

University of Windsor

Scholarship at UWindor

Electronic Theses and Dissertations

Theses, Dissertations, and Major Papers

1983

A study of the volcanic rocks on the southern half of Carriacou, Grenadines, West Indies.

Gary. Caldwell
University of Windsor

Follow this and additional works at: <https://scholar.uwindsor.ca/etd>

Recommended Citation

Caldwell, Gary., "A study of the volcanic rocks on the southern half of Carriacou, Grenadines, West Indies." (1983). *Electronic Theses and Dissertations*. 821.
<https://scholar.uwindsor.ca/etd/821>

This online database contains the full-text of PhD dissertations and Masters' theses of University of Windsor students from 1954 forward. These documents are made available for personal study and research purposes only, in accordance with the Canadian Copyright Act and the Creative Commons license—CC BY-NC-ND (Attribution, Non-Commercial, No Derivative Works). Under this license, works must always be attributed to the copyright holder (original author), cannot be used for any commercial purposes, and may not be altered. Any other use would require the permission of the copyright holder. Students may inquire about withdrawing their dissertation and/or thesis from this database. For additional inquiries, please contact the repository administrator via email (scholarship@uwindsor.ca) or by telephone at 519-253-3000ext. 3208.

CANADIAN THESES ON MICROFICHE

I.S.B.N.

THESES CANADIENNES SUR MICROFICHE



National Library of Canada
Collections Development Branch

Canadian Theses on
Microfiche Service

Ottawa, Canada
K1A 0N4

Bibliothèque nationale du Canada
Direction du développement des collections

Service des thèses canadiennes
sur microfiche

NOTICE

The quality of this microfiche is heavily dependent upon the quality of the original thesis submitted for microfilming. Every effort has been made to ensure the highest quality of reproduction possible.

If pages are missing, contact the university which granted the degree.

Some pages may have indistinct print especially if the original pages were typed with a poor typewriter ribbon or if the university sent us a poor photocopy.

Previously copyrighted materials (journal articles, published tests, etc.) are not filmed.

Reproduction in full or in part of this film is governed by the Canadian Copyright Act, R.S.C. 1970, c. C-30. Please read the authorization forms which accompany this thesis.

THIS DISSERTATION
HAS BEEN MICROFILMED
EXACTLY AS RECEIVED

AVIS

La qualité de cette microfiche dépend grandement de la qualité de la thèse soumise au microfilmage. Nous avons tout fait pour assurer une qualité supérieure de reproduction.

S'il manque des pages, veuillez communiquer avec l'université qui a conféré le grade.

La qualité d'impression de certaines pages peut laisser à désirer, surtout si les pages originales ont été dactylographiées à l'aide d'un ruban usé ou si l'université nous a fait parvenir une photocopie de mauvaise qualité.

Les documents qui font déjà l'objet d'un droit d'auteur (articles de revue, examens publiés, etc.) ne sont pas microfilmés.

La reproduction, même partielle, de ce microfilm est soumise à la Loi canadienne sur le droit d'auteur, SRC 1970, c. C-30. Veuillez prendre connaissance des formules d'autorisation qui accompagnent cette thèse.

LA THÈSE A ÉTÉ
MICROFILMÉE TELLE QUE
NOUS L'AVONS REÇUE

A STUDY OF THE VOLCANIC ROCKS
ON THE SOUTHERN HALF OF CARRIACOU,
GRENADINES, WEST INDIES.

by

© GARY CALDWELL

A thesis submitted to the Faculty of
Graduate Studies of the University
of Windsor in partial fulfilment
of requirements for the degree
of MASTER OF SCIENCE.

(GEOLOGY)

1983

© GARY FRANCIS CALDWELL 1983

ALL RIGHTS RESERVED

783482

ABSTRACT

Carriacou is a small island located in the southern part of the Lesser Antilles, West Indies. The field relations, petrography and geochemistry of the lavas found on the southern half of the island were examined in order to determine their petrogenesis and relationship to the rest of the volcanic arc.

It was found that there are six main volcanic units, which, from the oldest to youngest, include the clinopyroxene-phyric basalt (CPB) sequence, the amphibole-phyric andesite (APA) sequence, the clinopyroxene-megaphyric basalt (CMB) sequence, the olivine-microphyric basalt (OMB) sequence, the clinopyroxene-phyric andesite (CPA) sequence and the amphibole-megaphyric andesite (AMA) sequence. Volcaniclastic deposits are associated with the APA, CMB, and AMA sequences. The APA sequence is calc-alkaline, whereas the other five sequences are tholeiitic.

Sr isotope and REE data suggest that these rocks were derived from a partial melt(s) of a garnet peridotite deep within the mantle. The OMB lavas represent the closest composition to the primary melt(s). Variation diagrams, petrography, and REE

variations further suggest that the compositional variation in the volcanic rocks are due to low pressure fractional crystallization of the OMB magmas. The fractionation of approximately 17% clinopyroxene and 20% olivine (plus smaller amounts of magnetite, picotite and later plagioclase) is responsible for the evolution of the basaltic sequences. The subsequent fractionation of clinopyroxene and magnetite (plus smaller amounts of plagioclase and later amphibole) is responsible for the evolution of the andesitic sequences.

Compared to the islands which lie to the north, the basalts on the southern half of Carriacou contain high Ni, Cr and V, and all the lavas contain high Sr isotope ratios. In addition, the OMB lavas contain high MgO and low Al_2O_3 . These variations may be accounted for in a model where slower rates of subduction in the southern part of the arc lead to greater degrees of both partial melting and contamination. In addition, there are no alkali basalts on Carriacou, and in spite of the relative proximity to Grenada, and the parallel evolutionary mechanisms for the volcanic rocks on both islands, the lavas on Carriacou contain much lower ranges in Rb, Ba, K, and Sr contents than those lavas on Grenada, and are

therefore thought to have been derived from tholeiitic
parental melts.

ACKNOWLEDGEMENTS

I would like to thank Dr. T. Smith for his valuable suggestions, constructive criticism, and constant enthusiasm. The aid from Dr. C. H. Huang in carrying out the geochemical analyses was also very much appreciated. I would also like to thank my fiancée, Connie Squires, and my father, Frank Caldwell for both their direct and indirect help. Finally, I would like to thank Wilcox Bain (Plate 18) for his general aid, and Nipper (Plate 17) for his constant companionship while carrying out the field mapping on Carriacou.

TABLE OF CONTENTS

	Page
ABSTRACT	iv
ACKNOWLEDGEMENTS	vii
CHAPTER 1	
INTRODUCTION	1
1.1 GEOGRAPHY	1
1.2 PREVIOUS WORK	3
1.3 GEOLOGICAL SETTING	3
1.4 THE AREA OF STUDY AND THE METHOD. AND PURPOSE OF INVESTIGATION	5
CHAPTER 2	
GEOLOGY OF THE VOLCANIC ROCKS IN THE SOUTHERN HALF OF CARRIACOU	8
2.1 FIELD OBSERVATIONS	8
2.1.1 THE CLINOPYROXENE-PHYRIC BASALT SEQUENCE	9
2.1.2 THE AMPHIBOLE-PHYRIC ANDESITE SEQUENCE	12
2.1.3 THE CLINOPYROXENE-MEGAPHYRIC BASALT SEQUENCE	14
2.1.4 THE OLIVINE-MICROPHYRIC BASALT SEQUENC	15
2.1.5 THE CLINOPYROXENE-PHYRIC ANDESITE SEQUENCE	16
2.1.6 THE AMPHIBOLE-MEGAPHYRIC ANDESITE SEQUENCE	17
CHAPTER 3	
THIN-SECTION PETROGRAPHY	20
3.1 GENERAL OBSERVATIONS	20
3.1.1 THE CLINOPYROXENE-PHYRIC BASALT LAVAS	21
3.1.2 THE AMPHIBOLE-PHYRIC ANDESITE LAVAS	23
3.1.3 THE CLINOPYROXENE-MEGAPHYRIC BASALT LAVAS	25
3.1.4 THE OLIVINE-MICROPHYRIC BASALT LAVAS	27
3.1.5 THE CLINOPYROXENE-PHYRIC ANDESITE LAVAS	29

3.1.6 THE AMPHIBOLE-MEGAPHYRIC ANDESITE LAVAS	30
3.1.7 MAFIC PLUTONIC BLOCKS	32
3.2 THIN-SECTION PETROGRAPHY - A SUMMARY	33
CHAPTER 4	
GEOCHEMISTRY	37
4.1 METHOD	37
4.2 GEOCHEMICAL RESULTS	39
4.3 GEOCHEMICAL RESULTS WITHIN THE VOLCANIC SEQUENCES ON THE SOUTHERN HALF OF CARRIAOU	41
4.4 THE GEOCHEMISTRY OF THE LAVAS ON THE SOUTHERN HALF OF CARRIAOU IN COMPARISON TO THOSE FOUND THROUGHOUT THE LESSER ANTILLES VOLCANIC ARC	58
4.5 REE COMPOSITIONS AND Sr ISOTOPE RATIOS FROM THE LAVAS ON THE SOUTHERN HALF OF CARRIAOU	65
4.6 CLASSIFICATION OF THE VOLCANIC LAVAS ON THE SOUTHERN HALF OF CARRIAOU	65
CHAPTER 5	
PETROGENESIS	74
5.1 Sr ISOTOPES	74
5.2 REE VALUES	80
5.3 POSSIBLE MECHANISMS FOR COMPOSITIONAL VARIATIONS OF THE VOLCANIC ROCKS ON THE SOUTHERN HALF OF CARRIAOU	81
5.3.1 MIXING MODEL	83
5.3.2 PARTIAL MELTING AND FRACTIONAL CRYSTALLIZATION	84
5.4 FRACTIONAL CRYSTALLIZATION AS A MODEL FOR THE VARIATIONS IN COMPOSITION OF THE VOLCANIC ROCKS ON THE SOUTHERN HALF OF CARRIAOU	88
5.5 PETROGENESIS - A SUMMARY AND DISCUSSION	97
CHAPTER 6	
THE LESSER ANTILLES VOLCANIC-ARC SYSTEM	102
6.1 REGIONAL AND TECTONIC CHARACTERISTICS OF THE LESSER ANTILLES VOLCANIC-ARC SYSTEM	102
6.2 GEOCHEMICAL CHARACTERISTICS OF THE LESSER ANTILLES VOLCANIC ARC SYSTEM	105
6.3 MODELS FOR THE GEOCHEMICAL VARIATION ALONG THE LESSER ANTILLES VOLCANIC-ARC SYSTEM	108

CHAPTER 7

CONCLUSIONS	111
PLATES	115
REFERENCES CITED	149

LIST OF FIGURES

Figure	Page
1.1 The Lesser Antillés, with the Grenadines shown in inset	2
1.2 Geography and location map for the island of Carriacou	4
1.3 Geology of Carriacou (After Jackson 1970, 1980)	6
2.1 Geology of the southern half of Carriacou (Modified after Jackson 1970, 1980)	11
4.1a Major oxide (wt. %) vs. SiO ₂ (wt. %) for the lavas on Carriacou	59
4.1b Trace element (ppm) vs. SiO ₂ (wt. %) for the lavas on Carriacou	61
4.2 Alkaline vs. subalkaline classification diagrams for the lavas on the southern half of Carriacou	69
4.3 Subalkaline classification diagrams for the lavas on the southern half of Carriacou	71
4.4 Classification diagram for the andesites found on the southern half of Carriacou	73
5.1 Chondrite normalised REE patterns for four lavas from the southern half of Carriacou	82
5.2 Residual or incompatible element vs. non-residual or compatible element variation diagrams for the lavas on the southern half of Carriacou	85
5.3a Major oxide (wt. %) vs. MgO (wt. %) for the lavas on Carriacou	89
5.3b Trace element (ppm) vs. MgO (wt. %) for the lavas on Carriacou	91
6.1 Geological and structural trends for the Lesser Antilles volcanic-arc system	104

LIST OF TABLES

Table	Page
2.1 Geological formations (Modified after Jackson, 1970, 1980)	10
3.1 The volume percentages and dimensions for the intratelluric minerals of the main lava sequences that are exposed on the southern half of Carriacou	22
4.1 Basic operating conditions and precision for the major oxide and trace element analyses on the X-ray Spectrometer	40
4.2 Geochemistry of the volcanic lavason Carriacou	42
4.3 Geochemistry of an amphibole (taken from AMA volcanoclastics) and a clinopyroxene (taken from CMB volcanoclastics)	51
4.4 The ranges, averages and standard deviations of the major oxide and trace element geochemistry for the lavas on the southern half of Carriacou	53
4.5 The geochemistry of volcanic lavas found on Carriacou (After Jackson 1970, 1980)	66
5.1 Initial Sr isotope ratios from the Lesser Antilles	76
5.2 Silica, potassium, rubidium, strontium, and nickel contents and initial $^{87}\text{Sr}/^{86}\text{Sr}$ ratios of rocks belonging to three volcanic suites from the Lesser Antilles (After Hedge and Lewis, 1971)	79

CHAPTER 1

INTRODUCTION

1.1 GEOGRAPHY

Carriacou (Lat. 12°N , Long. 61°W) is a small island lying in the southern part of the Lesser Antilles volcanic-arc in the West Indies. It is the largest island of the Grenadines, and lies between St. Vincent and Grenada (Figure 1.1). Carriacou, approximately thirty-four square kilometers in area, is roughly boomerang-shaped, with its apex pointing southeast. A series of high ridges and hills is found throughout the island. The highest summits, which are over 313 m in height, are located in the north (High North) and southwest (Chapeau Carre). An east-dipping escarpment, which represents the western edge of the Miocene limestone beds, runs through the central area, and reaches over 270 m in height. Large alluvium-filled coastal flats are present along Tyrrel, Watering, Bretache and Hillsborough Bays (Plate 1). Elsewhere, the coast is very rugged, and often contains steep cliffs. The island contains many small settlements, of which Hillsborough is the largest. A

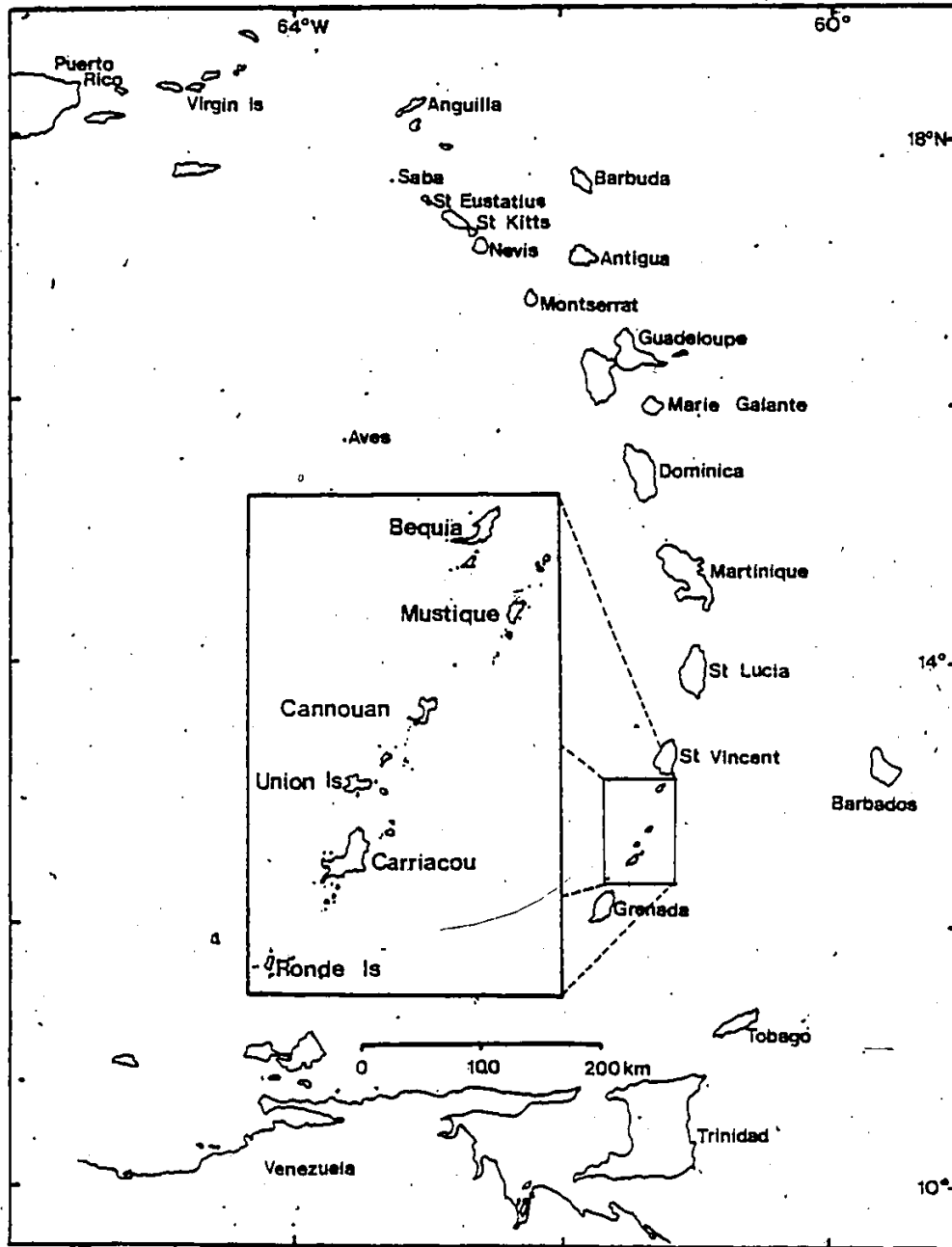


Fig. 1.1 The Lesser Antilles, with the Grenadines shown in inset

number of narrow roads and paths make predominantly all areas of the island accessible for study (Figure 1.2).

1.2 PREVIOUS WORK

The entire island's stratigraphy was examined by Martin-Kaye (1958) and Robinson and Jung (1972). However, these authors concentrated on the study of the age relationships and the lithologies of the marine sedimentary rocks. Later, Jackson (1970, 1980) mapped the island, concentrating on the geology of the volcanic rocks. Briden et al. (1978) dated some of these volcanic rocks using the K-Ar method.

1.3 GEOLOGICAL SETTING

Miocene marine sedimentary rocks, which are over 350 m in total thickness, and which are predominantly composed of fossiliferous calcareous deposits, are exposed mainly in the eastern part of the island. They form an open syncline, the eastern flank of which is cut off by the coast. In addition, a few scattered outcrops of limestone and tuffs in the northern part of the island contain fossils of Oligocene-Eocene age (Martin-Kaye, 1958, Robinson and Jung, 1972). The

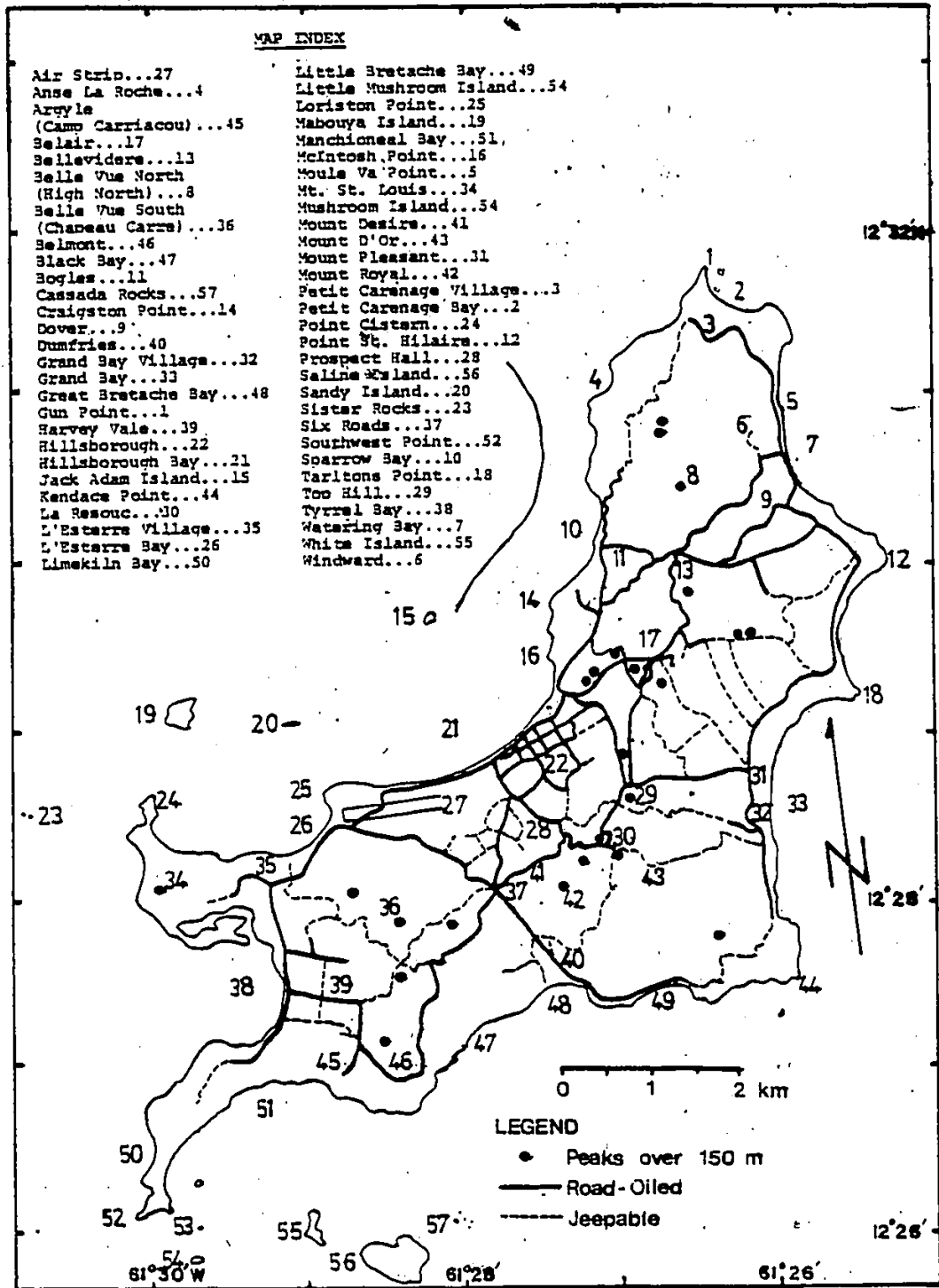


Fig. 1.2 Geography and location map for the island of Carriacou

remaining two-thirds of the island is composed of lava flows, volcanoclastics, and sub-volcanic dykes and plugs that range from Miocene to Pliocene in age (Briden et al., 1978, Jackson, 1970, 1980).

Jackson (1970, 1980) and Briden et al. (1978) established a volcanic sequence involving three main volcanic units, which has since been shown to be incomplete. They are, in order of oldest to youngest, the clinopyroxene-megaphyric basalt lavas and associated volcanoclastics (CMB sequence), the olivine-microphyric basalt lavas (OMB sequence) and the andesite lavas and associated volcanoclastic sequence. The Miocene marine sedimentary sequences, which include, from oldest to youngest, the Belmont Formation (composed predominantly of conglomerates and arenites), and the Carriacou and Grand Bay Limestone Formations (Plates 2 and 3), are stratigraphically above the CMB volcanic sequence and below the OMB and andesite sequences (Figure 1.3).

1.4 THE AREA OF STUDY AND THE METHOD AND PURPOSE OF INVESTIGATION

The volcanic deposits in the southern half of the island were chosen for study. These deposits represent

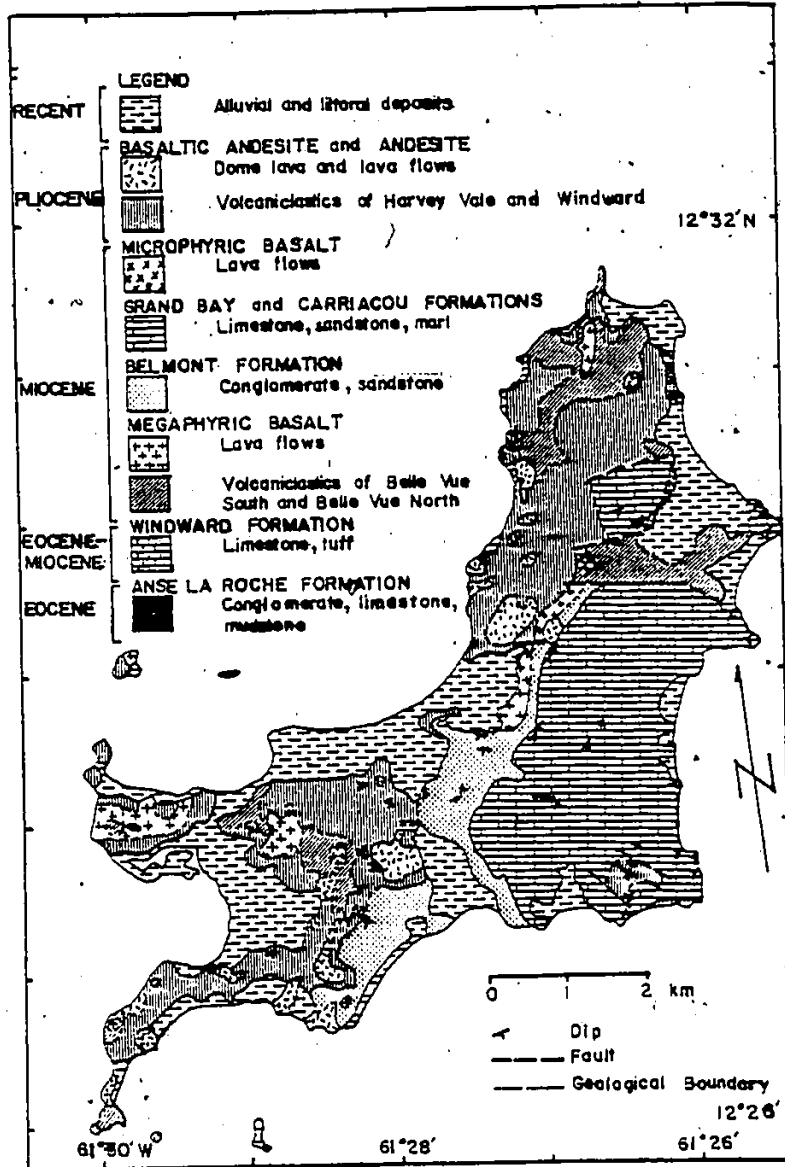


Fig. 1.3 Geology of Carriacou (After Jackson, 1970, 1980)

7

7

a complete and complex succession of all the volcanic material found on the island.

The study began with a thorough examination of the volcanic deposits in the field. ~~This~~ was followed by a study of their petrography and geochemistry in the laboratory. Using the above information, a complete and integrated description, classification, and petrogenesis was derived for the volcanic rocks on Carriacou. This information was subsequently compared with the overall trends and characteristics of the Lesser Antilles volcanic-arc system.

CHAPTER 2

GEOLOGY OF THE VOLCANIC ROCKS IN THE SOUTHERN
HALF OF CARRIACOU

2.1. FIELD OBSERVATIONS

New observations have established that there are six main volcanic units in the southern half of Carriacou. The oldest volcanic sequence, which was not mapped by Jackson (1970, 1980), is a small basaltic unit outcropping at Southwest Point (Figure 2.1). Additionally, stratigraphic relationships and petrography show that the andesite sequence mapped by Jackson (1970, 1980) can be separated into three units. These three units are the amphibole-phyric andesite lavas and associated volcanoclastics (APA sequence), which are older than the CMB and OMB volcanic sequences, and the amphibole-megaphyric andesite lavas and associated volcanoclastics, and clinopyroxene-phyric andesite lavas (AMA and CPA sequences respectively) which are younger than the CMB and OMB volcanic sequences. All of the andesites contain abundant plagioclase phenocrysts (up to 25%), however, the andesites can be divided into three groups

according to their mafic phenocryst assemblage. The APA lavas predominantly contain small amphibole phenocrysts, while the AMA lavas predominantly contain large amphibole phenocrysts, and the CPA lavas contain small amounts of predominantly clinopyroxene phenocrysts. In addition, weathered surfaces of the APA and AMA lavas are light grey in colour, while those of the CPA lavas are red-brown in colour.

The stratigraphic sequence, occurrence and lithologies of the volcanic and marine sedimentary units exposed on the southern half of Carriacou are summarized in Table 2.1.

2.1.1 THE CLINOPYROXENE-PHYRIC BASALT SEQUENCE

The CPB sequence outcrops at Southwest Point (Figure 2.1) and occurs as a lava flow which is brecciated in most places. The unit is over 10 m in thickness, and underlies APA volcanoclastics. The lavas are weathered to a light red colour and contain small (2 mm) clinopyroxene and plagioclase phenocrysts.

TABLE 2.1 - GEOLOGICAL FORMATIONS
(Modified after Jackson, 1970, 1980)

UNIT	OCCURRENCE	ROCK TYPE
Amphibole-megaphyric (AMA) and Clinopyroxene-phyric (CPA) andesite sequences	-lava flows, plugs, dykes and volcaniclastics	-mainly andesite; minor amounts of leucocratic basalts
Olivine-microphyric basalt (OMB) sequence	-dykes and scattered boulders	-basalt
Grand Bay and Carriacou Formations	-marine sedimentary beds	-limestone, sandstone, marl
Belmont Formation	-marine sedimentary beds	-conglomerate, sandstone
Clinopyroxene-megaphyric basalt (CMB) sequence	-lava flows, dykes and volcaniclastics	-basalt
Amphibole-phyric andesite (APA) sequence	-lava flows and volcaniclastics	-andesite
Clinopyroxene-phyric basalt (CPB) sequence	-lava flow (partly brecciated)	-basalt

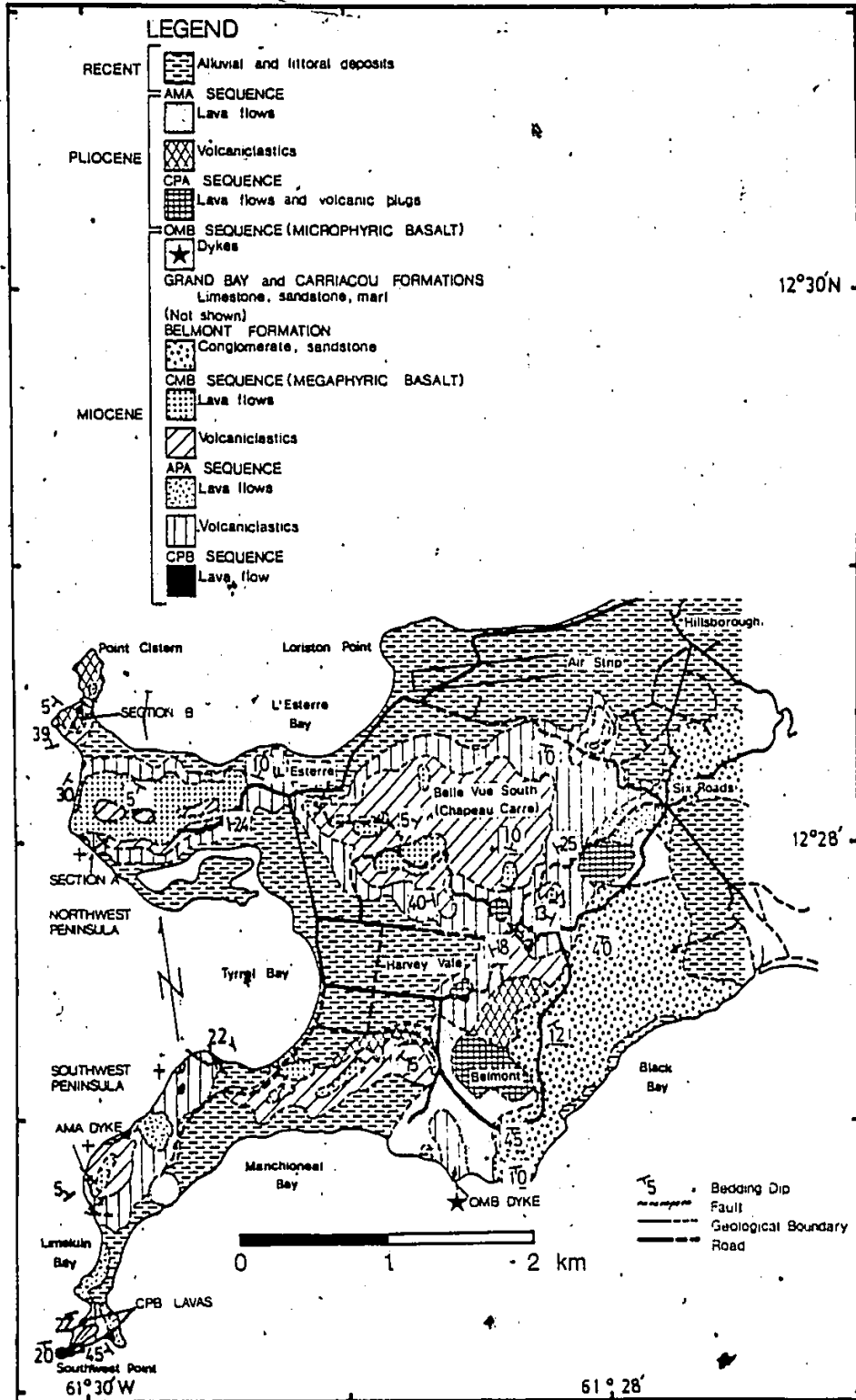


Fig. 2.1 Geology of the southern half of Carriacou (Modified after Jackson, 1970, 1980)

2.1.2 THE AMPHIBOLE-PHYRIC ANDESITE SEQUENCE

The APA lava sequence outcrops on the southwest peninsula and west of Six Roads (Figure 2.1). These flows reach over 80 m in thickness.

On the north shore of Limekiln Bay (Figure 2.1), volcanoclastic material, which contains fragments, similar in lithology to the adjacent andesite flows, conformably underlies CMB volcanoclastics. These andesites, together with the blocks found within the volcanoclastics, contain abundant and large plagioclase phenocrysts (up to 5 mm and 20 % by volume). The amphibole and clinopyroxene phenocrysts are very small (2 mm) and generally make up less than 5 % of the rock by volume.

The volcanoclastic deposits associated with the andesites above, generally form the base for most of the volcanic deposits on the southern half of the island (Figure 2.1). Accumulations of these volcanoclastics reach over 70 m in thickness. They include airfall material, which generally contains accretionary lapilli (Plates 4 and 5), and cold avalanche deposits. The cold avalanche deposits are made up of a framework of predominantly monolithic and angular boulders set in a finer rudaceous matrix of

similar material (Plates 6). However, massive to well bedded, often faulted and broken-up epiclastic material is predominant (Plates 7 and 8). The epiclastic material weathers to light green, yellow or red colours and generally contains fragments of andesite and mudstone, as well as small crystals of amphibole and clinopyroxene. These deposits include mudflows, paraconglomerates, pebbly greywackes and arenites. The mudflows contain a large range, in both size and composition, of andesitic clasts set in a muddy matrix (Plate 9).

In a steep shoreline section on the western shore of the northwest peninsula (Section A in Figure 2.1), approximately 10 m of a massive, pebbly arkosic greywacke, at the base of the cliff is overlain by over 15 m of horizontally bedded crystal tuffs and/or arkosic greywackes. Rudaceous fragments in the lower unit are primarily andesitic in composition. The crystal tuffs and/or arkosic greywackes are made up of predominantly weathered plagioclase (10 % by volume) and clinopyroxene (approximately 5 % by volume) crystals set in a marly matrix. The beds continue north along the shore and begin to dip towards the northeast at about 25° , where they are unconformably overlain by a thick CMB lava flow (approximately 80 m

thick).

2.1.3 THE CLINOPYROXENE-MEGAPHYRIC BASALT SEQUENCE

The next major volcanic unit includes CMB lava flows, dykes and volcanoclastics. The main CMB lava flows outcrop to the west of Chapeau Carre and on the northwest peninsula (Figure 2.1). The latter deposit (which is over 80 m thick) was emplaced in a basin, and unconformably overlies APA volcanoclastic deposits. The lavas characteristically weather to a black colour and contain large, stubby-prismatic clinopyroxene (3 to 5 mm in diameter) and abundant plagioclase (generally less than 1 mm in diameter) phenocrysts. Olivine phenocrysts are often readily visible.

CMB dykes, ranging from 1 to 4 m in thickness, were intruded along the Belmont and APA contact at Six Roads, into the volcanoclastics on the north shore of Limekiln Bay, and into the APA volcanoclastics at Southwest Point (Figure 2.1). These observations help show that the CMB sequence is younger than the Belmont and APA deposits.

The CMB volcanoclastics, which generally occupy the highest regions in the southern half of the island, are most abundant at Chapeau Carre and the north shore of Limekiln Bay (Plate 10), on the southwest peninsula (Figure 2.1). These deposits are generally

sub-horizontally bedded (Plate 11) and reach over 100 m in thickness. The volcanoclastic material is generally composed of a mud-supported framework of crystals and/or lithic clasts. The mud characteristically weathers to a dark green colour, and the lithic clasts, which range from sand to boulder size, are predominantly CMB fragments. The crystals, which are generally most abundant towards the bottom of the beds, include clinopyroxene (3 to 5 mm in diameter) and plagioclase (1 mm in diameter) crystals (Plate 12). The large sections are either too poorly exposed, or too steep for a detailed study of their stratigraphy.

2.1.4 THE OLIVINE-MICROPHYRIC BASALT SEQUENCE

The OMB sequence is observed in place as dykes intruding the APA volcanoclastics on the eastern shore of Manchioneal Bay and the Miocene limestone beds west of Mount D'Or (Figures 1.3 and 2.1 respectively). The presence of these dykes shows that the OMB sequence is younger than the APA and Miocene limestone deposits.

OMB boulders, found scattered both south and northeast of Belmont (Figure 2.1), may have once represented lava flows. There are no volcanoclastic

units assigned to this sequence.

The OMB lavas weather to a black colour, and contain abundant, and predominantly small (1 mm) phenocrysts of olivine.

2.1.5 THE CLINOPYROXENE-PHYRIC ANDESITE SEQUENCE

The CPA sequence exists as a volcanic plug at Belmont (Plate 13) and lava flows between Belmont and Six Roads, and on the western shoreline at Point Cistern. In addition, a large block of CPA lava, approximately 10 m in diameter, is present in the scree on the western shore of the southwest peninsula (Figure 2.1). There are no volcanoclastic deposits associated with this sequence.

At Point Cistern, partly brecciated CPA lava beds, which dip to the northeast, are believed to overlie layered CMB crystal tuffs, which continue to the southeast. Therefore, this section shows that the CPA lavas are younger than the CMB deposits. However, large amounts of scree cover obscure the boundary with the adjacent AMA volcanoclastic sequence, so that their stratigraphic relationship is not clear.

The CPA lavas characteristically contain approximately 5 % clinopyroxene (less than 3 mm in

diameter) with trace amounts of amphibole (less than 1 mm in diameter) phenocrysts.

2.1.6 THE AMPHIBOLE-MEGAPHYRIC ANDESITE SEQUENCE

The AMA lavas, which characteristically contain large (between 5 and 10 mm) amphibole phenocrysts, outcrop north and south of Six Roads and on the eastern shore of Manchioneal Bay (Figure 2.1). These flows reach more than 7 m in thickness. AMA basalts, which contain abundant (up to 20 % by volume) and large amphibole and clinopyroxene phenocrysts set in a leucocratic groundmass, outcrop on the southwest peninsula (Figure 2.1). Here they occur as both a 4 m wide, sub-vertical dyke intruding the CMB layered volcanoclastic sequence on the north shore of Limekiln Bay, and as a flow on the west shore of Manchioneal Bay. In addition, AMA lavas unconformably overlie the Belmont Formation on the eastern shore of Manchioneal Bay (Figure 2.1). The Belmont Formation continues eastward along the shore where it includes abundant CMB basalt cobbles. These observations show that the AMA sequence is younger than the Belmont and CMB deposits.

The AMA volcanoclastic deposits predominantly occur as small, scattered exposures that include cold

avalanche and airfall deposits, mudflows (Plate 14) and other epiclastic material (Figure 2.1). These deposits commonly contain andesitic clasts with large amphibole phenocrysts, while a few deposits contain minor amounts of sub-rounded CMB blocks. In addition, large amphibole crystals and/or mafic to ultramafic plutonic blocks are generally found within these deposits.

A good exposure of the volcanoclastic sequence is found at Point Cistern (Figure 2.1), where it reaches more than 70 m in thickness. This sequence overlies CMB mudflows and bedded crystal tuffs. The AMA volcanoclastics weather from a light brown to a white colour. Where they have been extensively hydrothermally altered, the rocks weather to a dark red-brown colour due to the presence of abundant hematite veins. Where they have not been brecciated (Plate 15), the sequence exists as massive to laminated crystal tuffs over 12 m in thickness. The crystals include abundant plagioclase and amphibole approximately 1 mm in size. Larger crystals of amphibole exist in places, and may reach 3 cm in length. This sequence continues upwards into sub-horizontally bedded layers of predominantly oligomictic breccia and epiclastic arkose and mudstone.

Throughout the sequence, mafic to ultramafic plutonic blocks are incorporated within the fragmental material. Similar plutonic blocks can also be found in thick andesite dykes exposed along the shoreline north of Hillsborough (Plate 16) and in andesitic volcanoclastic material exposed along the shoreline at the southern end of Tyrrel Bay (Figures 1.3 and 2.1 respectively).

CHAPTER 3

THIN-SECTION PETROGRAPHY

3.1 GENERAL OBSERVATIONS

Representative lavas (and a few plutonic blocks) from the six main volcanic sequences exposed on the southern half of Carriacou, were chosen for thin-section study. The lavas were porphyritic, with an aphanitic, holocrystalline groundmass, having an intergranular texture (Plate 19). However, a few of the CPA samples had a hypohyaline to hypocrySTALLINE groundmass. Glomerophenocrysts were present in most of the volcanic thin-sections. All of the intratelluric and groundmass pyroxenes were monoclinic, with a light green colour in plane polarized light. Intratelluric clinopyroxenes commonly showed a high dispersion in cross polars, and most showed oscillatory or non-oscillatory zoning (Plate 21). The intratelluric olivines, which only occurred in the basalts, were optically unzoned. In contrast, all of the intratelluric plagioclase phenocrysts showed normal and/or oscillatory zoning (Plate 21). Amphibole phenocrysts were pleochroic green in plane light, and

commonly exhibited patchy zoning in cross polars. The mineralogical abundances (along with their dimensions) for the intratelluric phases of the volcanic lavas are given in Table 3.1.

3.1.1 The CLINOPYROXENE-PHYRIC BASALT LAVAS

The groundmass of the CPB samples is predominantly made up of plagioclase, clinopyroxene and magnetite. Small amounts of olivine, which are pseudomorphed by iddingsite, are also present.

The intratelluric phases make up approximately 33% of the rock, and comprise less than 1% magnetite, 3% olivine, 10% clinopyroxene and 20% plagioclase (Table 3.1).

Magnetite crystals are euhedral to subhedral, and are generally less than 0.5 mm in diameter.

Olivines occur as mostly euhedral crystals which are generally less than 0.5 mm in diameter. The phenocrysts are either partially or completely pseudomorphed by iddingsite. Euhedral magnetite is commonly found within the olivine crystals.

Clinopyroxenes are present as mostly euhedral crystals which are generally less than 2 mm in diameter. The phenocrysts commonly show fritted

TABLE 3.1 - The volume percentages and dimensions for the intratelluric minerals of the main lava sequences that are exposed in the southern half of Carriacou.

Volcanic Lava Sequence	CPB	APA	CMB	OMB	CPA	AMA
% Intratelluric Phases (Total)	33	20-25	35-70	20-40	15-30	30-35
% Picotite (Diameter in mm)	-	-	0-1 <0.02	<1 <0.02	-	-
% Magnetite (Diameter in mm)	<1 <0.5	<1 <1	<3 <1	<2 <1	<2 <1	<1 <0.5
% Olivine (Diameter in mm)	3 <0.5	-	5-10 <3	10-20 <4	-	-
% Clinopyroxene (Diameter in mm)	10 <2	1-2 <0.5	5-20 <5	0-25 <1	3-5 <3	3-10 <5
% Plagioclase (Diameter in mm) (% An content)	20 <2 70	15-20 <5 55-60	10-50 <4 65-75	<1 <1 -	10-25 <4 50-65	15-25 <3 55-65
% Amphibole (Diameter in mm)	-	3 <2	-	-	<2 <1	5-10 <10
% Quartz (Diameter in mm)	-	<1 <1	-	-	-	<1 <1
% Apatite (Diameter in mm)	-	-	-	-	-	<1 <0.5

marginal overgrowths. Euhedral magnetite, and a few euhedral plagioclase crystals, are generally found within the clinopyroxene phenocrysts.

Plagioclase phenocrysts occur as mostly euhedral crystals which are generally less than 2 mm in diameter. The composition of the plagioclase is approximately An₇₀. Most phenocrysts show variable degrees of internal melt channel corrosion. A few of the crystals surround euhedral clinopyroxene.

The inclusion of smaller, euhedral minerals in larger phenocrysts, as observed above, indicates a crystallization sequence beginning with magnetite, followed by olivine (?), and clinopyroxene and plagioclase.

3.1.2 THE AMPHIBOLE-PHYRIC ANDESITE LAVAS

The groundmass of the APA samples is made up of plagioclase and magnetite, with small amounts of clinopyroxene.

The intratelluric phases make up between 20 and 25% of the rock, and comprise less than 1% magnetite, 1 to 2% clinopyroxene, 15 to 20% plagioclase, and 3% amphibole. One sample contained less than 1% quartz phenocrysts (Table 3.1).

Magnetite crystals are subhedral to euhedral, and are generally less than 1 mm in diameter. Many of these crystals exhibit dendritic quench overgrowths.

Clinopyroxenes are present as mostly euhedral crystals which are generally less than 0.5 mm in diameter. Euhedral magnetite is commonly found within the clinopyroxenes.

Plagioclase phenocrysts are present as mostly euhedral crystals which are generally less than 5 mm in diameter. The plagioclase composition lies in the labradorite range (An_{55} to An_{60}). Most of the plagioclase phenocrysts contain extensive internal melt channel corrosion with marginal overgrowths (Plate 21).

Amphibole phenocrysts are present as predominantly euhedral crystals which are generally less than 2 mm in length. The prismatic phenocrysts are marginally or entirely pseudomorphed by fine opaques (Plate 21). Euhedral clinopyroxene and plagioclase crystals are commonly found within the amphiboles.

Quartz phenocrysts are present as subhedral to anhedral crystals which are less than 1 mm in diameter. The margins are generally resorbed to rounded edges.

The inclusion of smaller, euhedral minerals in larger phenocrysts, as observed above, indicates a

crystallization sequence beginning with magnetite, followed by clinopyroxene and plagioclase (?), and amphibole (+ quartz).

3.1.3 THE CLINOPYROXENE-MEGAPHYRIC BASALT LAVAS

The groundmass of the CMB samples is made up of plagioclase, clinopyroxene, and magnetite (+ intergrowths of larger phlogopite (Plate 22) and red amphibole; ± olivine, altering to a green micaceous mineral).

The intratelluric phases make up between 35 and 70% of the rock, and comprise 0 to 1% picotite, less than 3% magnetite, 5 to 10% olivine, 5 to 20% clinopyroxene, and 10 to 50% plagioclase (Table 3.1).

Picotite occurs as small (0.02 mm in diameter), euhedral crystals found only within some of the olivine phenocrysts.

Magnetite crystals are subhedral to euhedral, and are generally less than 1 mm in diameter. Most of these magnetite crystals exhibit a dendritic quench overgrowth (Plate 23), while some show marginal resorption.

Olivines are present as subhedral to euhedral crystals which are generally less than 3 mm in

diameter. Many contain euhedral magnetite and/or picotite. A few of the olivine phenocrysts show marginal resorption, while all generally exhibit some degree of alteration to iddingsite or a green micaceous mineral along internal fractures.

Clinopyroxenes are present as predominantly euhedral crystals which are generally less than 5 mm in diameter. These phenocrysts commonly exhibit fritted overgrowths along their margins (Plate 24), and a few contain internal melt channel corrosion. Euhedral olivine, plagioclase and magnetite are sometimes found within the clinopyroxenes (Plates 25 and 26).

Plagioclase phenocrysts occur as predominantly euhedral crystals which are generally less than 4 mm in diameter. The plagioclase composition lies in the upper labradorite - lower bytownite range (An_{65} to An_{75}). They generally show internal melt channel corrosion, and a few of the phenocrysts contain euhedral magnetite.

The inclusion of smaller, euhedral minerals in larger phenocrysts, as observed above, indicates a crystallization sequence beginning with picotite and magnetite, followed by olivine, and clinopyroxene and plagioclase.

3.1.4 THE OLIVINE-MICROPHYRIC BASALT LAVAS.

The groundmass of the OMB samples (Plate 19) is predominantly made up of plagioclase, clinopyroxene, and magnetite (\pm phlogopite).

The intratelluric phases make up between 20 and 40% of the rock, and comprise less than 1% picotite, less than 2% magnetite, 10 to 20% olivine and 0 to 25% clinopyroxene. Trace amounts of plagioclase megacrysts are present in some of the samples (Table 3.1).

Picotite occurs as small (0.02 mm in diameter), euhedral crystals, and are generally very abundant within the olivine phenocrysts (Plate 27):

Magnetite crystals are euhedral to subhedral, and are generally less than 1 mm in diameter. A few of the crystals exhibit either a dendritic quench overgrowth, or internal and marginal corrosion.

Olivines are present as predominantly euhedral phenocrysts which are generally less than 4 mm in diameter. The crystals commonly contain euhedral magnetite and/or picotite. A few of the olivine phenocrysts display some degree of alteration to iddingsite or a green micaceous mineral along internal fractures.

Clinopyroxenes are present as euhedral to

subhedral phenocrysts which are generally less than 1 mm in diameter. These clinopyroxenes generally contain fritted marginal overgrowths and/or internal melt channel corrosion (Plate 28). Euhedral magnetite is commonly found within the clinopyroxenes.

Plagioclase megacrysts are present as euhedral to subhedral crystals which are less than 1 mm in diameter (Plate 29). The plagioclase is generally internally altered to a fine opaque dust.

The inclusion of smaller, euhedral minerals in larger phenocrysts, as observed above, indicates a crystallization sequence beginning with picotite and magnetite, followed by olivine and clinopyroxene. In addition, the absence of intratelluric clinopyroxene in one of the OMB samples (Plate 30) indicates that olivine crystallized before clinopyroxene.

Holocrystalline, fine-grained cognate xenoliths, with a dunite composition, are often present in the OMB samples (Plate 31). These xenoliths range up to 1 cm in diameter, and contain up to 5% corroded magnetite. Both the olivine and magnetite crystals are believed to represent cumulate phases.

3.1.5 THE CLINOPYROXENE-PHYRIC ANDESITE LAVAS

The groundmass of the CPA samples is made up of plagioclase and magnetite (\pm clinopyroxene, which is commonly replaced by calcite).

The intratelluric phases make up between 15 and 30% of the rock, and include less than 2% magnetite, 3 to 5% clinopyroxene, and 10 to 25% plagioclase. A few of the samples contained less than 2% amphibole phenocrysts (Table 3.1)

Magnetite crystals as subhedral to euhedral, and are generally less than 1 mm in diameter. A few of the phenocrysts exhibit dendritic quench overgrowths.

Clinopyroxenes occur as predominantly euhedral crystals, which are generally less than 3 mm in diameter. They commonly exhibit fritted marginal overgrowths. Euhedral magnetite is commonly found within the clinopyroxene phenocrysts.

Plagioclase phenocrysts occur as mostly euhedral crystals which are less than 4 mm in diameter. The composition lies in the labradorite range (An_{50} to An_{65}). Many of these phenocrysts exhibit internal melt channel corrosion (Plate 32). Euhedral magnetite is sometimes found within the plagioclase:

Amphibole phenocrysts are euhedral to subhedral

phenocrysts which are generally less than 1 mm in length. The margins are commonly altered to fine opaques. Euhedral plagioclase and clinopyroxene crystals are commonly found within the amphibole phenocrysts.

The inclusion of smaller, euhedral minerals in larger phenocrysts, as observed above, indicates a crystallization sequence beginning with magnetite, followed by clinopyroxene and plagioclase (\pm later amphibole).

3.1.6 THE AMPHIBOLE-MEGAPHYRIC ANDESITE LAVAS

The groundmass of the AMA samples is made up of plagioclase and magnetite (\pm clinopyroxene, which is commonly replaced by calcite).

The intratelluric phases make up between 30 and 35% of the rock, and include less than 1% magnetite, 3 to 10% clinopyroxene (being most abundant in the leucocratic basalts), 15 to 25% plagioclase and 5 to 10% amphibole. One of the samples contains trace amounts of quartz and apatite (Table 3.1).

Magnetite crystals are subhedral to euhedral, and are generally less than 0.5 mm in diameter. A few of the crystals exhibit dendritic quench overgrowths.

Clinopyroxenes are present as mostly euhedral phenocrysts which are generally less than 5 mm in diameter. Euhedral magnetite is commonly found within the clinopyroxenes.

Plagioclase phenocrysts are present as predominantly euhedral crystals which are generally less than 3 mm in diameter. The plagioclase composition lies in the labradorite range (An_{55} to An_{65}). The crystals commonly show internal melt channel corrosion, and a few of the phenocrysts contain euhedral magnetite.

Amphibole phenocrysts are present as mostly euhedral crystals which are generally less than 10 mm in length. The amphiboles are commonly altered to fine opaques around their margins. Euhedral magnetite and plagioclase, and anhedral clinopyroxene are often found within the amphibole phenocrysts (Plate 33). The latter relationship seems to be the result of reaction between the clinopyroxene and amphibole phases.

Quartz and apatite are present as anhedral to subhedral crystals which are less than 1 and 5 mm in diameter, respectively. Both phases are generally marginally altered.

The inclusion of smaller, euhedral minerals in larger phenocrysts, as observed above, indicates a

crystallization sequence beginning with magnetite, followed by plagioclase and clinopyroxene, and amphibole (\pm quartz and apatite).

3.1.7 MAFIC PLUTONIC BLOCKS

The mafic plutonic blocks are all medium-grained, with holocrystalline, hypidiomorphic-granular textures. According to the gabbroic classification by the IUGS Subcommittee (1973), the rocks fall into the pyroxene-hornblende gabbronorite field. The mineralogy includes less than 5% magnetite, 5 to 20% clinopyroxene, 10 to 25% amphibole and 60 to 70% plagioclase.

Magnetite occurs as predominantly anhedral, interprecipitate crystals. A few subhedral, precipitate crystals of magnetite are included in all of the other phases present.

Clinopyroxenes are present as subhedral to anhedral precipitate crystals, and some display compositional zoning (non-oscillatory), internal melt channel corrosion and/or exsolution lamellae. Many of the clinopyroxenes are mantled by amphibole.

Amphibole is generally pleochroic green in plane polarized light, except for one sample, where the

amphibole is pleochroic red-brown. The red-brown amphibole has been identified as an oxyhornblende (Ujike, 1974) which has a high Fe^{3+}/Fe^{2+} ratio. All of the amphiboles display subhedral to anhedral shapes that represent both interprecipitate and precipitate crystals. These amphiboles commonly include euhedral to subhedral plagioclase, clinopyroxene and magnetite.

Plagioclase crystals are present as precipitate phases with euhedral to subhedral shapes. The plagioclase composition lies in the lower bytownite range (An_{70} to An_{75}). A few of the plagioclase crystals display faint normal zoning.

The inclusion of smaller, euhedral crystals in larger precipitate crystals indicates a crystallization sequence beginning with magnetite, followed by plagioclase and clinopyroxene, and amphibole. In addition, the presence of interprecipitate amphibole and magnetite indicate that these crystals were the last to crystallize.

3.2 THIN-SECTION PETROGRAPHY - A SUMMARY

The order of crystallization of the intratelluric phases for each of the three basaltic sequences (CPB, CMB, and OMB) is given in the following list:

1. Magnetite, followed by olivine (?), and clinopyroxene and plagioclase for the CPB lavas.
2. Picotite and magnetite, followed by olivine, and clinopyroxene and plagioclase for the CMB lavas.
3. Picotite and magnetite, followed by olivine² (\pm later clinopyroxene) for the OMB lavas.

The CPB and CMB lavas both contain abundant plagioclase phenocrysts, and picotite crystals are either absent or present in very small amounts (i.e. in a few of the CMB lavas). However, the clinopyroxene phenocrysts are generally much larger in the CMB lavas.

The OMB lavas generally contain abundant picotite crystals, and the clinopyroxene phenocrysts are very small (and may be absent). Plagioclase phenocrysts are very rare, while dunite xenoliths are common (Table 3.1).

The order of crystallization for each of the three andesitic sequences (APA, CPA and AMA) is given in the following list:

1. Magnetite, followed by clinopyroxene and plagioclase (?), and amphibole (\pm quartz) for the APA lavas.

2. Magnetite, followed by clinopyroxene and plagioclase (\pm later amphibole) for the CPA lavas.
3. Magnetite, followed by clinopyroxene and plagioclase, and amphibole (\pm quartz and apatite) for the AMA lavas.

In addition, the crystallization sequence for the mafic plutonic blocks begins with magnetite, which is followed by clinopyroxene and plagioclase, and amphibole. The occurrence of interprecipitate amphibole and magnetite indicates that these are the last minerals to crystallize.

The APA lavas contain large plagioclase phenocrysts; small amphibole phenocrysts, and minor amounts of small clinopyroxene phenocrysts. The CPA lavas predominantly contain plagioclase and clinopyroxene phenocrysts; with minor amounts of small amphibole phenocrysts, while the AMA lavas contain significant amounts of large amphibole phenocrysts. (Table 3.1).

However, there are many similar mineralogical characteristics between the main lava sequences. Picotites are only found within the olivine phenocrysts of both the CMB and OMB lavas. All of the plagioclase phenocrysts of the CPB, CMB, and andesitic sequences

show normal and/or oscillatory zoning, and many exhibit internal melt channel corrosion. The plagioclase compositions for the andesitic sequences all lie in the range An_{50} to An_{65} , while those for the CPB and CMB sequences lie in the range An_{65} to An_{75} . All of the intratelluric clinopyroxenes are light green in plane polarized light, with a high dispersion in cross polars, while all of the amphibole phenocrysts (for the lavas) are pleochroic green in plane polarized light, and show some degree of marginal alteration to opaque minerals. Special textures (i.e. dendritic quench overgrowths on intratelluric magnetite, and fritted overgrowths on clinopyroxenes) are present in most of the lavas. Groundmass phlogopite is present in many of the basaltic lavas. In addition, the lava sequences show identical to overlapping mineralogies, with similar crystallization evolutions. In view of all these common characteristics, and the spacial and temporal association of these volcanic sequences, there is good reason to believe that the rocks on the southern half of Carriacou are genetically related.

CHAPTER 4

GEOCHEMISTRY

4.1. METHOD

The chemical analyses were carried out on glass discs and rock powder pellets using a Phillips PW 1410 Universal Vacuum X-ray Spectrometer. The contents of 10 major oxides (SiO_2 , Al_2O_3 , TiO_2 , Fe_2O_3 , MnO , MgO , CaO , Na_2O , K_2O and P_2O_5), plus 10 trace elements (V, Cr, Co, Ni, Rb, Sr, Y, Zr, Nb and Ba) were determined on 43 representative lava samples, using glass disc and rock powder pellets respectively. The major oxides were also determined on both a clinopyroxene and amphibole mineral.

Lanthanum oxide was used in the fusion mixture for the glass discs to lower the background to a uniform level for the analysis of major elements. However, the use of rock powder pellets was necessary for the trace element analysis because of overlapping background effects produced by the lanthanum oxide over smaller trace element peaks. The rock powder pellets were also used to keep the count rates at a reasonably high

level, since the concentration of any given element is greater than in glass discs. Loss on ignition was also determined on each sample (1050°C for 1 hour).

The rock powder for both the glass discs and powder pellets was prepared in a shatter box after being crushed by both the jaw crusher and micro-crusher. The samples were dried at 105°C for 12 hours, and then stored in a dessicator.

For the preparation of rock powder pellets, 2.5 g of rock powder was thoroughly mixed with 4 drops of a 2% solution of polyvinyl alcohol. This mixture was encased in 4 g of boric acid by applying 9 tons of pressure for 15 seconds in a 32 mm die. The pellets were allowed to dry for 24 hours.

For the preparation of glass discs, 1.875 g of fusion mixture (28.5 g Li tetraborate - anhydrous, 22.2 g Li carbonate, and 9.9 g lanthanum oxide) was melted down with 0.350 g of rock powder in a platinum crucible. The discs were formed in brass rings on a polished brass plate that was heated to 450°C. The glass was then annealed between two asbestos mats on a second hotplate that was heated to 250°C. The discs were allowed to slowly cool to room temperature, and then stored individually in labelled plastic bags.

Regression lines, produced from the count rates

for the standards GSP-1, pure quartz, G-2, BCR-1, AGV-1, BR, GA, and DTS-1 (U.S.G.S. and C.P.R.G) were used to derive the concentration of the major oxides and trace elements of the samples. Dead time corrections were carried out for all of the analyses. Background corrections on fixed time calculations, were carried out on all but CaO, K₂O, Fe₂O₃ and TiO₂ (because of their high peak/background intensity ratios) and mass absorption corrections were calculated for all the trace elements, using values derived from various Compton scatter peaks. Matrix effects were uniform for the major element analyses since the glass discs contained lanthanum oxide, and since the concentrations of the oxides were relatively diluted. The basic operating conditions for the X-ray Spectrometer and the precision for each of the major oxides and trace elements are given in Table 4.1.

4.2 GEOCHEMICAL RESULTS

Table 4.2 lists the results of the major oxide and trace element analyses of 43 representative lavas found predominantly in the southern half of Carriacou. The locations of the samples and their normative mineralogy is also given in Table 4.2. The rocks are divided into

TABLE 4.1 - Basic operating conditions and precision for the major oxide and trace element analyses on the X-ray spectrometer

Major Oxide or Trace Element	X-ray Tube	Crystal	Counter	*Precision
SiO ₂	Cr	TLAP	FC500	±0.2013
Al ₂ O ₃	Cr	TLAP	FC500	±0.5303
TiO ₂	Cr	LiF200	FC498	±0.4461
Fe ₂ O ₃	Cr	LiF200	FC500	±3.1829
MnO	W	LiF200	FC500	±1.1307
MgO	Cr	ADP	FC515	±1.3183
CaO	Cr	LiF200	FC500	±0.0136
Na ₂ O	Cr	TLAP	FC520	±10.0146
K ₂ O	Cr	TLAP	FC500	±0.2275
P ₂ O ₅	Cr	GERM	FC500	±1.1242
V	W	LiF220	FC480	±1.3211
Cr	W	LiF200	FC500	±3.3459
Co	Cr	LiF220	FC500	±8.1338
Ni	Ag	LiF220	SC230	±4.4046
Rb	Mo	LiF220	SC225	±1.9211
Sr	Mo	LiF220	SC225	±0.6030
Y	Ag	LiF220	SC220	±1.5652
Zr	Ag	LiF220	SC220	±0.8542
Nb	Ag	LiF220	SC216	±2.8678
Ba	Cr	LiF200	FC496	±0.8762

* Precision is given as the % standard deviation of the count rates for a repeated standard.

5 groups, the APA, CMB, OMB, CPA, and AMA respectively (there were no unweathered CPB samples available for geochemical analysis), and ordered within each group from lowest to highest SiO_2 contents. Each analysis is recalculated to 100 % using anhydrous major oxides. Five analyses give rather high L.O.I. (>3.00 wt. %) values (CU-46, CU-3, CU-44, CU-11, and CU-78), which is due to extensive secondary and/or deuteritic alteration effects as seen in thin-section study. Therefore, these rocks were not used in the study and interpretation of the geochemistry of volcanic lavas found on Carriacou. In addition, the major oxides and corresponding normative mineralogies for both a clinopyroxene (taken from CMB volcanoclastics) and amphibole (taken from AMA volcanoclastics) are given in Table 4.3.

4.3 GEOCHEMICAL VARIATION WITHIN THE VOLCANIC SEQUENCES ON THE SOUTHERN HALF OF CARRIACOU

The ranges and averages of the major oxide and trace element geochemistry for the lavas in Table 4.2 are given in Table 4.4.

Together, the CMB and OMB lavas contain the lowest Na_2O , SiO_2 , K_2O , Rb, Ba, Nb, and Zr compositions and

TABLE 4.2 - Geochemistry of volcanic lavas on Carriacou

Sample #:Cu-86	Cu-85	Cu-1E	Cu-83	Cu-82	
Name: Andesite (APA)	Andesite (APA)	Andesite (APA)	Andesite (APA)	Andesite (APA)	
Long.(W): 61°29'.90"	61°30'.00"	61°29'.75"	61°30'.00"	61°29'.90"	
Lat.(N): 12°26'.20"	12°26'.30"	12°27'.00"	12°26'.40"	12°26'.50"	
Major Elements in Dry Weight % (Recalculated to 100 %)					
SiO ₂ :	58.26	59.98	60.34	61.01	62.58
Al ₂ O ₃ :	18.03	17.16	17.59	17.77	17.49
TiO ₂ :	0.61	0.55	0.59	0.52	0.51
*Fe ₂ O ₃ :	7.52	6.85	7.11	6.61	6.62
MnO:	0.15	0.13	0.08	0.15	0.13
MgO:	3.62	2.30	2.53	2.83	1.85
CaO:	7.93	7.34	6.96	5.39	6.20
Na ₂ O:	2.95	4.68	3.59	3.19	3.44
K ₂ O:	0.81	0.88	0.96	0.90	1.05
P ₂ O ₅ :	0.12	0.13	0.13	0.14	0.14
L.O.I.:	1.49	2.23	2.58	1.47	1.58
*FeO/MgO:	1.87	2.87	2.53	2.10	3.21
Trace Elements in ppm					
V:	167	133	175	129	119
Cr:	53	49	98	45	56
Co:	17	13	21	13	6
Ni:	10	2	12	9	1
Rb:	23	28	25	28	30
Sr:	302	312	318	319	309
Y:	34	23	29	42	25
Zr:	33	88	82	85	92
Nb:	4	4	3	4	5
Ba:	230	270	243	270	290
K/Rb:	298	262	298	272	287
Rb/Sr:	0.075	0.090	0.078	0.086	0.098
Y/Nb:	8.74	5.30	10.07	11.74	4.98
+ Normative Mineralogy					
Q:	13.19	9.95	15.33	17.24	19.38
Or:	4.86	5.23	5.18	5.39	6.32
Ab:	28.88	42.23	32.66	29.03	31.37
An:	34.00	23.30	29.74	31.98	29.68
Ne:	0.00	0.00	0.00	0.00	0.00
Di:	4.16	10.01	3.60	1.52	0.63
Wo:	0.00	0.00	0.00	0.00	0.00
Hy:	13.58	6.11	10.29	11.71	9.50
Ol:	0.00	0.00	0.00	0.00	0.00
Mt:	2.24	2.15	2.21	2.14	2.13
Il:	0.87	0.76	0.83	0.74	0.72
Ap:	0.23	0.26	0.26	0.27	0.27

*FeO=Total Iron as FeO

*Fe₂O₃=Total Iron as Fe₂O₃+ For the weight % in the normative calculation,
Fe₂O₃=1.5*TiO₂ and FeO=0.8998(*Fe₂O₃-Fe₂O₃)

TABLE 4.2 (Cont'd)

Sample #:	Cu-18	Cu-75	Cu-53	Cu-100	Cu-43
Name:	Cpx.Mega. Basalt	Cpx.Mega. Basalt	Cpx.Mega. Basalt	Cpx.Mega. Basalt	Cpx.Mega. Basalt
Long.(W):	61°28'50"	61°29'90"	61°28'70"	61°28'20"	61°28'25"
Lat.(N):	12°27'00"	12°26'80"	12°27'90"	12°27'80"	12°27'65"
Major Elements in Dry Weight % (Recalculated to 100 %)					
SiO ₂ :	45.15	46.06	46.20	46.89	47.04
Al ₂ O ₃ :	17.53	15.10	15.86	17.10	17.14
TiO ₂ :	1.00	0.92	0.91	1.00	1.02
*Fe ₂ O ₃ :	13.25	12.43	11.77	11.23	11.24
MnO:	0.21	0.17	0.17	0.17	0.17
MgO:	6.63	9.26	9.57	7.74	8.05
CaO:	13.70	14.55	13.42	13.17	13.24
Na ₂ O:	1.60	0.88	1.68	1.95	1.30
K ₂ O:	0.75	0.51	0.26	0.60	0.64
P ₂ O ₅ :	0.18	0.12	0.15	0.15	0.17
L.O.I.:	1.73	1.09	1.01	1.76	2.03
*FeO/MgO:	1.80	1.21	1.11	1.31	1.26

Trace Elements in ppm

V:	386	353	336	372	370
Cr:	116	452	590	377	351
Co:	36	44	40	36	39
Ni:	22	121	164	29	111
Rb:	14	10	6	13	13
Sr:	836	457	390	437	469
Y:	31	20	25	29	28
Zr:	47	37	42	49	50
Nb:	5	1	4	4	7
Ba:	208	148	154	183	186
K/Rb:	457	419	365	391	417
Rb/Sr:	0.016	0.022	0.015	0.029	0.027
Y/Nb:	6.50	38.68	5.58	7.46	3.89

+ Normative Mineralogy

Q:	0.00	0.00	0.00	0.00	0.00
Or:	4.56	3.10	1.57	3.61	3.86
Ab:	12.11	8.03	15.27	17.68	11.83
An:	39.33	36.45	35.28	36.58	39.69
Ne:	1.57	0.00	0.00	0.00	0.00
Di:	23.32	29.17	24.81	22.90	20.83
Wo:	0.00	0.00	0.00	0.00	0.00
Hy:	0.00	7.67	1.55	0.76	12.72
Ol:	14.65	11.47	17.40	14.13	6.61
Mt:	2.67	2.58	2.54	2.64	2.68
Il:	1.42	1.31	1.28	1.41	1.45
Ap:	0.37	0.24	0.31	0.31	0.33

*FeO=Total Iron as FeO

*Fe₂O₃=Total Iron as Fe₂O₃

+ For the weight % in the normative calculation,

Fe₂O₃=1.5*TiO₂ and FeO=0.8998(*Fe₂O₃-Fe₂O₃)

TABLE 4.2 (Cont'd).

Sample #:	Cu-52	Cu-59	Cu-23	Cu-14	Cu-7B
Name:	Cpx.Mega. Basalt	Cpx.Mega. Basalt	Cpx.Mega. Basalt	Cpx.Mega. Basalt	Cpx.Mega. Basalt
Long. (W):	61°28'60"	61°28'90"	61°30'00"	61°29'20"	61°26'35"
Lat. (N):	12°27'75"	12°28'60"	12°28'10"	12°27'20"	12°31'35"

Major Elements in Dry Weight % (Recalculated to 100 %)					
SiO ₂ :	47.33	47.45	47.46	48.42	48.56
Al ₂ O ₃ :	17.03	17.95	16.73	19.74	18.02
TiO ₂ :	1.02	0.92	0.81	0.86	0.92
*Fe ₂ O ₃ :	10.71	12.30	11.49	11.05	10.97
MnO:	0.17	0.24	0.18	0.18	0.17
MgO:	7.92	5.46	7.78	4.77	5.62
CaO:	13.79	12.76	13.24	11.62	11.33
Na ₂ O:	1.27	2.38	1.70	2.61	3.80
K ₂ O:	0.61	0.43	0.48	0.64	0.49
P ₂ O ₅ :	0.15	0.12	0.13	0.11	0.12
L.O.I.:	2.28	1.56	1.22	1.28	1.27
*FeO/MgO:	1.22	2.02	1.93	2.09	1.76

Trace Elements in ppm					
V:	375	344	323	319	319
Cr:	350	128	244	56	106
Co:	30	35	36	31	38
Ni:	102	27	57	4	18
Rb:	12	7	10	14	8
Sr:	414	383	454	408	333
Y:	26	26	25	28	30
Zr:	49	49	44	47	60
Nb:	6	3	2	2	4
Ba:	180	141	144	154	151
K/Rb:	439	539	418	371	408
Rb/Sr:	0.028	0.017	0.021	0.035	0.024
Y/Nb:	4.19	8.24	13.14	12.51	8.36

+ Normative Mineralogy					
Q:	0.00	0.00	0.00	0.00	0.00
Or:	3.68	2.59	2.90	3.86	2.88
Ab:	11.58	21.77	15.51	23.78	26.43
An:	39.56	37.80	37.14	40.88	30.81
Ne:	0.00	0.00	0.00	0.00	4.72
Di:	23.22	20.83	22.99	13.64	19.95
Wo:	0.00	0.00	0.00	0.00	0.00
Hy:	12.44	2.36	8.07	6.89	0.00
Ol:	5.11	10.53	9.53	7.03	11.16
Mt:	2.67	2.58	2.45	2.50	2.54
Il:	1.44	1.30	1.15	1.21	1.28
Ap:	0.30	0.25	0.26	0.21	0.24

*FeO=Total Iron as FeO

*Fe₂O₃=Total Iron as Fe₂O₃

+ For the weight % in the normative calculation,

Fe₂O₃=1.5+TiO₂ and FeO=0.8998(*Fe₂O₃-Fe₂O₃)

TABLE 4.2 (Cont'd)

Sample #:	Cu-13	Cu-22	Cu-44	Cu-6	Cu-20
Name:	Cpx.Mega. Basalt	Cpx.Mega. Basalt	Cpx.Mega. Basalt	Cpx.Mega. Basalt	Ol.Micro. Basalt
Long. (W):	61° 27' 10"	61° 29' 30"	61° 27' 80"	61° 26' 50"	61° 28' 00"
Lat. (N):	12° 28' 80"	12° 28' 15"	12° 28' 10"	12° 31' 40"	12° 27' 75"
Major Elements in Dry Weight % (Recalculated to 100 %)					
SiO ₂ :	48.61	48.70	50.77	51.56	46.95
Al ₂ O ₃ :	15.34	19.38	15.41	13.18	13.52
TiO ₂ :	0.89	0.93	0.74	0.88	0.78
*Fe ₂ O ₃ :	11.36	11.42	10.48	10.90	12.56
MnO:	0.13	0.19	0.19	0.20	0.18
MgO:	9.94	4.67	2.35	4.61	12.16
CaO:	11.20	11.17	9.99	10.15	12.00
Na ₂ O:	1.75	2.78	1.97	2.76	1.26
K ₂ O:	0.61	0.58	0.90	0.55	0.48
P ₂ O ₅ :	0.12	0.19	0.19	0.21	0.12
L.O.I.:	0.95	1.74	4.85	0.38	0.97
*FeO/MgO:	1.03	2.20	1.01	2.13	0.93
Trace Elements in ppm					
V:	289	309	198	250	271
Cr:	862	59	837	72	1750
Co:	48	30	40	30	53
Ni:	258	7	216	7	416
Rb:	15	7	44	3	9
Sr:	283	513	448	396	419
Y:	25	31	22	36	21
Zr:	53	61	90	84	44
Nb:	3	3	8	4	3
Ba:	162	135	256	175	161
K/Rb:	329	683	172	563	452
Rb/Sr:	0.059	0.014	0.097	0.020	0.021
Y/Nb:	7.58	10.69	2.70	9.67	7.96
+ Normative Mineralogy					
Q:	0.00	0.00	0.00	3.03	0.00
Or:	3.64	3.46	5.35	3.31	2.85
Ab:	15.80	25.34	17.81	25.27	11.38
An:	32.47	39.37	30.74	36.24	30.03
Ne:	0.00	0.00	0.00	0.00	0.00
Di:	18.27	12.69	14.39	11.02	23.41
Wo:	0.00	0.00	0.00	0.00	0.00
Hy:	17.84	9.18	27.69	16.92	12.04
Ol:	7.99	5.69	0.26	0.00	16.56
Mt:	2.52	2.58	2.36	2.54	2.40
Il:	1.25	1.32	1.04	1.25	1.10
Ap:	0.24	0.37	0.38	0.42	0.23

*FeO=Total Iron as FeO

*Fe₂O₃=Total Iron as Fe₂O₃

+ For the weight % in the normative calculation.

Fe₂O₃=1.5+TiO₂ and FeO=0.8998(*Fe₂O₃-Fe₂O₃)

TABLE 4.2 (Cont'd)

Sample #:	Cu-19	Cu-28	Cu-111	Cu-93	Cu-30
Name:	Ol.Micro. Basalt	Ol.Micro. Basalt	Ol.Micro. Basalt	Ol.Micro. Basalt	Ol.Micro. Basalt
Long. (W):	61°28.25"	61°28.10"	61°26.50"	61°28.45"	61°28.65"
Lat. (N):	12°27.00"	12°27.85"	12°29.85"	12°26.75"	12°26.80"
Major Elements in Dry Weight % (Recalculated to 100 %)					
SiO ₂ :	47.08	47.08	47.10	47.25	47.36
Al ₂ O ₃ :	13.66	13.49	14.10	13.61	13.59
TiO ₂ :	0.77	0.79	0.91	0.78	0.77
*Fe ₂ O ₃ :	12.59	12.34	11.88	12.57	12.48
MnO:	0.19	0.18	0.17	0.18	0.19
MgO:	11.85	12.18	11.03	11.87	11.94
CaO:	11.92	12.00	12.85	11.93	11.98
Na ₂ O:	1.30	1.34	1.37	1.17	1.16
K ₂ O:	0.51	0.51	0.50	0.52	0.49
P ₂ O ₅ :	0.13	0.11	0.10	0.12	0.14
L.O.I.:	0.35	0.34	1.31	0.61	0.46
*FeO/MgO:	0.96	0.91	0.97	0.95	0.95
Trace Elements in ppm					
V:	260	266	297	254	266
Cr:	1613	1794	958	1657	1712
Co:	64	59	50	63	59
Ni:	382	430	271	393	395
Rb:	10	11	8	10	10
Sr:	440	464	353	412	440
Y:	25	21	18	23	23
Zr:	49	43	48	46	49
Nb:	3	4	4	4	2
Ba:	174	183	160	185	214
K/Rb:	440	377	507	429	394
Rb/Sr:	0.022	0.024	0.023	0.024	0.023
Y/Nb:	7.91	5.48	4.26	6.26	10.38
+ Normative Mineralogy					
Q:	0.00	0.00	0.00	0.00	0.00
Or:	3.06	3.02	2.99	3.08	2.91
Ab:	11.76	12.07	12.37	10.56	10.54
An:	30.16	29.47	31.12	30.67	30.71
Ne:	0.00	0.00	0.00	0.00	0.00
Di:	22.98	23.79	26.10	22.66	22.77
Wo:	0.00	0.00	0.00	0.00	0.00
Hy:	12.41	10.92	8.90	15.71	16.54
Ol:	15.92	17.00	14.50	13.58	12.78
Mt:	2.39	2.41	2.55	2.40	2.40
Il:	1.08	1.11	1.29	1.10	1.09
Ap:	0.25	0.22	0.19	0.25	0.27

*FeO=Total Iron as FeO

*Fe₂O₃=Total Iron as Fe₂O₃

+ For the weight % in the normative calculation,

Fe₂O₃=1.5+TiO₂ and FeO=0.8298(*Fe₂O₃-Fe₂O₃)

TABLE 4.2 (Cont'd)

Sample #:	Cu-88	Cu-25	Cu-11	Cu-10B	Cu-10E
Name:	Ol.Micro. Basalt	Ol.Micro. Basalt	Ol.Micro. Basalt	Ol.Micro. Basalt	Ol.Micro. Basalt
Long. (W):	61°28'60"	61°27'00"	61°26'85"	61°28'80"	61°27'00"
Lat. (N):	12°26'75"	12°28'25"	12°29'45"	12°29'35"	12°28'90"

Major Elements in Dry Weight % (Recalculated to 100 %)					
SiO ₂ :	47.69	47.80	48.31	48.47	49.46
Al ₂ O ₃ :	13.55	13.36	14.13	14.03	14.96
TiO ₂ :	0.82	0.86	0.78	0.79	0.82
*Fe ₂ O ₃ :	12.42	11.59	11.99	11.74	11.05
MnO:	0.18	0.17	0.17	0.17	0.16
MgO:	11.96	11.92	12.64	12.69	10.20
CaO:	11.85	12.20	10.27	10.44	10.76
Na ₂ O:	1.13	1.37	1.17	1.12	1.58
K ₂ O:	0.32	0.60	0.45	0.45	0.84
P ₂ O ₅ :	0.08	0.13	0.08	0.08	0.17
L.O.I.:	1.39	1.84	4.1	2.88	2.59
*FeO/MgO:	0.93	0.87	0.8	0.83	0.97

Trace Elements in ppm					
V:	257	273	257	246	241
Cr:	1192	1292	1269	1304	918
Co:	65	62	57	55	48
Ni:	371	417	468	472	252
Rb:	5	14	10	10	24
Sr:	567	409	214	219	480
Y:	22	19	21	18	24
Zr:	35	52	43	42	74
Nb:	2	4	2	3	5
Ba:	109	157	115	112	237
K/Rb:	582	365	395	379	293
Rb/Sr:	0.008	0.033	0.045	0.046	0.049
Y/Nb:	13.78	5.20	13.49	6.93	4.77
+ Normative Mineralogy					
Q:	0.00	0.00	0.00	0.00	0.00
Or:	1.92	3.55	2.67	2.68	4.98
Ab:	10.23	12.35	10.55	10.11	14.31
An:	31.25	28.70	32.14	32.06	31.48
Ne:	0.00	0.00	0.00	0.00	0.00
Di:	22.10	25.11	14.90	15.61	17.07
Wo:	0.00	0.00	0.00	0.00	0.00
Hy:	20.97	12.83	28.07	28.92	24.18
Ol:	9.78	13.53	8.03	6.95	4.05
Mt:	2.45	2.48	2.40	2.40	2.44
Il:	1.15	1.21	1.10	1.10	1.15
Ap:	0.16	0.25	0.15	0.15	0.33

*FeO=Total Iron as FeO

*Fe₂O₃=Total Iron as Fe₂O₃

+ For the weight % in the normative calculation,

Fe₂O₃=1.5+TiO₂ and FeO=0.8998(*Fe₂O₃-Fe₂O₃)

TABLE 4.2 (Cont'd)

Sample #:	Cu-1	Cu-73	Cu-27	Cu-98	Cu-68
Name:	Basalt (CPA)	Andesite (CPA)	Andesite (CPA)	Andesite (CPA)	Andesite (CPA)
Long. (W):	61°27'.10"	61°29'.70"	61°28'.10"	61°28'.00"	61°30'.00"
Lat. (N):	12°29'.40"	12°27'.05"	12°27'.90"	12°27'.90"	12°28'.50"
Major Elements in Dry Weight % (Recalculated to 100 %)					
SiO ₂ :	52.67	53.19	53.31	54.88	55.42
Al ₂ O ₃ :	18.14	19.42	17.76	18.70	20.36
TiO ₂ :	0.89	0.79	0.77	0.83	1.01
*Fe ₂ O ₃ :	9.72	9.27	9.52	8.88	8.80
MnO:	0.22	0.23	0.21	0.19	0.05
MgO:	3.70	2.42	3.54	3.57	0.94
CaO:	9.26	10.54	9.43	9.26	8.19
Na ₂ O:	4.59	3.11	4.75	3.04	4.23
K ₂ O:	0.59	0.77	0.53	0.47	0.93
P ₂ O ₅ :	0.22	0.26	0.17	0.18	0.28
L.O.I.:	2.25	2.96	2.44	0.54	1.55
*FeO/MgO:	2.37	3.45	2.42	2.24	9.37
Trace Elements in ppm					
V:	226	221	174	194	268
Cr:	59	63	69	70	45
Co:	25	17	23	19	11
Ni:	11	0	9	8	4
Pb:	21	17	11	17	15
Sr:	402	499	303	319	510
Y:	32	34	30	28	24
Zr:	93	79	79	76	104
Nb:	5	4	3	3	6
Ba:	135	222	157	157	254
K/Rb:	235	384	387	229	455
Rb/Sr:	0.051	0.033	0.038	0.053	0.030
Y/Nb:	6.65	9.19	9.40	11.04	3.65
+ Normative Mineralogy					
Q:	0.00	5.35	0.00	8.50	7.07
Or:	3.48	4.63	3.15	2.24	4.96
Ab:	41.37	28.45	42.83	27.71	38.54
An:	27.31	37.46	25.66	36.58	34.66
Ne:	0.00	0.00	0.00	0.00	0.00
Di:	14.04	11.40	16.23	7.21	3.97
Wo:	0.00	0.00	0.00	0.00	0.00
Hy:	5.65	8.65	4.84	13.16	6.18
Ol:	3.97	0.00	3.49	0.00	0.00
Mt:	2.51	2.44	2.38	2.49	2.66
Il:	1.25	1.12	1.08	1.13	1.42
Ap:	0.42	0.52	0.34	0.36	0.55

*FeO=Total Iron as FeO

*Fe₂O₃=Total Iron as Fe₂O₃

+ For the weight % in the normative calculation,

Fe₂O₃=1.5+TiO₂ and FeO=0.8998(*Fe₂O₃-Fe₂O₃)

TABLE 4.2 (Cont'd)

Sample #:	Cu-46	Cu-3A	Cu-3	Cu-87	Cu-78
Name:	Andesite (CPA)	Andesite (CPA)	Dacite (CPA)	Basalt (AMA)	Basalt (AMA)
Long. (W):	61°28'.40"	61°26'.75"	61°29'.75"	61°29'.65"	61°29'.95"
Lat. (N):	12°27'.70"	12°29'.35"	12°27'.35"	12°26'.70"	12°26'.80"
Major Elements in Dry Weight % (Recalculated to 100 %)					
SiO ₂ :	57.68	57.75	66.91	48.12	49.51
Al ₂ O ₃ :	17.51	19.50	15.02	18.43	17.97
TiO ₂ :	0.68	0.53	0.58	0.89	0.86
*Fe ₂ O ₃ :	8.43	7.06	4.89	11.95	11.45
MnO:	0.23	0.19	0.12	0.24	0.21
MgO:	2.31	1.96	1.18	4.39	6.77
CaO:	8.72	8.52	6.17	12.77	19.11
Na ₂ O:	3.59	3.38	3.35	2.44	2.23
K ₂ O:	0.65	0.80	0.76	0.59	0.69
P ₂ O ₅ :	0.21	0.29	0.12	0.18	0.21
L.O.I.:	3.79	1.92	3.11	2.19	3.11
*FeO/MgO:	3.29	3.24	3.72	2.45	1.52
Trace Elements in ppm					
V:	139	79	119	275	273
Cr:	60	23	61	96	111
Co:	10	10	8	27	30
Ni:	4	3	1	13	26
Pb:	14	19	11	12	12
Sr:	403	549	200	519	359
Y:	37	40	34	29	27
Zr:	121	103	93	58	74
Nb:	5	6	1	3	3
Ba:	204	225	165	186	178
K/Rb:	402	342	589	420	459
Rb/Sr:	0.034	0.035	0.051	0.023	0.035
Y/Nb:	6.80	6.76	45.60	10.07	8.58
+ Normative Mineralogy					
Q:	11.10	12.08	28.02	0.00	0.00
Or:	3.33	4.79	4.58	3.58	4.11
Ab:	32.84	30.75	30.67	22.41	20.27
An:	30.22	36.20	26.70	38.44	37.57
Ne:	0.00	0.00	0.00	0.00	0.00
Di:	10.02	3.97	3.06	20.24	9.68
Wo:	0.00	0.00	0.00	0.00	0.00
Hy:	3.20	8.75	3.69	4.64	23.69
Ol:	0.00	0.00	0.00	6.51	0.55
Mt:	2.31	2.15	2.22	2.55	2.50
Il:	0.89	0.75	0.82	1.27	1.22
Ap:	0.42	0.56	0.23	0.36	0.41

*FeO=Total Iron as FeO

*Fe₂O₃=Total Iron as Fe₂O₃

+ For the weight % in the normative calculation,

Fe₂O₃=1.5+TiO₂ and FeO=0.8998(*Fe₂O₃-Fe₂O₃)

TABLE 4.2 (Cont'd)

Sample #:	Cu-33	Cu-21	Cu-12B
Name:	Andesite (AMA)	Andesite (AMA)	Andesite (AMA)
Long. (W):	61°28'.45"	61°27'.75"	61°27'.75"
Lat. (N):	12°26'.75"	12°27'.90"	12°27'.90"

Major Elements in Dry Weight % (Recalculated to 100 %)			
SiO ₂ :	59.58	60.89	61.40
Al ₂ O ₃ :	19.76	18.16	18.65
TiO ₂ :	0.57	0.43	0.45
*Fe ₂ O ₃ :	5.93	5.62	5.85
MnO:	0.11	0.27	0.19
MgO:	1.45	1.33	1.08
CaO:	7.78	7.97	7.21
Na ₂ O:	3.63	4.20	4.02
K ₂ O:	0.95	0.96	0.95
P ₂ O ₅ :	0.24	0.19	0.20
L.O.I.:	1.12	1.55	0.61
*FeO/MgO:	3.67	3.81	4.86
Trade Elements in ppm			
V:	121	63	74
Cr:	44	51	49
Co:	8	3	3
Ni:	3	1	1
Rb:	23	29	30
Sr:	567	614	625
Y:	41	41	38
Zr:	119	131	136
Nb:	8	5	6
Ba:	243	288	278
K/Rb:	348	277	265
Rb/Sr:	0.040	0.047	0.048
Y/Nb:	4.91	7.74	6.27
+ Normative Mineralogy			
Q:	14.35	13.61	15.71
Or:	5.68	5.70	5.69
Ab:	32.95	38.00	36.50
An:	35.21	28.10	30.35
Ne:	0.00	3.00	0.00
Di:	1.90	3.51	3.72
Wo:	0.00	0.00	0.00
Hy:	6.45	3.07	4.96
Ol:	0.00	0.00	0.00
Nt:	2.17	2.04	2.06
Il:	0.80	0.61	0.63
Ap:	0.46	0.37	0.39

*FeO=Total Iron as FeO

*Fe₂O₃=Total Iron as Fe₂O₃+ For the weight % in the normative calculation,
Fe₂O₃=1.5+TiO₂ and FeO=0.8998(*Fe₂O₃-Fe₂O₃)

TABLE 4.3 - Geochemistry of an amphibole (taken from AMA volcanoclastics) and a clinopyroxene (taken from CMB volcanoclastics)

+Mineral:	Amphibole	Clinopyroxene
	-----	-----
Major-Elements in Weight %		
SiO ₂ :	43.31	50.13
Al ₂ O ₃ :	16.09	7.32
TiO ₂ :	1.59	0.76
*Fe ₂ O ₃ :	12.55	8.02
MnO:	0.12	0.12
MgO:	9.71	10.49
CaO:	10.95	21.29
Na ₂ O:	2.11	0.25
K ₂ O:	0.49	0.09
P ₂ O ₅ :	0.05	0.00
L.O.I.:	1.95	1.11
TOTAL:	98.92	99.58
* Normative Mineralogy		
Q:	0.00	2.72
Or:	2.99	0.56
Ab:	15.92	2.34
An:	34.28	19.18
Ne:	2.25	0.00
Di:	17.46	71.36
Wo:	0.00	0.29
Hy:	0.00	0.00
Ol:	21.36	0.00
Mt:	3.35	2.45
Il:	2.29	1.10
Ap:	0.10	0.00

+ The amphibole is classified as tschermakitic hornblende (using the classification of amphiboles by Leake, 1978) while the clinopyroxene plots as having a salite composition (using the system Mg-Ca-Fe+Mn by Poldervaart and Hess, 1951)

*Fe₂O₃=Total Iron as Fe₂O₃

* For the weight % in the normative calculation,

Fe₂O₃=1.5+TiO₂ and FeO=0.8998(*Fe₂O₃-Fe₂O₃)

highest K/Rb and Fe_2O_3 compositions of all the lavas found on the southern half of the island. In addition, the CMB lavas contain the highest TiO_2 , CaO and V compositions while the OMB lavas contain the highest MgO, Co, Ni, Cr compositions and the lowest P_2O_5 , Al_2O_3 and Y compositions.

In contrast, the andesitic lava sequences (APA, CPA and AMA sequences) show the lowest TiO_2 , Fe_2O_3 , CaO, Co, V, Cr, K/Rb and Ni compositions and highest SiO_2 , Al_2O_3 , Na_2O , K_2O , Zr, Ba, Rb and Nb compositions of all the lava sequences found on the southern half of the island. In addition, except for a few outlying compositions, the AMA and CPA lavas contain the highest MnO, P_2O_5 , Sr and Y compositions while the APA lavas contain the lowest MnO concentrations and highest Rb/Sr ratios (0.075 - 0.098).

Finally, relative to the AMA and CPA lava sequences, the APA lavas contain lower MnO, Al_2O_3 , CaO, P_2O_5 , Y and Sr compositions, and higher SiO_2 and MgO compositions.

TABLE 4.4 - THE RANGES, AVERAGES AND STANDARD DEVIATIONS OF THE MAJOR OXIDE AND TRACE ELEMENT GEOCHEMISTRY FOR THE LAVAS ON THE SOUTHERN HALF OF CARRIACOU

SEQUENCE: AMPHIBOLE-PHYRIC ANDESITE LAVAS

	RANGE	AVERAGE	ST. DEV.
MAJOR OXIDES			
IN WT. %			
SiO ₂ :	58.26-62.58	60.47	1.57
Al ₂ O ₃ :	17.16-18.03	17.61	0.32
TiO ₂ :	0.51-0.61	0.56	0.04
*Fe ₂ O ₃ :	6.61-7.55	6.94	0.38
MnO:	0.08-0.15	0.13	0.03
MgO:	1.85-3.62	2.63	0.66
CaO:	6.20-7.93	7.06	0.64
Na ₂ O:	2.95-4.68	3.57	0.67
K ₂ O:	0.81-1.05	0.90	0.09
P ₂ O ₅ :	0.12-0.14	0.13	0.01
*FeO/MgO:	1.87-3.21	2.48	0.52
TRACE ELEMENTS			
IN PPM			
V:	119-175	145	24.80
Cr:	45-98	60	21.53
Co:	6-21	14	5.57
Ni:	1-12	7	4.97
Rb:	23-30	27	2.77
Sr:	302-319	312	6.96
Y:	23-42	31	7.64
Zr:	82-92	86	4.06
Nb:	3-5	4	0.71
Ba:	230-290	261	23.91
K/Rb:	262-298	281	14.28
Rb/Sr:	0.075-0.098	0.085	0.01
Y/Nb:	4.98-11.74	8.37	2.75

*Fe₂O₃ = Total iron as Fe₂O₃.

*FeO = Total iron as FeO.

TABLE 4.4 - (Cont'd)

SEQUENCE* CLINOPYROXENE-MEGAPHYRIC BASALT LAVAS

	RANGE	AVERAGE	ST. DEV.
MAJOR OXIDES			
IN WT. %			
SiO ₂ :	45.15-51.56	47.87	1.75
Al ₂ O ₃ :	15.10-19.74	17.10	1.46
TiO ₂ :	0.81-1.02	0.93	0.06
*Fe ₂ O ₃ :	10.71-13.25	11.47	0.75
MnO:	0.17-0.24	0.19	0.02
MgO:	4.61-9.94	7.24	1.94
CaO:	10.15-13.79	12.38	1.44
Na ₂ O:	0.88-3.80	2.03	0.77
K ₂ O:	0.26-0.75	0.55	0.21
P ₂ O ₅ :	0.11-0.21	0.15	0.03
*FeO/MgO:	1.03-2.20	1.53	0.44
TRACE ELEMENTS			
IN PPM			
V:	250-386	334	38.62
Cr:	56-862	329	275
Co:	30-48	37	5.42
Ni:	4-258	87	81.85
Rb:	6-15	11	3.13
Sr:	263-836	443	128.78
Y:	25-36	28	3.18
Zr:	37-84	52	11.69
Nb:	1-7	4	1.65
Ba:	141-208	167	20.49
K/Rb:	329-683	453	96.61
Rb/Sr:	0.014-0.097	0.025	0.012
Y/Nb:	3.89-38.68	10.50	8.93

*Fe₂O₃ = Total iron as Fe₂O₃.
 *FeO = Total iron as FeO.

TABLE 4.4 - (Cont'd)

SEQUENCE: OLIVINE-MICROPHYRIC BASALT LAVAS

	RANGE	AVERAGE	ST. DEV.
MAJOR OXIDES			
IN WT. %			
SiO ₂ :	46.95-49.46	47.69	0.78
Al ₂ O ₃ :	13.49-14.96	13.82	0.46
TiO ₂ :	0.77-0.91	0.81	0.04
*Fe ₂ O ₃ :	11.05-12.59	12.11	0.50
MnO:	0.16-0.19	0.18	0.01
MgO:	10.20-12.69	11.85	0.70
CaO:	10.44-12.85	11.79	0.69
Na ₂ O:	1.12-1.58	1.27	0.14
K ₂ O:	0.32-0.84	0.52	0.13
P ₂ O ₅ :	0.08-0.17	0.11	0.03
*FeO/MgO:	0.83-0.97	0.92	0.05
TRACE ELEMENTS			
IN PPM			
V:	241-297	262	15.06
Cr:	918-1794	1405	315
Co:	48-65	53	18.36
Ni:	252-472	388	70.31
Rb:	5-24	11	4.82
Sr:	218-567	420	90.32
Y:	18-25	20	6.58
Zr:	35-74	48	9.84
Nb:	2-5	3	1.01
Ba:	109-214	164	41.15
K/Rb:	293-582	418	77.38
Rb/Sr:	0.008-0.049	0.027	0.01
Y/Nb:	4.26-13.78	7.85	3.34

*Fe₂O₃ = Total iron as Fe₂O₃.

*FeO = Total iron as FeO.

TABLE 4.4 - (Cont'n)

SEQUENCE: CLINOPYROXENE-PHYRIC ANDESITES

	RANGE	AVERAGE	ST. DEV.
MAJOR OXIDES			
IN WT. %			
SiO ₂ :	52.67-57.58	54.54	1.90
Al ₂ O ₃ :	18.14-20.36	18.98	0.96
TiO ₂ :	0.53-1.01	0.80	0.16
*Fe ₂ O ₃ *	7.06-9.72	8.88	0.96
MnO:	0.05-0.23	0.18	0.07
MgO:	0.84-3.70	2.67	1.14
CaO:	8.19-10.54	9.20	0.82
Na ₂ O:	3.04-4.75	3.85	0.77
K ₂ O:	0.47-0.83	0.67	0.15
P ₂ O ₅ :	0.17-0.29	0.23	0.05
*FeO/MgO:	2.24-9.37	3.85	2.75
TRACE ELEMENTS			
IN PPM			
V:	79-268	194	64.58
Cr:	23-70	55	18.03
Co:	11-25	18	6.12
Ni:	0-11	6	4.17
Rb:	11-21	17	3.44
Sr:	303-549	430	104
Y:	24-40	31	5.47
Zr:	76-104	89	12.70
Nb:	3-6	5	1.38
Ba:	157-254	200	39.87
K/Rb:	229-455	339	90.23
Rb/Sr:	0.030-0.053	0.040	0.01
Y/Nb:-	3.65-11.04	7.78	2.63

*Fe₂O₃ = Total iron as Fe₂O₃.

*FeO = Total iron as FeO.

TABLE 4.4 - (Cont'n)

SEQUENCE: AMPHIBOLE-MEGAPHYRIC ANDESITE LAVAS

	RANGE	AVERAGE	ST. DEV.
MAJOR OXIDES			
IN WT. %			
SiO ₂ :	48.12-61.40	57.50	6.30
Al ₂ O ₃ :	18.16-19.76	18.75	0.70
TiO ₂ :	0.43-0.89	0.59	0.21
*Fe ₂ O ₃ :	5.62-11.95	7.34	3.08
MnO:	0.11-0.27	0.20	0.07
MgO:	1.08-4.39	2.06	1.56
CaO:	7.21-12.77	8.93	2.58
Na ₂ O:	2.44-4.20	3.57	0.79
K ₂ O:	0.59-0.96	0.86	0.18
P ₂ O ₅ :	0.18-0.24	0.20	0.03
*FeO/MgO:	2.45-4.86	3.70	0.99
TRACE ELEMENTS			
IN PPM			
V:	63-275	133	97.79
Cr:	44-96	60	24.18
Co:	3-27	10	11.41
Ni:	1-13	5	5.74
Rb:	12-30	24	8.26
Sr:	519-625	581	48.53
Y:	29-41	37	5.69
Zr:	58-136	111	36.05
Nb:	3-8	6	2.08
Ba:	186-288	249	46.07
K/Rb:	277-420	328	71.72
Rb/Sr:	0.023-0.048	0.040	0.012
Y/Nb:	4.91-10.07	7.25	2.21

*Fe₂O₃ = Total iron as Fe₂O₃.

*FeO = Total iron as FeO.

4.4 THE GEOCHEMISTRY OF THE LAVAS ON THE SOUTHERN HALF OF CARRIACOU IN COMPARISON TO THOSE FOUND THROUGHOUT THE LESSER ANTILLES VOLCANIC-ARC

The geochemistry of the Lesser Antilles volcanic lavas is discussed and summarized by Brown *et al.* (1977) and Smith *et al.* (1980). The chemical variations of the lavas on the southern half of Carriacou were plotted against SiO_2 (Figure 4.1) and compared to this data. The major elements of the basalts and andesites are similar to the rest of the arc with respect to their high Al_2O_3 (16 to 20 wt. %), and low K_2O (less than 1 wt. %), total alkalis (less than 6 wt. %; shown in Figure 4.2a), and TiO_2 (less than 1 wt. %). However, the high MgO (11 to 13 wt. %) and low Al_2O_3 (13 to 16 wt. %) of the OMB lavas are characteristic of only a few of the basalts found on Grenada.

The trace element geochemistry of the basalts and andesites (Figure 4.1b) is similar to the rest of the arc with respect to their Zr contents, which lie between 30 and 140 ppm and increase with SiO_2 , and Sr contents, which stay fairly low and constant (200 to 600 ppm). Additionally, Ba compositions (100 to 300 ppm) and K/Rb ratios (200 to 600 ppm) are fairly low.

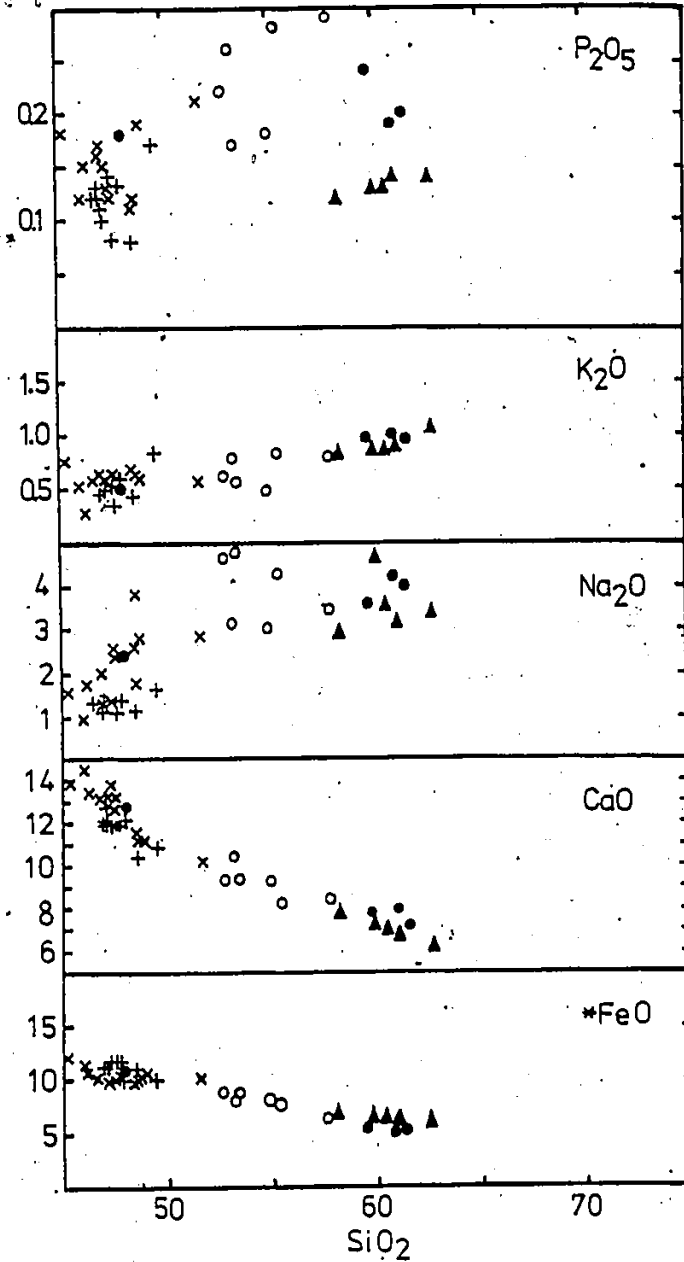


Fig. 4.1a Major oxide (wt. %) vs. SiO₂ (wt. %) for the lavas on Carriacou
 (*FeO = Total iron as FeO; ▲ = APA, x = CMB, + = OMB, ○ = CPA, ● = AMA)

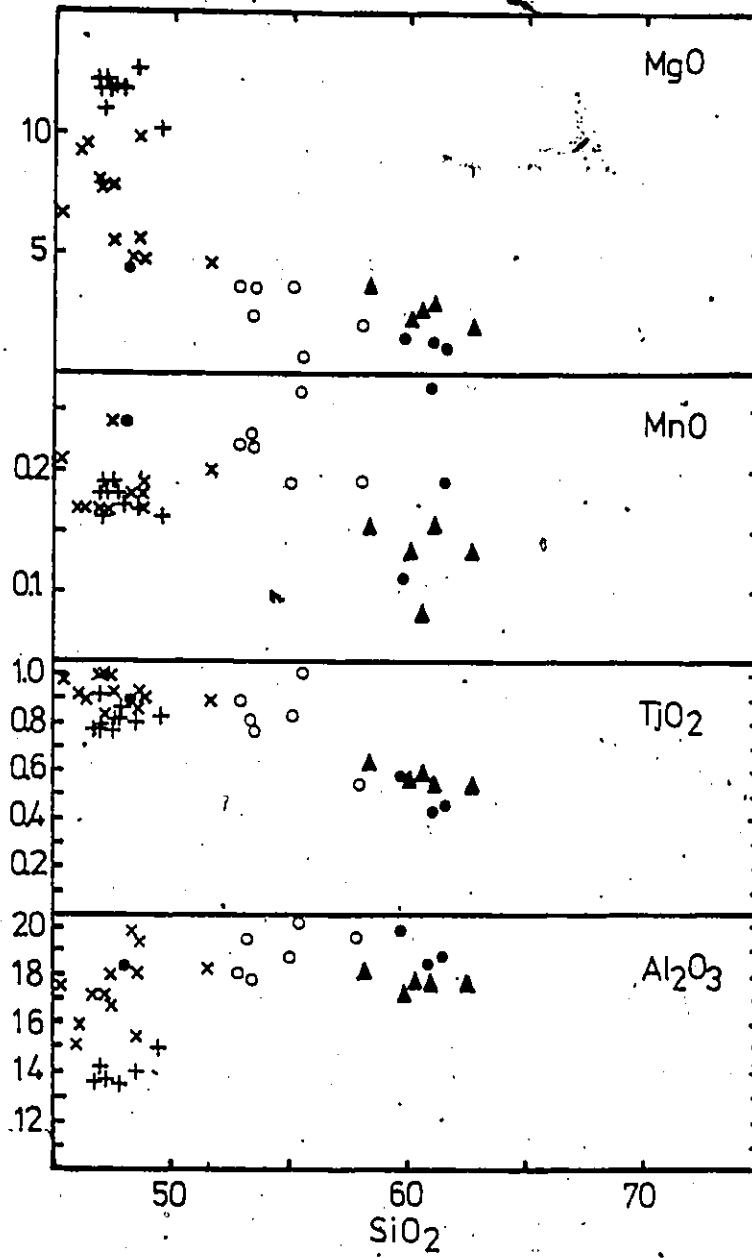


Fig. 4.1a (Cont'd)

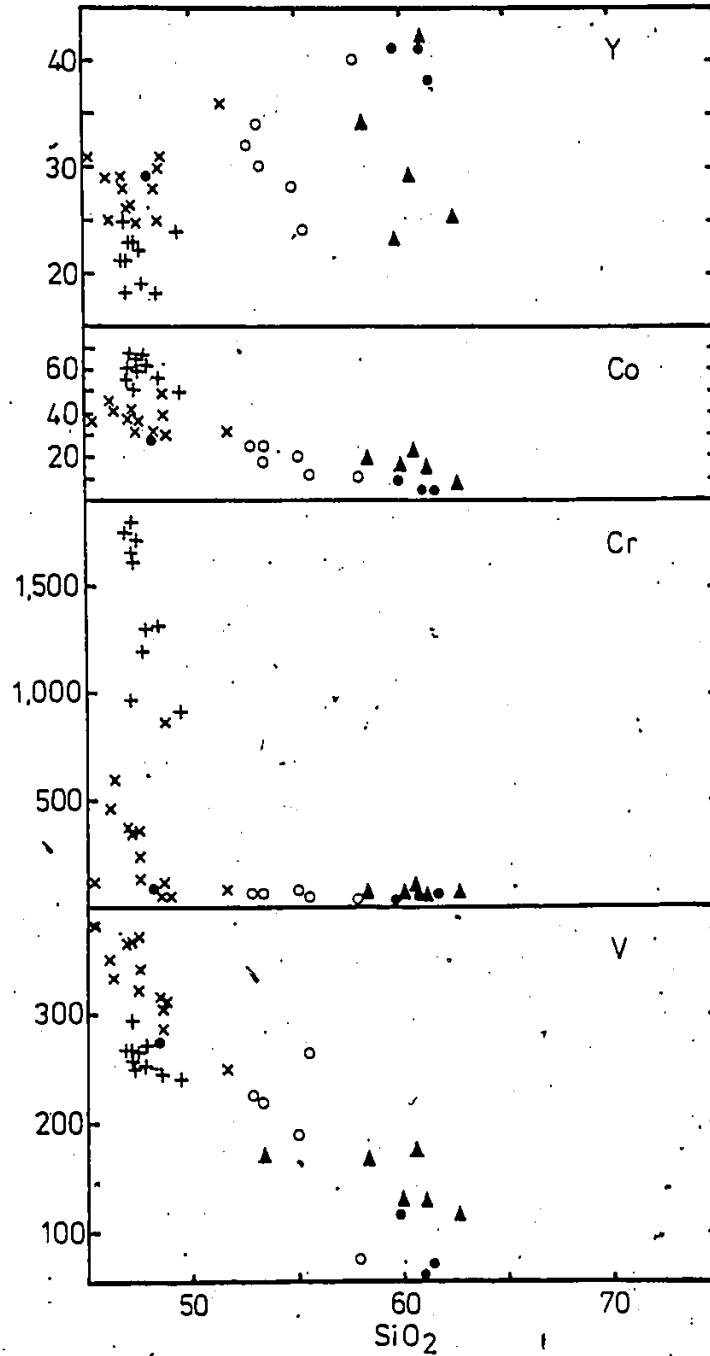


Fig. 4.1b Trace elements (ppm) vs. SiO₂ (wt. %) for the lavas on Carriacou (▲=APA, ×=CMB, +=OMB, ○=CPA, ●=AMA)

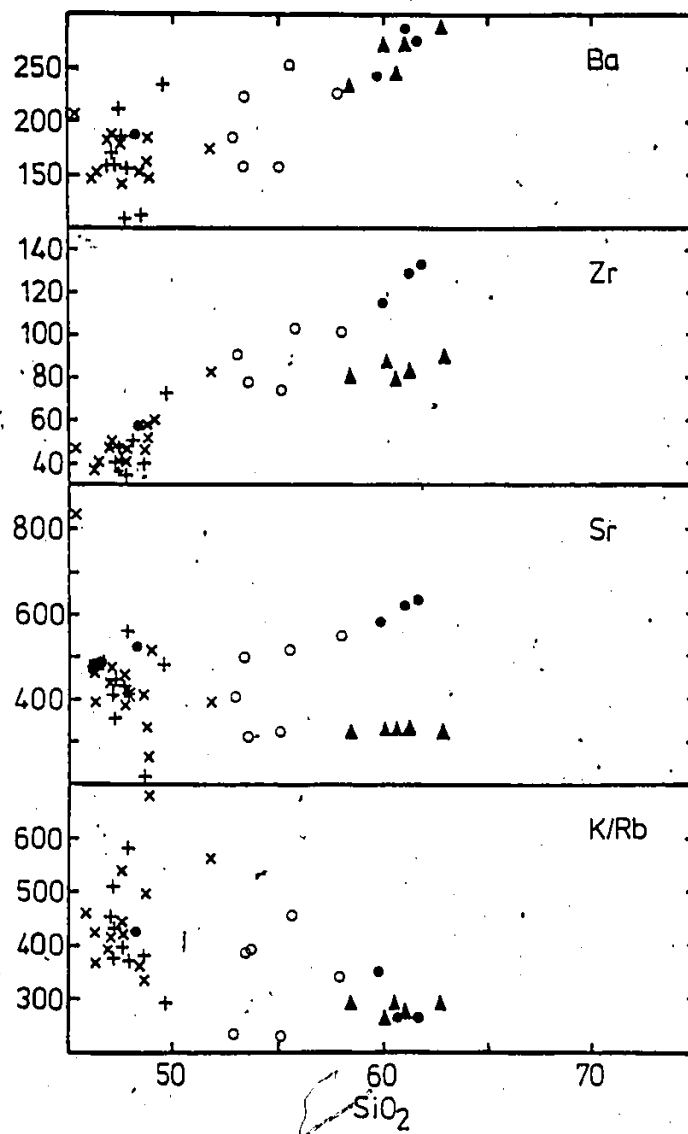


Fig. 4.1b. (Cont'd)

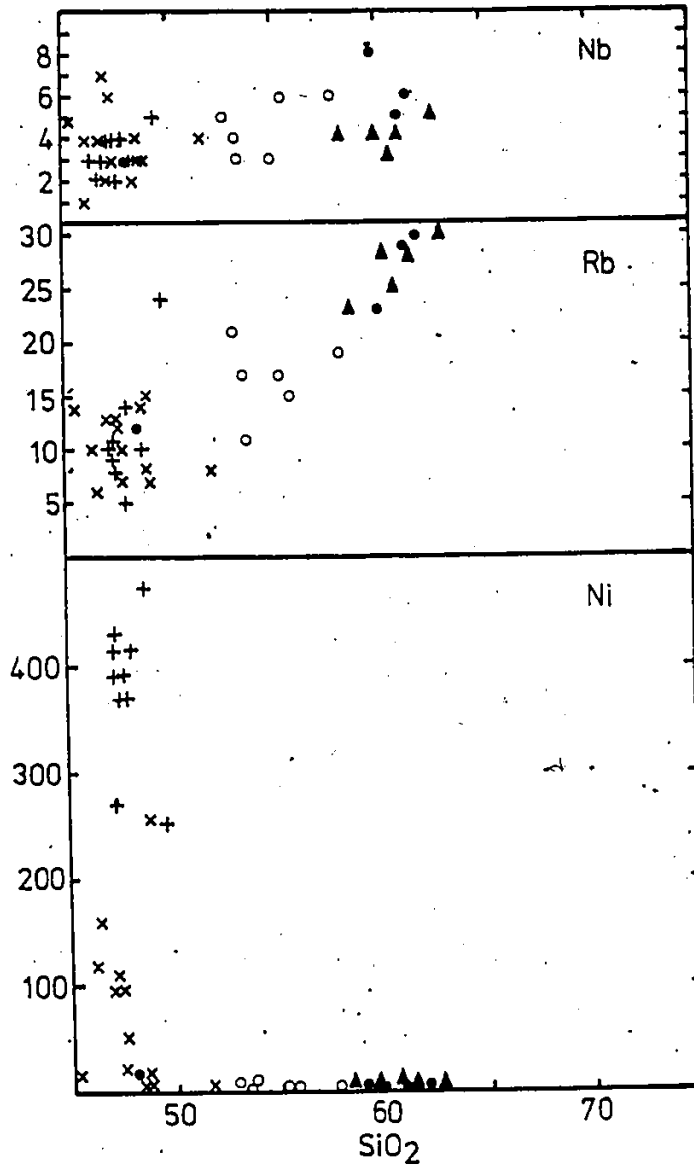


Fig. 4.1b (Cont'd)

However, high Cr and Ni contents in the basalts (up to 1794 ppm and 472 ppm respectively in the OMB lavas), which rapidly drops to very low values in the andesitic sequences, is characteristic of only those lavas found in the southern islands (especially Grenada).

Although, it should be noted that the K, Rb, Ba and Sr compositions of all the lavas found in Carriacou, are much lower than those found in Grenada, the latter of which contains alkali basalts and is often used as a type example for the southern islands (the geochemical ranges for K_2O , Rb, Ba and Sr for lavas found in Grenada are 0.5-2.5 wt. %, 15-100 ppm, 50-900 ppm, 400-1600 ppm respectively; Arculus, 1976).

The trace element geochemistry of the lavas found on the southern half of Carriacou also differs from the geochemistry of the rest of the arc with respect to higher Y contents in the andesites (30 to 40 ppm) and the higher V contents in the basalts (250 to 400 ppm). Additionally, the APA lavas all contain high Rb/Sr ratios (0.075 and 0.098), and the Cr contents in the OMB lavas (1000 to 1800 ppm) are even higher than those concentrations found in the basaltic lavas on Grenada, and therefore represent the highest in the Lesser Antilles (the highest Y, V, Rb/Sr, and Cr contents for the rest of the arc generally lie in the range of 30

ppm, 300 ppm, 0.080, and 850 ppm respectively; Smith et al., 1980, Brown et al., 1977).

4.5 REE COMPOSITIONS AND INITIAL Sr ISOTOPE RATIOS FOR THE LAVAS ON THE SOUTHERN HALF OF CARRIACOU

REE data (Table 4.5) were determined by T.A. Vogel (1981; pers. comm.) on 4 lava samples, supplied by Jackson (1970, 1980), by the N.A.A. method. Chondrite normalised values are relatively HREE depleted compared to the LREE values.

Initial Sr isotopes (Table 4.5) were determined on five volcanic samples (Hedge and Lewis, 1971) which were supplied by Jackson (1970, 1980). The major oxide and trace element data for these lavas are also given in Table 4.5 (Jackson, 1970, 1980). The initial Sr isotope ratios for Carriacou lie in the range of 0.7051 to 0.7054.

4.6 CLASSIFICATION OF THE VOLCANIC LAVAS IN THE SOUTHERN HALF OF CARRIACOU

The classification of the lavas on Carriacou was carried out in order to define the magma series to which they belong. Because of chemical variations along

TABLE 4.5 - The geochemistry of volcanic lavas found on Carriacou (after Jackson, 1970, 1980)

Sample #:	WCA097	WCA252	WCA144	WCA117
Name:	Ol.Micro. Basalt	Ol.Micro. Basalt	Ol.Micro. Basalt	Ol.Micro. Basalt
Long.(W):	61°29'.0"	61°28'.3"	61°28'.3"	61°29'.9"
Lat.(N):	12°28'.2"	12°25'.9"	12°27'.8"	12°26'.8"

Major Elements in Weight %

SiO ₂ :	45.70	46.65	46.85	48.75
Al ₂ O ₃ :	16.21	13.90	17.44	18.87
TiO ₂ :	1.01	0.76	0.86	0.90
Fe ₂ O ₃ :	2.53	2.26	2.36	2.40
FeO:	6.77	6.52	6.36	6.83
MnO:	0.11	0.15	0.15	0.20
MgO:	9.70	14.68	8.78	5.13
CaO:	12.33	9.78	11.71	10.99
Na ₂ O:	2.24	1.92	2.06	3.08
K ₂ O:	0.53	0.54	0.92	0.84
P ₂ O ₅ :	0.08	0.09	0.13	0.17
H ₂ O(T):	1.95	1.78	2.13	1.69
Total:	99.18	99.03	99.75	99.85

Trace Elements in ppm

V:	277	228	345	244
Cr:	507	1185	292	59
Co:	17	19	16	16
Ni:	169	385	126	21
Cu:	89	79	109	91
Zn:	57	63	87	68
Rb:	5	9	20	14
Sr:	428	360	553	461
Y:	29	29	31	36
Zr:	60	62	63	79
Ba:	117	113	160	150
Nb:	13	10	15	12
K/Rb:	880	498	382	498
Rb/Sr:	0.012	0.025	0.036	0.030
* ⁸⁷ Sr/ ⁸⁶ Sr:	0.7052	0.7051	0.7053	-

Chondrite Normalized REE(after T.A. Vogel, 1981, pers. comm.)

La:	-	30.30	-	39.39
Ce:	-	25.00	-	30.68
Sm:	-	17.13	-	24.31
Eu:	-	14.35	-	23.48
Tb:	-	10.21	-	13.83
Lu:	-	8.53	-	13.53

*Hedge and Lewis (1971)

TABLE 4.5 (Cont'd)

Sample #:	WCA223	WCA109	WCA050
Name:	Andesite (CPA)	Andesite (CPA)	Andesite (CPA)
Long.(W):	61°29'.7"	61°28'.4"	61°27'.9"
Lat.(N) :	12°27'.0"	12°27'.2"	12°27'.9"

Major Elements in Weight %

SiO ₂ :	53.63	56.91	61.71
Al ₂ O ₃ :	19.72	19.59	18.26
TiO ₂ :	0.61	0.57	0.37
Fe ₂ O ₃ :	2.11	2.07	1.87
FeO:	6.10	4.40	2.40
MnO:	0.20	0.17	0.13
MgO:	1.40	1.34	0.71
CaO:	8.67	8.59	6.47
Na ₂ O:	3.55	4.00	4.51
K ₂ O:	0.92	0.96	1.27
P ₂ O ₅ :	0.22	0.17	0.15
H ₂ O(T):	1.88	1.40	1.22
Total:	99.01	100.17	99.07

Trace Elements in ppm

V:	180	118	63
Cr:	25	29	36
Co:	16	12	7
Ni:	16	1	1
Cu:	55	32	-
Zn:	287	77	53
Rb:	33	21	33
Sr:	742	409	576
Y:	34	27	46
Zr:	67	104	151
Ba:	213	201	369
Nb:	11	13	12
K/Rb:	231	380	320
Rb/Sr:	0.044	0.051	0.057
* ⁸⁷ Sr/ ⁸⁶ Sr:	-	0.7053	0.7054

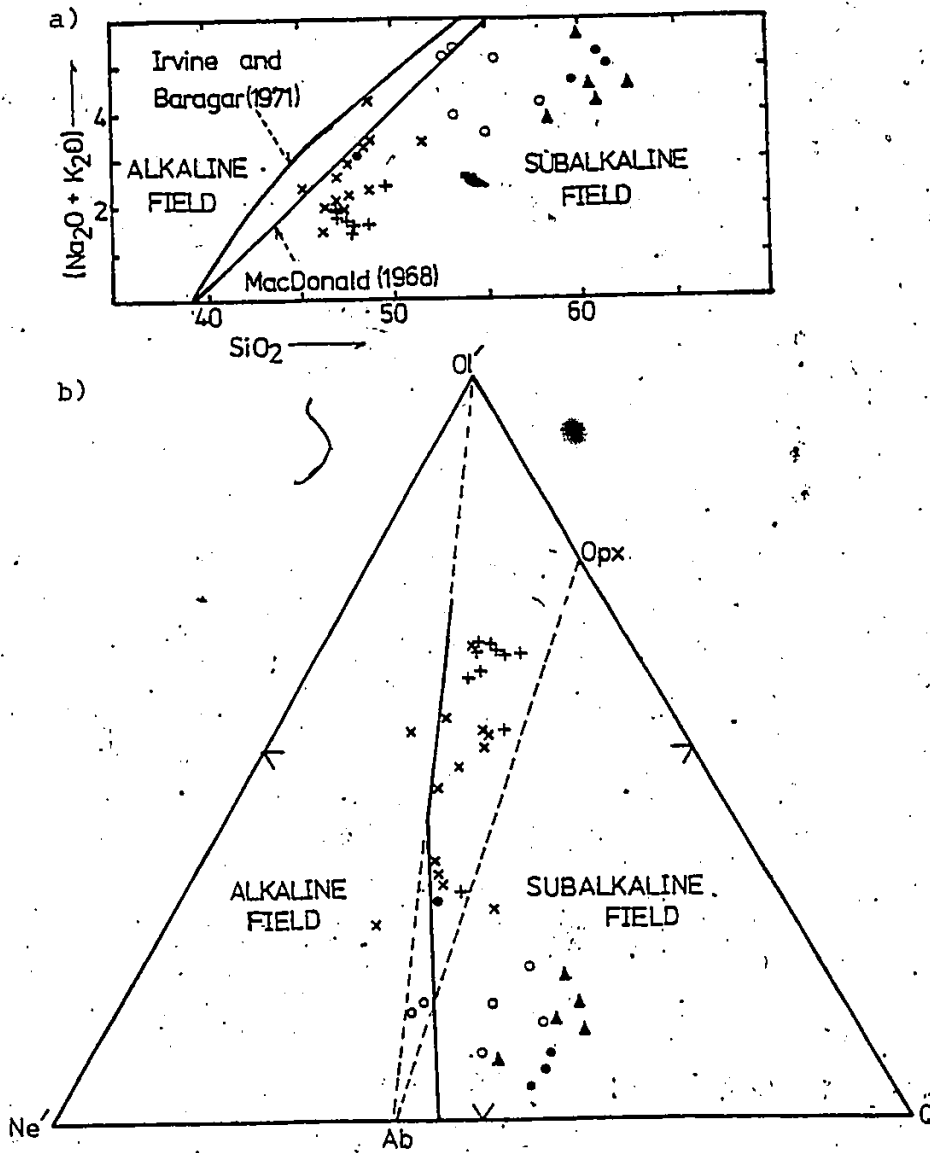
Chondrite Normalized REE(after T.A. Vogel, 1981, pers. comm.)

La:	45.45	-	63.64
Ce:	32.95	-	43.18
Sm:	28.17	-	31.49
Eu:	22.75	-	24.93
Tb:	17.66	-	15.53
Lu:	15.59	-	17.35

*Hedge and Lewis (1971)

the arc (and even within single islands) there exists a large degree of controversy over which magma series the lavas belong to in certain sections of the arc.

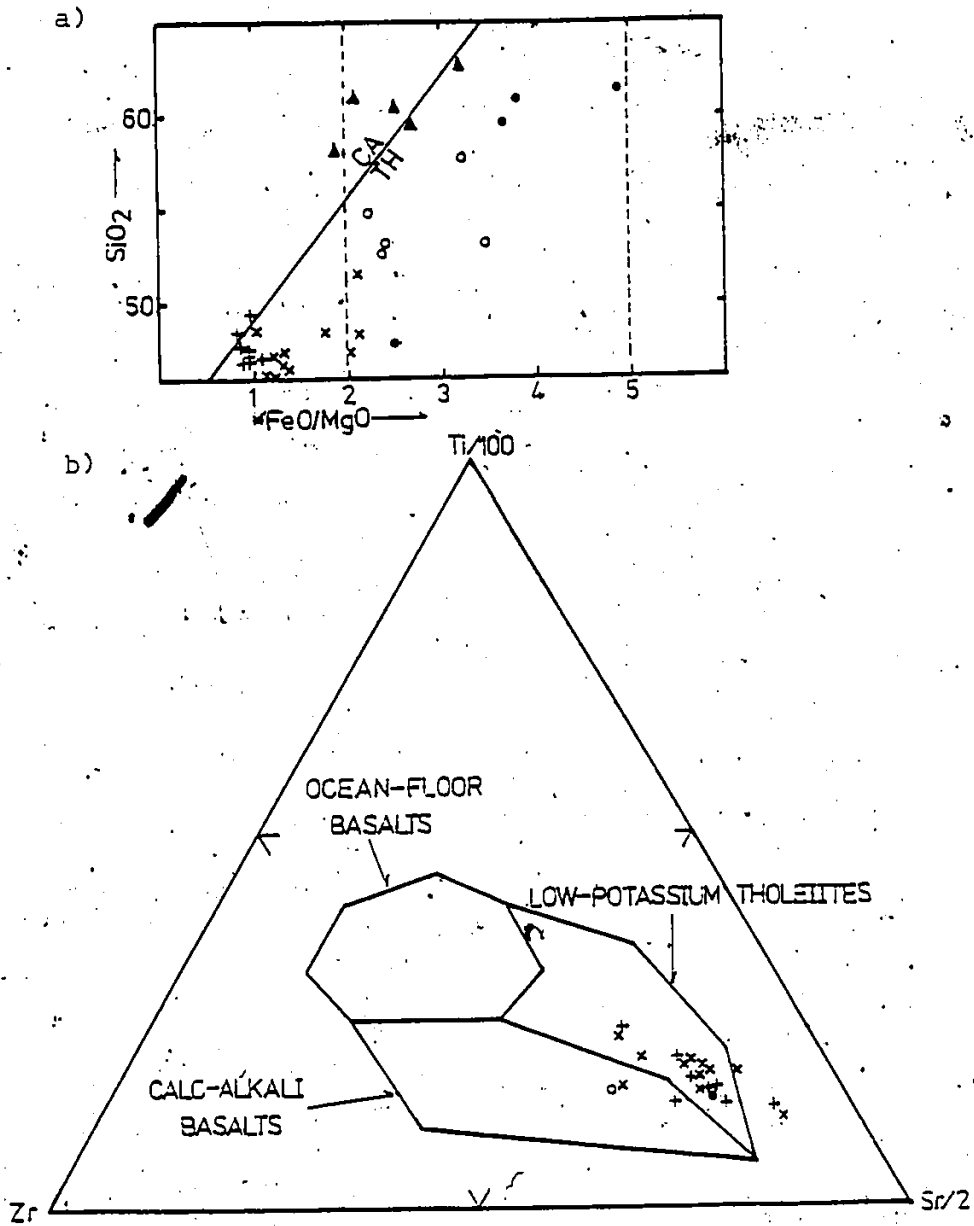
The volcanic lavas were first plotted on the SiO_2 vs. $\text{Na}_2\text{O}+\text{K}_2\text{O}$ and $\text{Ol}'\text{-Q}'\text{-Ne}'$ diagrams (Irvine and Barager, 1971) to determine if they are alkaline or subalkaline in nature (Figure 4.2a and b). Four rocks (two CMB lavas, CU-18 and CU-7; and two CPA lavas, CU-1 and CU-27), which contained high Na_2O compositions, plotted in the alkaline fields. As a consequence, the two CMB lavas contained nepheline in their normative mineralogy (Table 4.2). However, alteration affects, which do not show up in high L.O.I. contents (>3.00 wt. %), may have been responsible for high Na_2O contents, since Na is a mobile element, and since the remainder of the rocks (which show similar petrological characteristics) plotted in the subalkaline field. In addition, all of the remaining basalts contained normative hypersthene (Table 4.2); all of the basalts (including CU-18 and CU-7) contained Y/Nb ratios (Pearce and Cann, 1973) greater than 2 (Table 4.2); and the normative mineralogy of the CMB clinopyroxene did not include nepheline (Table 4.3). These characteristics all indicate that the basalts do not have alkaline affinities.



Figs. 4.2a and b. Alkaline vs. subalkaline classification diagrams (Irvine and Barager, 1971) for the lavas on the southern half of Carriacou (\blacktriangle =APA, \times =CMB, $+$ =OMB, \circ =CPA, \bullet =AMA; $Ne = Ne + 3/5Ab$, $Q = Q + 2/5Ab + 1/4Opx$, $O1 = O1 + 3/4Opx$)

The volcanic lavas were then plotted on the FeO/MgO vs. SiO₂ diagram (Miyashiro, 1974) to determine if the rocks belong to the calc-alkaline or tholeiitic magma series (Figure 4.3a). The majority of the APA samples plotted as calc-alkaline, which was also reflected in their relatively lower P₂O₅ contents (Anderson and Gottfried, 1971). However, all of the remaining andesites, including some of the hypersthene-normative CMB basalts which fell into the critical field of classification (FeO/MgO greater than 2 and less than 5), plotted as tholeiitic lavas. The relatively shallow slope of the plot was also characteristic of tholeiitic lavas. In addition, using the stable element triangle diagram (Ti/100-Zr-Sr/2) for fresh basalts (Pearce and Cann, 1973), the majority of the CMB and OMB lavas plotted as low-potassium (island-arc) tholeiites (Figure 4.3b). This conclusion differs from that of Jackson (1970, 1980), who believes that the CMB lavas, and all of the rocks in the andesitic sequence(s) are calc-alkaline.

All of the andesites on the southern half of Carriacou (hypersthene-normative rocks with SiO₂ contents from 53 to 63 wt. %, calculated on an anhydrous basis) can be classified as true orogenic andesites (Gill, 1981; where wt. % K₂O is less than



Figs. 4.3a and b. Subalkaline classification diagrams for the lavas on the southern half of Carriacou (5.6a=general rock classification by Miyashiro, 1974; 5.6b=basaltic classification by Pearce and Cann, 1973; \blacktriangle = APA, \times = CMB, $+$ = OMB, \circ = CPA, \bullet = AMA)

0.145(wt. % SiO_2 - 5.135) and TiO_2 is less than 1.75 wt. %). Therefore, these rocks do not belong to the shoshonitic series (Gill, 1981). These andesites were plotted on the SiO_2 vs. K_2O andesite classification by Gill (1981). All of the samples plotted around the low-K/medium-K dividing line. The CPA lavas plotted as predominantly basic andesites, while the APA and AMA lavas plotted as acid andesites (Figure 4.4).

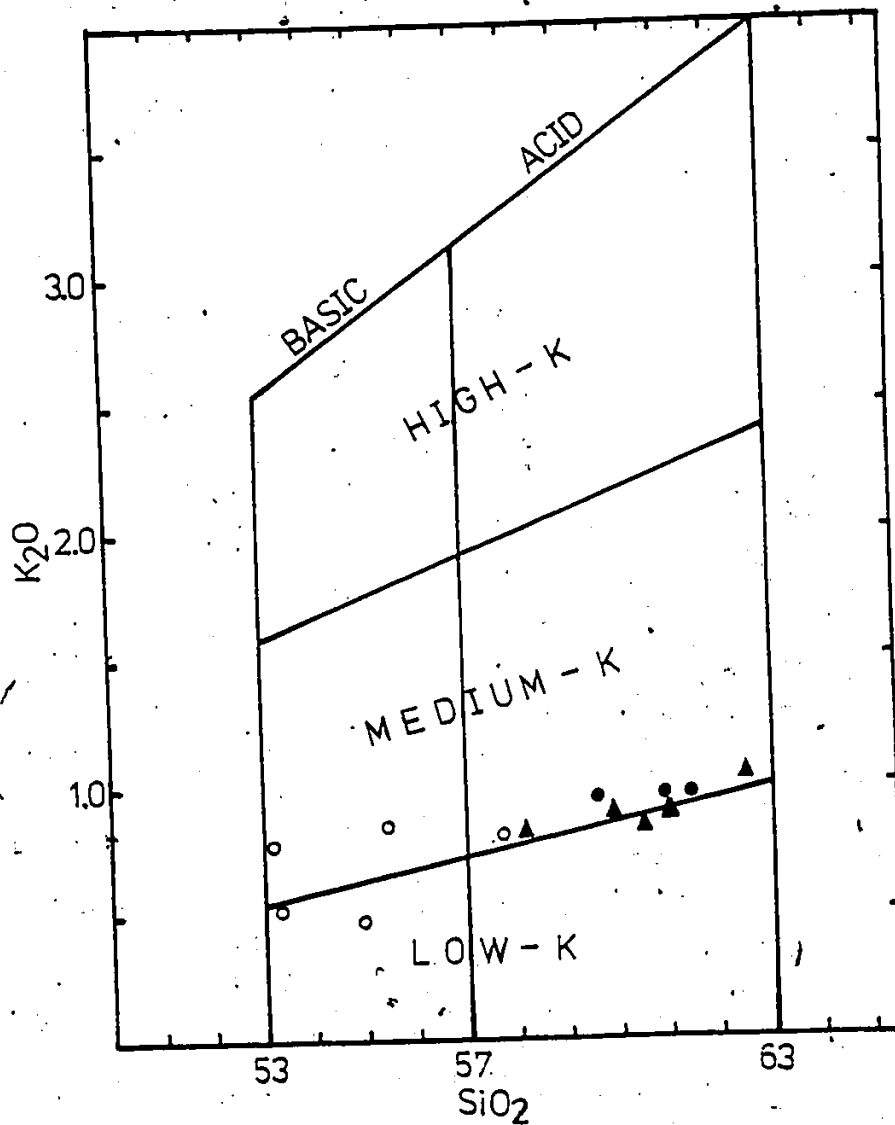


Fig. 4.4 Classification diagram for andesites (Gill, 1981) found on the southern half of Carriacou (▲=APA, ○=CPA, ●=AMA)

CHAPTER 5

PETROGENESIS

In the following sections, a model for the petrogenesis of the volcanic rocks, found on the southern half of Carriacou, will be constructed. The Sr isotope and REE data will first be examined to determine the source(s) of the primary melt(s) which gave rise to these rocks. In view of these conclusions, the possible mechanisms for the variation in the composition of the volcanic rocks will be listed and individually discussed. Finally, the resultant model for the petrogenesis of the volcanic rocks will be further discussed using information from both petrological and geochemical observations.

5.1 INITIAL Sr ISOTOPE RATIOS

The initial $^{87}\text{Sr}/^{86}\text{Sr}$ values for the 5 samples found on the southern half of Carriacou lie in the range 0.7051 and 0.7054 (Table 4.5). These ratios, which include those for both the basalts and andesites, and which are fairly uniform, fall within the range of ratios found in ocean island basalts (0.7025 to

0.7055), and therefore represent a mantle origin (Hedge and Lewis, 1971).

One of the geochemical trends of the Lesser

Antilles is the general increase in the Sr isotope ratios toward the south (Table 5.1). This characteristic may be explained by one of the following reasons:

1. Sr contamination from continental detritus in the subducted crust
2. Long-term variation in the Rb/Sr ratios between respective mantle sources (Hedge and Lewis, 1971)
3. Sr contamination from occluded seawater and seawater affected material in the subducted crust (Hawkesworth *et al.*, 1979)

In view of the relative proximity to South America, Sr contamination from continental sedimentary material is an attractive mechanism for the increase in the initial Sr isotope ratios for the rocks produced in the southern part of the arc. IRS fluids (fluids rich in incompatible trace elements, radiogenic isotopes, and silica), which are derived from the subducted crust and sedimentary material (Gill, 1981), would mix with those melts derived from the mantle, causing an increase in the Sr isotope values. Dasch (1969) found that the marine sediments in this part of the Atlantic

TABLE 5.1 - Initial Sr isotope ratios from the Lesser Antilles

ISLAND	RANGE	AVERAGE VALUE
Saba	0.7036-0.7042a	0.7039
Statia	0.7034-0.7042a	0.7039
St. Kitts	0.7036-0.7046b,c	0.7039
Nevis	0.7036-0.7041a	-
Montserrat	0.7034-0.7034d	0.7034
Guadeloupe	0.7031-0.7043a,c	0.7037
Dominica	0.7045-0.7068c,e	-
Martinique	0.7034-0.7084a,f	0.7048
St. Lucia	0.7037-0.7092e,f	0.7067
St. Vincent	0.7039-0.7043h	0.7041
Carriacou	0.7051-0.7054b	0.7052
Grenada	0.7039-0.7058g	-

- a) Nagle and Stipp (unpublished data)
 b) Hedge and Lewis (1971)
 c) Donnelly et al. (1971)
 d) Réa (1974)
 e) Pushkar (1968)
 f) Pushkar et al. (1973)
 g) Hawkesworth et al. (1979)

Ocean have $^{87}\text{Sr}/^{86}\text{Sr}$ values of approximately 0.72. At the present rate of convergence (1.4 cm/yr; which was calculated by Chase, 1978, using euler vectors), and given that the southern segment of the Atlantic lithosphere subducts approximately 150 km east of the arc at about a 30 degree dip to the west (Tomblin, 1975), it would take approximately 12 Ma to subduct these sediments beneath the arc. Therefore, substantial amounts of sedimentary material must have been at the site of subduction over 30 Ma ago since the oldest volcanic rocks on Carriacou, that were dated by Briden *et al.* (1978), were approximately 18.1 Ma old. These sediments may have been clays which were transported northward by long-shore currents along the northeastern coast of South America. At present, the bulk of the sediments transported by longshore currents are derived from the Amazon River (Van Andel, 1967).. The Amazon river (and possibly the Orinoco River) is thought to have been originated as a result of a mid-Tertiary (30 Ma) uplift of the Andes (Grabert, 1971). Therefore, it is quite possible to derive higher initial Sr isotope ratios from the contamination by continental detritus in the subducted crust.

Hedge and Lewis (1971), who studied geochemical analyses from various lavas found on three islands in

the Lesser Antilles (St. Kitts, St. Vincent, and Carriacou) also found a general increase in the initial Sr isotope ratios towards the south. However, the authors noted that the Rb/Sr ratios from the corresponding rocks did not increase towards the south, as might be expected due to higher initial Sr isotope ratios (Table 5.2). They concluded that the sedimentary component in the downgoing slab did not play a major role in causing higher initial Sr isotope ratios, and instead was caused by long-term mantle heterogeneity. They believed that the respective mantle sources are so old that the isotopic differences could have been generated by small differences in the Rb/Sr ratios (which were obscured by the volcanism).

The final explanation deals with the possibility that higher initial Sr isotope ratios were caused by contamination from occluded seawater and seawater affected material in the subducted crust. Hawkesworth et al. (1979), who carried out Nd and Sr isotope geochemistry for the lavas on Grenada, show that the Sr isotopes are displaced to higher values compared to those values derived from mid-oceanic ridge and ocean-island basalts, while the $^{143}\text{Nd}/^{144}\text{Nd}$ ratios remain the same. They point out that continental crust contains higher initial Sr isotope ratios and lower Nd

TABLE 5.2 - Silica, potassium, rubidium, strontium, and nickel contents and initial $^{87}\text{Sr}/^{86}\text{Sr}$ ratios of rocks belonging to three volcanic suites from the Lesser Antilles (After Hedge and Lewis, 1971)

(Each suite listed in order of increasing SiO_2 content)

Sample No.	SiO_2 (%)	K (%)	Rb (ppm)	Sr (ppm)	Ni (ppm)	Rb/Sr	$\text{Sr}^{87}/\text{Sr}^{86}$
Mt. Misery, St. Kitts							
14842	48.8	0.34	6.2	235	23	0.026	0.7036
14446	50.3	0.32	7.7	279	2	0.028	0.7036
14368	50.9	0.43	8.7	295	-	0.029	0.7037
14377	53.3	0.38	10.7	269	4	0.040	0.7040
14401	56.6	0.54	14.2	312	2	0.046	0.7037
14697	58.6	0.61	16.4	310	-	0.053	0.7038
14416	59.1	0.48	15.6	278	2	0.056	0.7040
14789	59.7	0.55	18.6	288	1	0.065	0.7037
14759	61.6	0.71	16.2	291	1	0.056	0.7039
Soufriere, St. Vincent							
37311	47.7	0.51	7.9	228	200	0.035	0.7040
37080	51.3	0.26	8.7	178	82	0.049	0.7043
37076	51.9	0.41	11.5	212	66	0.054	0.7042
37139	52.3	0.38	13.7	225	10	0.061	0.7040
37333	52.3	0.46	11.8	224	20	0.053	0.7040
37254	53.6	0.56	15.9	224	10	0.071	0.7041
37240	55	0.48	14.1	217	10	0.065	0.7039
37317	55.4	0.57	16.3	217	10	0.075	0.7039
Carriacou							
WCA097	45.7	0.44	5.4	412	169	0.013	0.7052
WCA252	46.7	0.45	9.1	339	385	0.027	0.7051
WCA144	46.9	0.76	18.6	455	126	0.039	0.7053
WCA109	56.9	0.80	21	383	1	0.055	0.7053
WCA050	61.7	1.05	35	628	1	0.056	0.7054

isotope ratios than the mantle, and that altered ocean floor basalt contains some Sr of continental origin derived from seawater, but apparently no Nd (O'Nions et al., 1977, O'Nions et al., 1978). Therefore, contamination from seawater affected material in the subducted crust may largely account for the higher initial Sr isotope ratios, with no change in Nd isotopes. However, the relative contribution from sedimentary material is not easily recognized since the oceanic sediments are not well-characterised as yet and they are likely to be mixtures of both continental detritus and authigenic material.

In addition, these authors also noted higher initial Sr isotope ratios in the SiO₂-undersaturated rocks which were unlikely to have been derived by melting of the subducted crust. They suggest that the higher alkalic elements can also be accounted for in a model whereby these elements are preferentially released during dehydration of the subducted lithosphere and contaminate the overlying mantle source region of the arc magmas.

5.2 REE VALUES

The REE data for 4 volcanic lavas found on the

southern half of Carriacou (Table 4.5 and Figure 5.1) shows HREE depletion (7 to 9 times chondrite) relative to the LREE values (17 to 19 times chondrite). This suggests that the primary magma(s) was derived by partial melting of a garnet-peridotite in the mantle (Gast, 1968) since garnet has a relatively higher compatibility with the HREE (i.e. $K_{Gar}^{Ce} = 0.01$ while $K_{Gar}^{Yb} = 4.0$; Shimizu and Kushiro, 1975). At a depth of over 100 km, garnet and clinopyroxene are important residual phases after small degrees (15 to 20 %) of melting and would therefore produce the patterns of normalised REE values shown by the volcanic rocks on the southern half of Carriacou in Figure 5.1 (Cox et al., 1979).

5.3 POSSIBLE MECHANISMS FOR COMPOSITIONAL VARIATIONS OF THE VOLCANIC ROCKS ON THE SOUTHERN HALF OF CARRIACOU

In view of the conclusion that the lavas on the southern half of Carriacou were initially derived from a partial melt of a garnet-peridotite within the mantle, the compositional variations of volcanic rocks may be accounted for by one of the three following possible mechanisms:

1. Mixing of a mantle derived basaltic magma with a mantle derived intermediate or acid

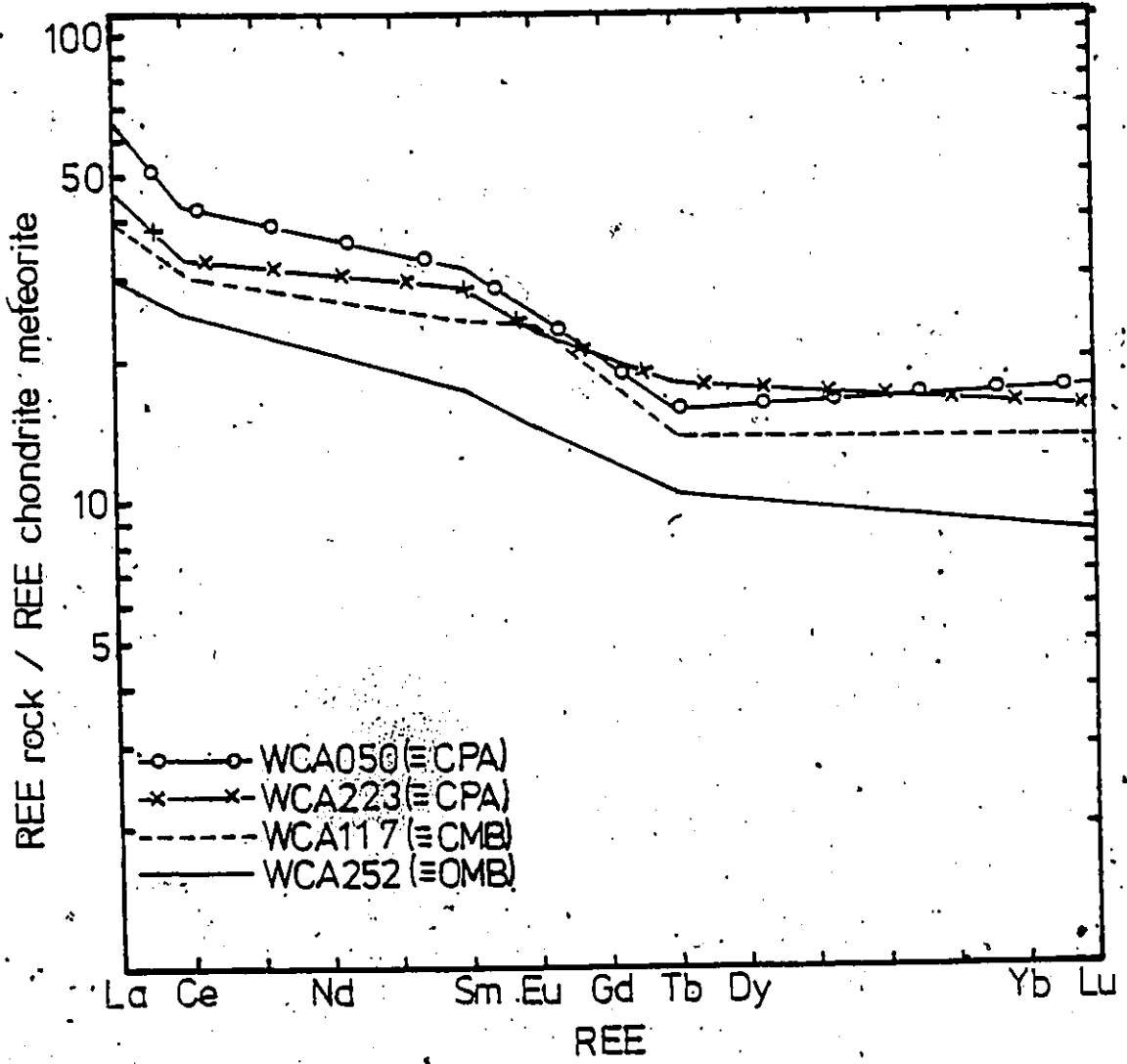


Fig. 5.1 Chondrite normalised REE patterns for four lavas from the southern half of Carriacou

magma.

2. Successive partial melting of the mantle at high pressures (where garnet is involved).
3. Low pressure (where garnet and/or orthopyroxene are not involved) fractional crystallization of a mantle derived partial melt(s).

These mechanisms are all consistent with those models that are presently considered to be operative in the genesis of island-arc magmas (Gill, 1981).

5.3.1 MIXING MODEL

Petrographic observations show that substantial mixing of two end-member magmas did not take place. There are no observed amphibole xenocrysts in the basaltic magmas, or olivine xenocrysts in the andesitic magmas. Additionally, intratelluric plagioclase displays only normal zoning. However, a few altered plagioclase megacrysts (which may have been xenocrysts) are found in the OMB lavas. In addition, samples commonly contain intratelluric plagioclase that display both internal melt channel corrosion, and no internal melt channel corrosion. However, all of these phenocrysts have similar An compositions.

Furthermore, experimental evidence suggests that an andesitic end-member could not have been produced from the mantle for those lavas that are found on Carriacou. In the presence of H₂O, which markedly lowers melting temperatures, andesite magmas can only be generated from a mantle peridotite under exceptional conditions (i.e. at depths less than 40 km where the temperature exceeds 1000°C). This depth of partial melting is inconsistent with the REE data, which suggests that a partial melt from a garnet-peridotite was derived approximately 100 km down in the mantle (garnet is not stable at 40 km). Additionally, if the andesites were produced in the upper lithosphere (since the crust is at least 30 km thick in the Lesser Antilles; Tomblin, 1975), the H₂O contents would be so high that the andesites could not reach the surface without extensive fractionation or solidification (Wyllie, 1982).

5.3.2 PARTIAL MELTING AND FRACTIONAL CRYSTALLIZATION

Compatible or non-residual element (i.e. Ni and Cr) vs. incompatible or residual element (i.e. Zr and K) variation diagrams are plotted in Figure 5.2 using the compositions of the volcanic lavas on the southern

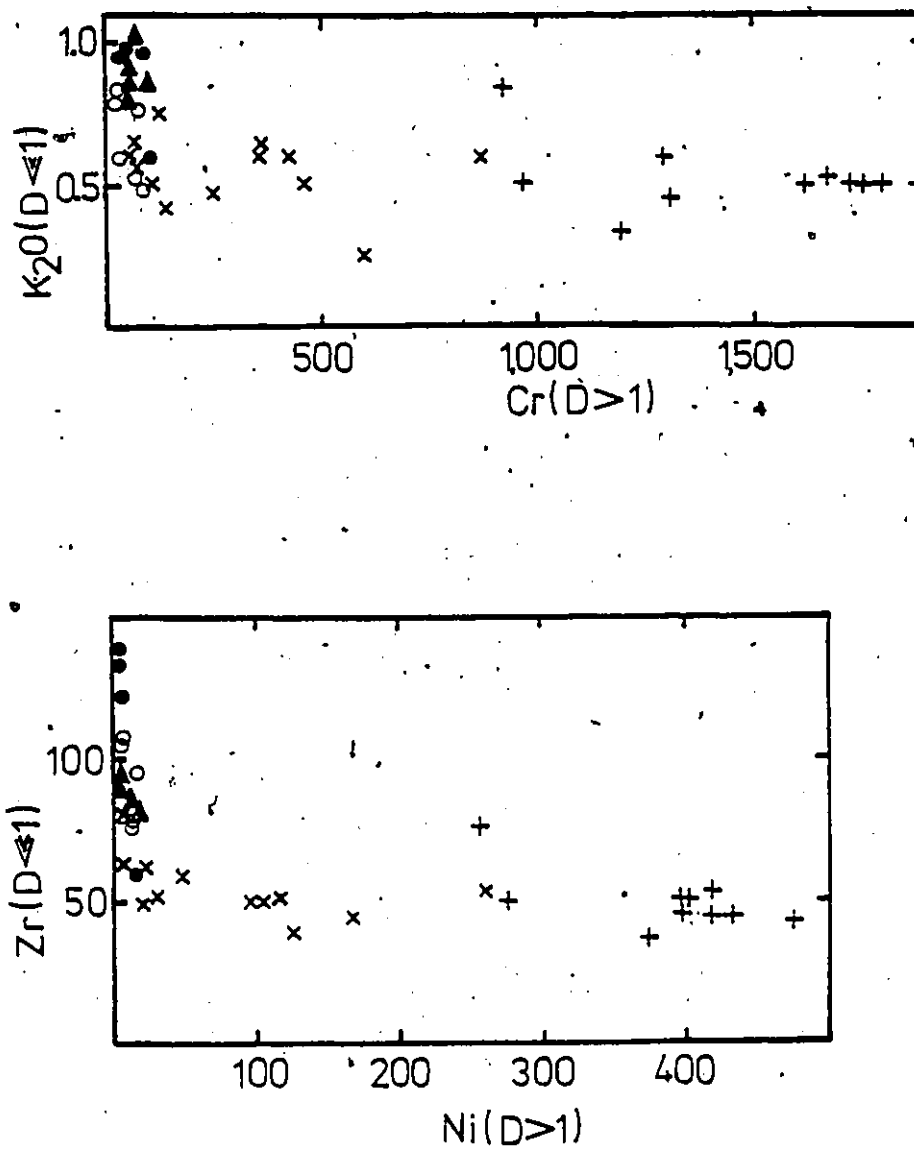


Fig. 3.2 Residual or incompatible element ($D < 1$) vs. non-residual or compatible element ($D > 1$) variation diagrams (K_2O in wt. %; Cr, Ni and Zr in ppm) for the lavas on the southern half of Carriacou (Δ =APA, \times =CMB, $+$ =OMB, \circ =CPA, \bullet =AMA)

half of Carriacou. These diagrams show large variations in compatible or non-residual element compositions relative to small variations in incompatible or residual element compositions. This feature is indicative of fractional crystallization rather than partial melting, since non-residual elements are depleted more rapidly than the residual elements are concentrated during fractional crystallization (Hanson, 1978).

Green et al. (1967) show that crystallization experiments carried out on an olivine tholeiite with a similar chemistry to the OMB lavas (i.e. high MgO, and low Al_2O_3 and K_2O) will only crystallize olivine, followed by clinopyroxene and plagioclase, at pressures between approximately 5 and 9 kb. Therefore, fractional crystallization must have taken place in a reservoir which was formed within the lower crust, since seismic data show that the crust beneath the Lesser Antilles is at least 30 km in thickness (Tomblin, 1975).

Parallel REE variations (Figure 5.1) are also consistent with a crystal fractionation model. Shimizu and Arculus (1975), who studied REE patterns of basanitoid and alkali olivine basalts on Grenada, have argued that REE variations of their volcanic rocks,

which show variations with rapid enrichment in the LREE, are best explained by batch partial melting of a garnet-peridotite. However, they point out that fractional crystallization at low pressures (where garnet and orthopyroxene are not involved) would produce parallel fractionation variations in basaltic liquids (Zielinski and Frey, 1970, Zielinski, 1974). This latter variation trend is similar to the REE pattern shown by the lavas on the southern half of Carriacou (Figure 5.1). Because the partition coefficients of REE for the main phenocrysts of the basaltic lavas on Carriacou are small (i.e. Schnetzler and Philpotts, 1970; $K_{Ol}^{Ce} = 0.009$, $K_{Ol}^{Yb} = 0.023$, $K_{Cpx}^{Ce} = 0.096$, $K_{Cpx}^{Yb} = 0.227$), the fractional crystallization of these phases would result in an increase of REE concentrations in the residual liquid. The partition coefficients for light and heavy REE only differ by a factor of about two for both olivine and clinopyroxene, so that the relative fractionation of REE in the residual liquid would be limited. As a result, the separation of olivine and clinopyroxene would result in an essentially parallel upward shift of the REE pattern in the residual melts. Furthermore, significant plagioclase fractionation can be ruled out because of the lack of an Eu anomaly.

5.4 FRACTIONAL CRYSTALLIZATION AS A MODEL FOR THE VARIATIONS IN COMPOSITION OF THE VOLCANIC ROCKS ON THE SOUTHERN HALF OF CARRIACOU

Petrographic observations support a crystallization sequence of picotite and magnetite, followed by olivine (\pm clinopyroxene) for the OMB sequence; a crystallization sequence of picotite and magnetite, followed by olivine, clinopyroxene and plagioclase for the CMB sequence; and a crystallization sequence of magnetite, followed by plagioclase and clinopyroxene, and amphibole (\pm quartz and apatite) for the andesitic sequences. Variation diagrams for the major oxide and trace element chemistry, using MgO as an abscissa (Figure 5.3), confirm the above crystallization sequences along with their fractionation. Liquid line(s) of descent show a complete evolution from the most primitive OMB lavas, through the CMB and andesitic lavas.

The initial fractional crystallization sequence, which includes that for the OMB and CMB sequences, is largely dominated by olivine and clinopyroxene (plus smaller amounts of magnetite, picotite and later plagioclase). This sequence changes when olivine stops crystallizing from the melt, and the fractional

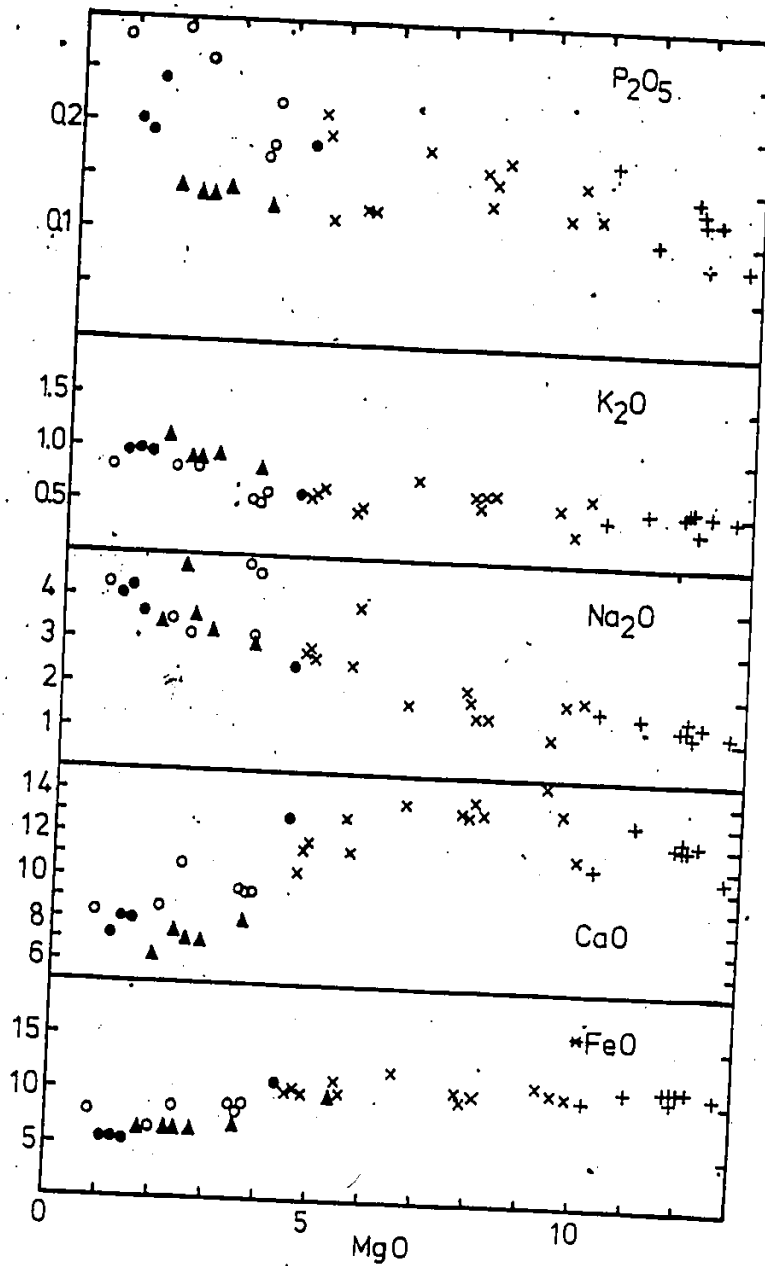


Fig. 5.3a Major oxides (wt. %) vs. MgO (wt. %) for the lavas on Carriacou
 (*FeO = Total iron as FeO; ▲ = APA,
 x = CMB, + = OMB, ○ = CPA, ● = AMA)

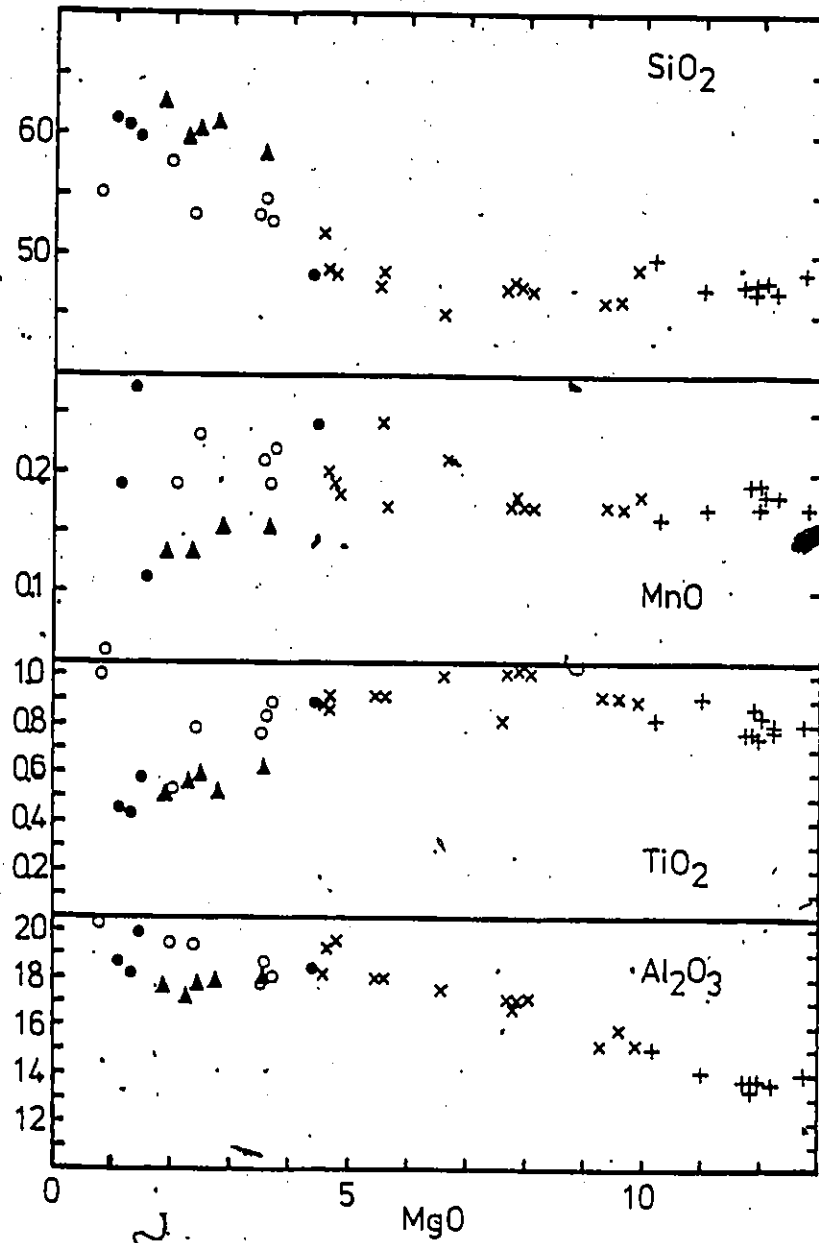


Fig. 5.3a (Cont'd)

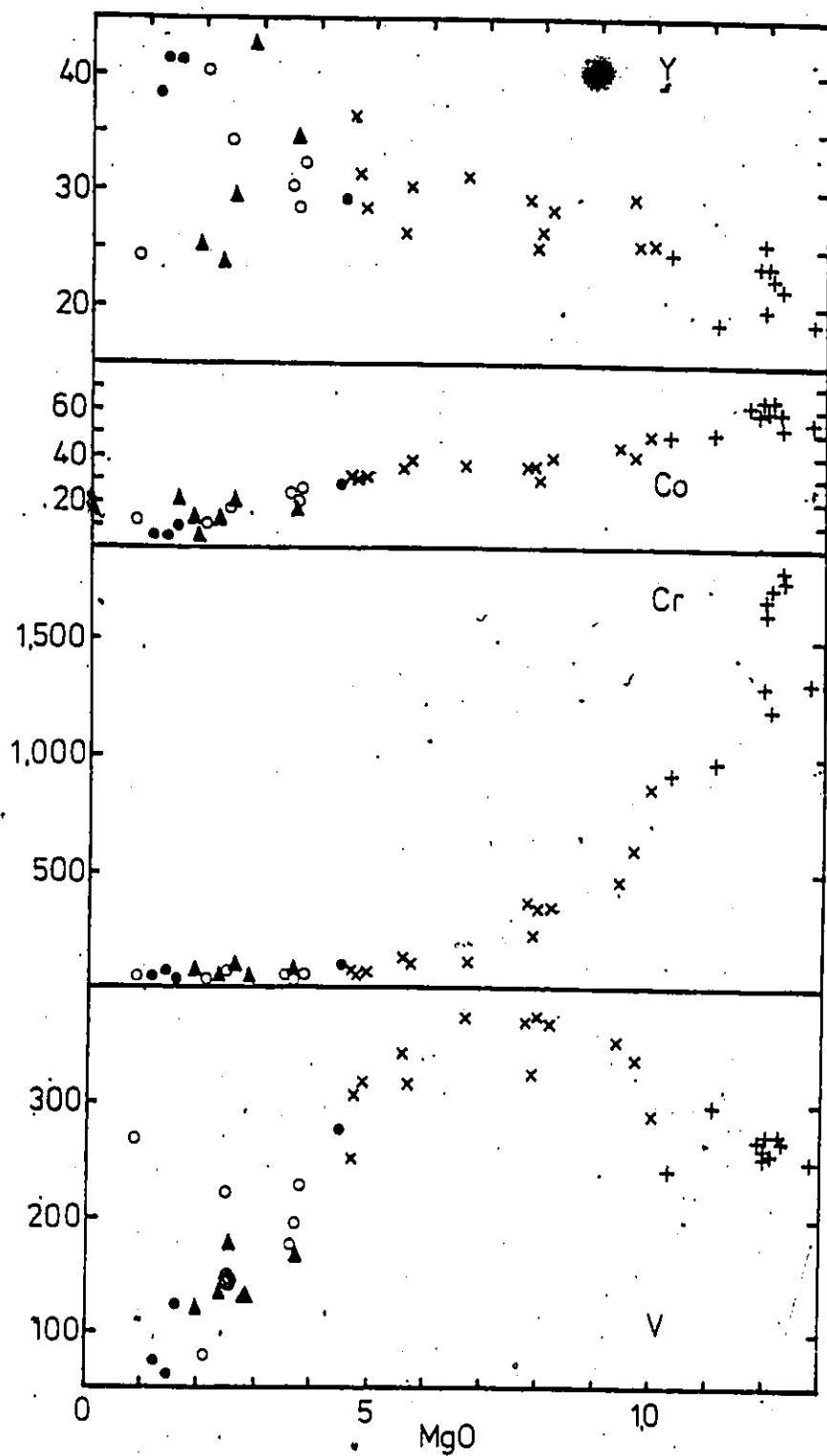


Fig. 5.3b Trace elements (ppm) vs. SiO_2 (wt. %) for the lavas on Carriacou (Δ =APA, \times =CMB, $+$ =OMB, \circ =CPA, \bullet =AMA)

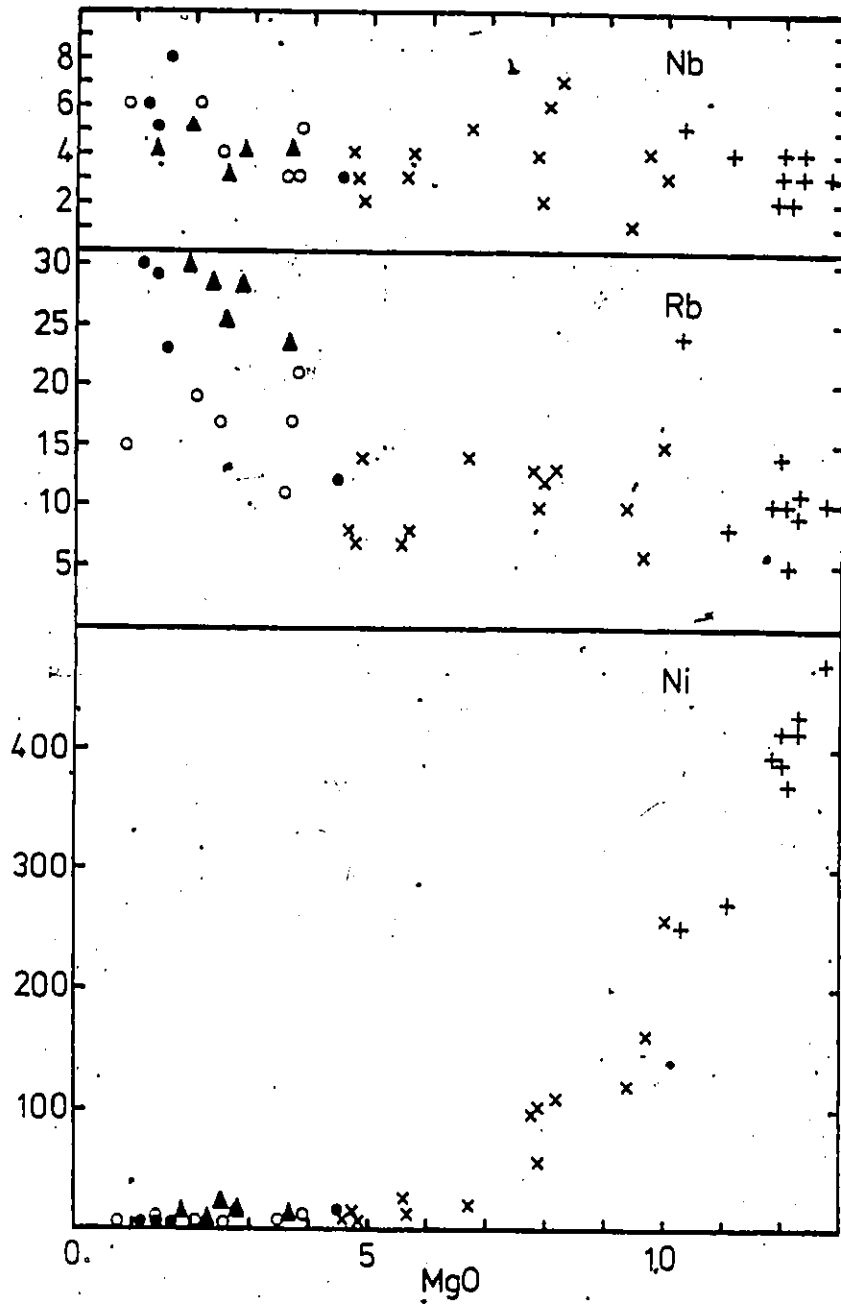


Fig. 5.3b (Cont'd)

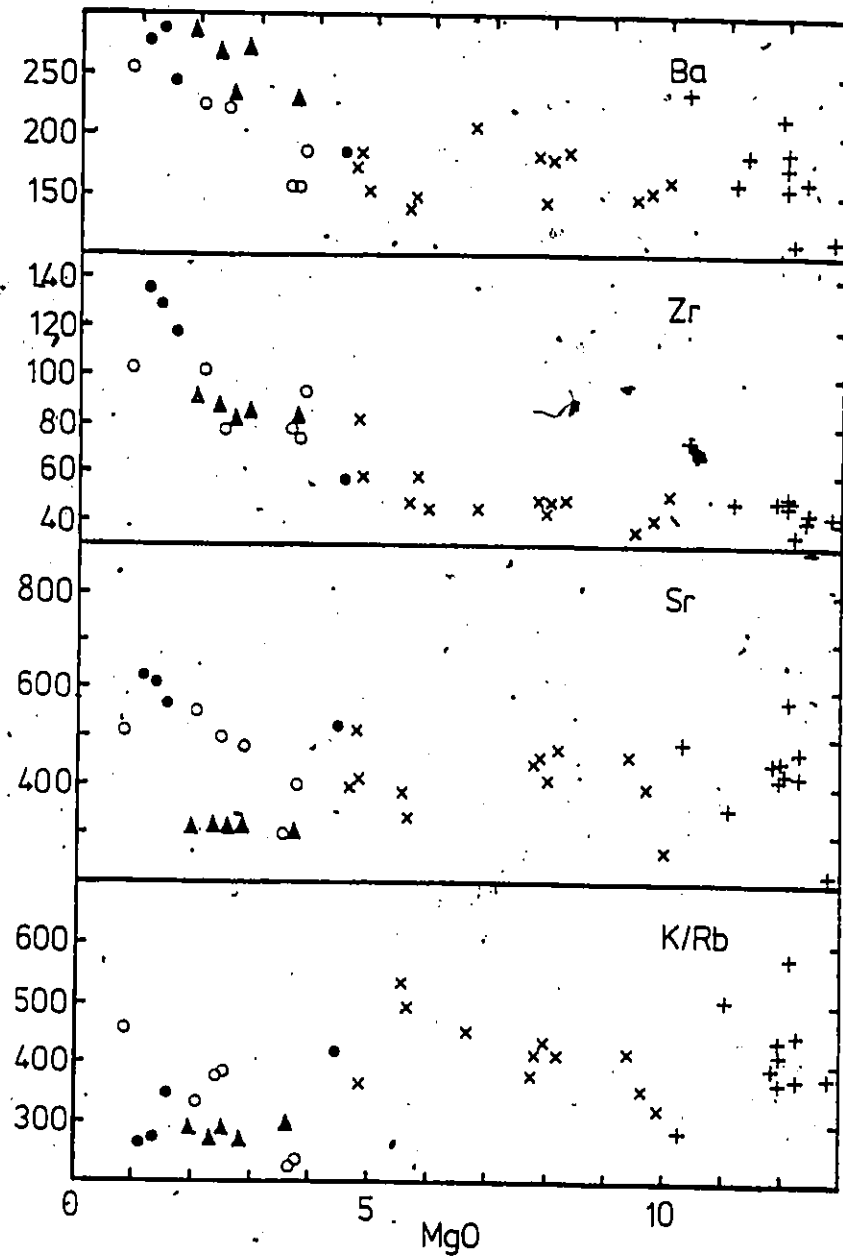


Fig. 5.3b (Cont'd)

crystallization trends, which give rise to the andesitic sequences, are dominated by the removal of magnetite and clinopyroxene (plus smaller amounts of plagioclase and later amphibole).

The initial removal of olivine, which is very forsteritic ($Fe_{0.2}$; determined by X-ray diffraction), accounts for the rapid depletion of MgO and Ni, while the initial removal of clinopyroxene accounts for the rapid removal of Cr. The fractionation of both clinopyroxene and olivine, which have low Al_2O_3 contents is a possible mechanism for the observed decrease in the Al_2O_3 . Major oxide analysis shows high CaO contents for the clinopyroxenes (Table 4.3), however, CaO depletion is masked by co-fractionating olivine, until olivine becomes less abundant in the fractionating sequence (Figure 5.3).

The contribution of fractionating magnetite must be relatively small since the bulk distribution coefficient is low enough to allow V to increase in the basaltic compositions. The lack of an Eu anomaly in the REE data, the lack of decreasing Al_2O_3 , and the uniform Sr levels (except for the APA lavas) indicate a rather small contribution by plagioclase to the fractionating assemblage throughout the evolution of the lavas (Figure 5.3). Furthermore, as observed in

thin-section, the picotites are very small, and therefore only fractionate in the olivines. As a result; the fractionation of very minor amounts of small picotites can only have negligible effects on the overall chemical evolution.

Therefore, by calculating basaltic bulk distribution coefficients for non-residual Co, Ni and Cr, where $K_{Cpx}^{Co} = 1.22$, $K_{Ol}^{Co} = 4.44$, $K_{Cpx}^{Ni} = 2.11$, $K_{Ol}^{Ni} = 18.54$ (Dale and Henderson, 1972), $K_{Cpx}^{Cr} = 18$ (Wager and Mitchell, 1951), and $K_{Ol}^{Cr} = 0.2$ (Cox et al., 1979), and using the Rayleigh equation (given below), approximately 17 % clinopyroxene and 20 % olivine must be removed to consistently account for the observed drops in Co, Ni and Cr.

Rayleigh Equation

$$C_L / C_0 = F^{(D-1)}$$

- Where: C_L = Concentration of the element in the residual liquid
 C_0 = Concentration of the element in original melt
 F = Proportion of the original liquid remaining
 D = Bulk distribution coefficient for a specific element
 $= \sum_{i=1}^n w_i K_{Di}$ where w_i = The weight proportion of each mineral in the fractionating assemblage and K_{Di} = The distribution coefficient for a specific element

This calculation is consistent with uniform residual element concentrations (Rb, Ba, Nb, Zr, Y and Sr) in the CMB and OMB basalt trends (Figure 5.3). For trace elements with very low distribution coefficients, there is generally an increase by only a factor of 1.5 for 37 % crystal fractionation (where $F=0.63$) of a given magma body.

The second main fractionating sequence of minerals begins when olivine takes a subordinate role in both crystallization and fractionation. This occurs at approximately 6 wt. % MgO, where inflection points are apparent on the majority of the variation diagrams (Figure 5.2). Inflection points are characteristic of crystal-liquid fractionation processes, and represent a change in the fractionation assemblage (Cox *et al.*, 1979).

At the inflection point, the rapid drop in V and CaO can only be accounted for by the removal of magnetite ($K_{Mg}^V=30$; Gill, 1981) and clinopyroxene respectively (Figure 5.2). Additionally, the removal of significant amounts of magnetite would account for the drops in TiO_2 and FeO, and the increase in SiO_2 (Gill, 1981). However, a small drop in the K/Rb ratios may indicate contributions from later amphibole ($K_{Amp}^V=32$; Gill, 1981) fractionation in the andesitic lavas (when there is at least 3 wt. % H_2O in the liquid).

phase; Burnham, 1979).

5.5 PETROGENESIS - A SUMMARY AND DISCUSSION

The OMB lavas, which are the most primitive magmas found on the southern half of Carriacou (containing the lowest *FeO/MgO ratios), represent the closest composition to the primary melt(s). REE and initial Sr isotope ratios indicate that this primary melt(s) was derived through partial melting of a garnet-peridotite deep within the mantle. Residual element vs. non-residual element variation diagrams, and REE variations are consistent with a fractional crystallization model to account for the compositional variations found within the volcanic rocks in the southern half of Carriacou. Variation diagrams, using MgO as an abscissa, show liquid lines of descent which represent a complete evolution through the CMB and andesitic sequences. Both the petrography and geochemical trends (i.e. the drops in Ni, Cr, and MgO and the increase in Al₂O₃ contents) suggest the early fractionation of clinopyroxene and olivine (plus smaller amounts of picotite, magnetite and later plagioclase). The lack of substantial plagioclase fractionation, in spite of its high abundance, is

supported by the lack of Sr and Al_2O_3 depletion, and by the lack of an Eu anomaly. By using the Rayleigh equation, approximately 17 % clinopyroxene and 20 % olivine must fractionate to yield the observed drops in the Cr, Co, and Ni contents of the basaltic sequences. These values are consistent with fairly uniform residual element concentrations.

The subsequent disappearance of olivine causes inflection points to appear at approximately 6 wt. % MgO on most of the variation diagrams, and marks the beginning of a new crystallization and fractionation sequence which eventually give rise to the andesitic sequences. Liquid lines of descent show an early and rapid depletion in V and CaO, which can only be accounted for by the fractionation of magnetite and clinopyroxene respectively. However, smaller amounts of plagioclase and later amphibole may also have contributed to the evolution of the andesitic sequences.

The above model is similar to that invoked for the evolution of the lavas on Grenada. The suite of basanitoid and alkali basalts on Grenada are believed to be the result of batch partial melting of a garnet-peridotite (Shimizu and Arculus, 1975). These undersaturated basalts are thought to evolve through

the fractional crystallization of olivine, clinopyroxene and spinel (and joined by later plagioclase and amphibole) to produce the associated subalkaline lavas (Sigurdsson et al., 1973, Arculus, 1976).

A fractional crystallization model was also used to explain the evolution of the lavas on Carriacou by Jackson (1970, 1980). However, Jackson (1970, 1980) believed that, because the most primitive basalts on Carriacou (the OMB sequence) only show similar geochemical characteristics to the subalkaline basalts found on Grenada (i.e. high MgO, Ni and Cr, and low Al₂O₃), the volcanic suite on Carriacou was also derived from a parental basanitoid or alkalic magma. However, because there are no alkali basalts exposed on Carriacou (a characteristic also noted by Jackson, 1970, 1980), and because all the lavas on Carriacou show a much lower range in Rb, Sr, Ba and K compositions than those found on Grenada, it is believed in this paper that the parental melt(s) is not the same as that for the volcanic rocks on Grenada.

REE variations, and experimental work on the crystallization of an olivine tholeiitic basalt (Green et al., 1967) indicate that the crystallization and fractionation of the lavas on the southern half of

Carriacou occurred at pressures which are indicative of those in the lower crust (i.e. approximately 5 to 9 kb). It should be stressed however, that all the magmas were not derived from one parental melt. It is more likely, given the time span, and the variable stratigraphic sequence, that different batches of magmas were tapped at various times throughout their fractionation history.

The plutonic blocks, which are found in the younger andesitic deposits, are thought to represent blocks brought up from older crustal intrusions of andesitic magmas. These blocks did not show any obvious cumulate textures and structures, and the presence of abundant subhedral plagioclase, which was shown not to fractionate in substantial amounts, supports an intrusive history.

The andesitic sequence which was mapped by Jackson (1970, 1980) was shown to be made up of two younger tholeiitic sequences (CPA and AMA sequences) and one older calcalkaline sequence (APA sequence). The observed variations in the Rb/Sr ratios and Al_2O_3 , CaO, Sr and SiO_2 contents in the APA lavas might all be accounted for by relatively larger amounts of plagioclase fractionation. This is supported by the model offered by Gill (1981), who believes that through

POAM fractionation (the fractionation of plagioclase + orthopyroxene or olivine + augite + magnetite) it is possible to derive calcalkaline magmas from tholeiitic magmas.

CHAPTER 6

THE LESSER ANTILLES VOLCANIC-ARC SYSTEM

In order to bring the volcanic rocks on Carriacou into a meaningful context with all those found in the Lesser Antilles, a summary of the arc's regional, tectonic and geochemical characteristics is given. This summary will also include various explanations used to model the above characteristics.

6.1 REGIONAL AND TECTONIC CHARACTERISTICS OF THE LESSER ANTILLES VOLCANIC ARC-SYSTEM

The Lesser Antilles volcanic arc is approximately 700 km long and stretches from Grenada in the south, to Saba in the north (Figure 1.1). To the northwest lies the Greater Antilles, which consists of deformed and metamorphosed sediments and volcanics of Jurassic to Eocene age. To the west of the Lesser Antilles lies the north to south striking Aves Ridge. The rocks from this ridge are thought to have calc-alkaline affinities (Fox and Heezen, 1975) and Keary (1974) favours an island arc origin in the Upper Cretaceous. The site of subduction has since moved 300 km eastward. Approximately

150 km east of the Lesser Antilles, the Atlantic lithosphere, which has a westward convergence rate of approximately 1.4 cm/year (Chase, 1978); begins to subduct beneath the Caribbean plate. The axis of negative isostatic anomaly (Figure 6.1), which splits in the south, is associated with a depression of the igneous crust and an oceanic trench filled with about 20 km of deformed sediments (Chase and Bunce, 1969; Westbrook et al., 1973). Seismic evidence shows that the Atlantic lithosphere is about 30 to 50 km in thickness, and that it dips approximately 20° west, north of Guadeloupe (reaching a depth of 80 to 100 km below the arc), 40° west, in the central parts (reaching a depth of 120 km below the arc) and 30° west, between St. Lucia and Grenada (reaching a depth of 100 km below the arc). The southern segment of the arc is characterized by a low level of recent seismicity. Beneath the Lesser Antilles, the minimum crustal root depth is about 30 km (Tomblin, 1972, 1975), which is quite thick relative to other island arc systems (Gill, 1981).

North of Dominica, two arcs can be recognized. To the east lie islands composed of pre-Miocene volcanics and shallow level intrusives, which are capped by Miocene and younger limestone, while to the west lie islands composed of Pliocene to recent volcanics

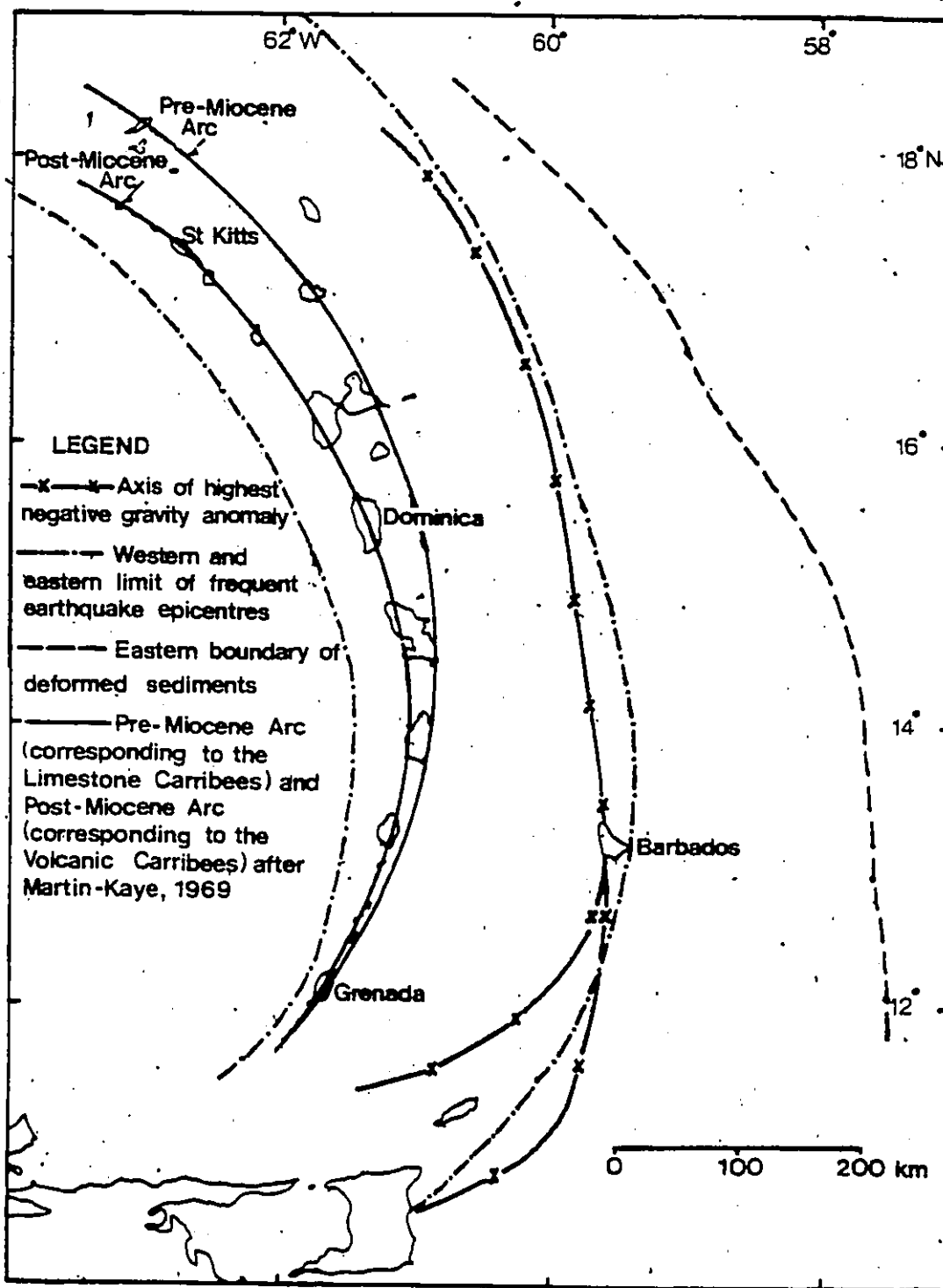


Fig. 6.1 Geological and structural trends for the Lesser Antilles volcanic-arc system

(Martin-Kaye, 1969). The two arcs merge and superimpose in the south (Figure 6.1). Bowen (1972) and Nagle et al. (1976) have shown that the shift in the northern arc segment occurred between 20 Ma and 7 Ma.

6.2 GEOCHEMICAL CHARACTERISTICS OF THE LESSER ANTILLES VOLCANIC ARC-SYSTEM

The most noteworthy characteristic of the Lesser Antilles island arc system is the regular compositional differences of the lavas along the arc without any significant change in the depth to the dipping seismic zone or in crustal thickness. In many other volcanic arc systems, where modest widths are available, across-the-arc increases in incompatible elements (especially K_2O contents), away from the plate margin are well documented (i.e. Tomita, 1935, was the first to identify a compositional polarity in the basalts of Japan). However, along with the Lesser Antilles, longitudinal compositional polarity, which is not as consistent as across-the-arc variation, is present in many other volcanic arc systems. Because of this inconsistency, Gill (1981) has subdivided these systems into four types:

1. Those that show random variations.
2. Those that are regular, but apparently unrelated to crustal thickness (i.e. the Lesser Antilles).
3. Those related to the thickness of the crust traversed.
4. Those that show edge effects (i.e. where convergent plate boundaries terminate at tear faults).

Volcanic arcs which also show regular compositional variations like that of the Lesser Antilles include the Banda arc, Indonesia (Jesek and Hutchison, 1978; Magaritz et al., 1978; Whitford and Jesek, 1979) and the western Bismark arc, Papua New Guinea (Johnson, 1976).

Brown et al. (1977), who studied major oxide and trace element variations of 1,518 lavas, from various islands in the Lesser Antilles, have divided the arc into the northern tholeiitic suite (represented by St. Kitts), the central calc-alkaline suite (represented by Dominica), and the southern alkalic suite (represented by Grenada). These authors found that the lavas on Grenada contained high Rb, Ba, and K, while Dominica and St. Kitts, which lie to the north, contained lavas that respectively showed lower concentrations. In

addition, Grenada contained lavas with the highest Sr, Ni and Cr contents. Grenada was also found to be the only island which contained alkali basalts, and the Sr isotope ratios of the southern islands as a whole contained higher values relative to the northern islands. However, Brown et al. (1977) mixed the data from different centers on each island, and then further smoothed the data by averaging on 2 wt. % SiO₂ intervals. This technique was later criticized (Smith et al., 1980) because of very large intra-volcano variation observed on single islands. In addition, authors who studied and compared lavas on more of the main islands (Smith et al., 1980; Rea and Baker, 1980), noted the lack of iron enrichment in the northern tholeiitic suites, and therefore claimed that both the central and northern islands contain lavas that belong to the low-K, island arc, calc-alkaline series. It should also be stressed that only some of the basalts on Grenada are alkali basalts, and that subalkaline basalts, andesites and dacites are also present (Sigurdsson et al., 1972; Brown et al., 1977; Arculus, 1976).

However, authors who have studied the compositions of lavas from all of the main islands in the Lesser Antilles have generally agreed that Grenada

and the southern Grenadines contain relatively higher Rb, Ba, K, Sr, Ni, and Cr contents in their volcanic products compared to the rest of the arc. In addition, Grenada is the only island that contains alkali basalts, and that the southern islands contain higher (but more variable) Sr isotopes (Smith et al., 1980). Rea and Baker (1980) point out that in terms of the total volume of erupted volcanic material, the northern islands contain higher proportions of andesitic lavas, the central islands contain higher proportions of acid lavas, while the southern islands contain higher proportions of basaltic lavas.

6.3 MODELS FOR THE GEOCHEMICAL VARIATION ALONG THE LESSER ANTILLES VOLCANIC ARC-SYSTEM

There is no satisfactory model for the geochemical variation along the Lesser Antilles volcanic arc, although various authors tentatively attribute this phenomenon to mantle heterogeneities (Brown et al., 1977), variation in subducted materials (Whitford and Jesik, 1979) or varying rates of subduction (Johnson et al., 1976). This last theory is enhanced by Smith et al. (1980), who draw attention to structural evidence for pivoting of the Atlantic lithosphere in the south

(the northern split of the arc; the absence of clear evidence for the presence of a transform fault separating the Caribbean plate from the South American-Atlantic plate in the south; the presence of the Barbados Ridge, which may be due to a crumpling of the Atlantic lithosphere) and suggests the lower rate of subduction accounts for the compositional differences in the southern part of the arc. Slower rates of subduction would cause an increase in the amounts of escaping volatiles from the subducted slab. These volatiles would cause greater degrees of melting, which would account for higher concentrations of compatible elements (i.e. Ni and Cr). Longer periods of heating and melting would also cause incompatible elements to be liberated from the subducted slab, and/or scavenged from the overlying mantle wedge.

Rea and Baker (1980) believe that, because of the relatively larger volumes of andesitic lavas (along with their low concentrations of Cr and Ni), the northern Lesser Antilles suite of volcanic rocks is produced by partial melting of the subducting oceanic crust, while those produced in the south are derived from partial melting of the mantle.

Finally, Gill (1980) makes the observation that, like other islands in volcanic arcs which contain

alkali basalts (i.e. at Samoa; Hawkins and Natland, 1975), the alkali suite on Grenada may be directly related to it being located at the lateral edge of a subducting lithosphere.

CHAPTER 7

CONCLUSIONS

There are six main volcanic sequences exposed on the southern half of Carriacou. These sequences are, from oldest to youngest, the clinopyroxene-phyric basalt (CPB) sequence, the amphibole-phyric andesite (APA) sequence, the clinopyroxene-megaphyric basalt (CMB) sequence, the olivine-microphyric basalt (OMB) sequence, the clinopyroxene-phyric andesite (CPA) sequence, and the amphibole-megaphyric andesite (AMA) sequence. Volcaniclastic deposits are associated with the APA, CMB, and AMA sequences. The stratigraphic relationship between the AMA and CPA sequences is unclear.

All of the lavas are tholeiitic, except for the APA lavas, which are calcalkaline. All of the andesites are classified as true orogenic andesites, with medium to low-K compositions (Gill, 1981).

Initial Sr isotope ratios and REE data suggest that the volcanic rocks in the southern half of Carriacou were derived by partial melting of a garnet-peridotite deep within the mantle.

REE variations, petrographic observations,

experimental work on the crystallization of an olivine tholeiite, and residual element vs. non-residual element variation diagrams all suggest that the compositional variations of the rocks on the southern half of Carriacou were caused by low-pressure fractional crystallization in the lower crust. Geochemical trends, and calculations based on the roles of both residual and non-residual elements indicate that, starting from a composition which is similar to that of the OMB lavas, approximately 17 % clinopyroxene and 20 % olivine (plus smaller amounts of picotite, magnetite and later plagioclase) fractionated to produce the variations in composition of the basaltic sequences. The subsequent change in the fractionation sequence to clinopyroxene and magnetite (plus smaller amounts of plagioclase and later amphibole) gave rise to the andesitic sequences.

The model for the evolution of the lavas on Carriacou is similar to that proposed by various authors who have studied the volcanic rocks on Grenada (Sigurdsson et al., 1972; Arculus, 1976). In addition, fractional crystallization is believed to be the dominant differentiating process for those rocks found in volcanic-arc settings (Gill, 1981).

Finally, the compositional differences between

Grenada and Carriacou, along with that between the southern, central and northern portions of the arc, may be due to one of many possible mechanisms, however, due to abundant structural evidence for the pivoting of the Atlantic lithosphere in the south, these chemical variations are thought to be largely due to variation in rates of subduction. A lower rate of subduction in the southern portion of the arc, which is supported by relatively low levels of recent seismicity (Tomblin, 1975), would allow material escaping from the subducting slab to play a greater role in the melting of the overlying mantle wedge (Smith *et al.*, 1980). An increase in escaping volatiles would lead to greater amounts of basaltic magma formed, and these magmas would contain much higher concentrations of compatible elements (i.e. Cr, Ni and V). Larger amounts of escaping volatiles, which contain higher Sr isotope ratios derived from occluded seawater and seawater affected material in the subducted crust, may cause sufficient contamination to account for higher Sr isotope ratios in the lavas formed in the southern part of the arc (Hawkesworth *et al.*, 1979). In addition, longer periods of heating and melting may cause higher concentrations of incompatible elements (i.e. K, Rb, Ba, and Sr) to be incorporated in the lavas (as with

those lavas found on Grenada). These elements may have either been scavenged from the mantle wedge, or taken from the subducting slab.

PLATES



PLATE 1 Hillsborough Bay, with Hillsborough in the foreground and the air-strip and Point Cistern in the background.

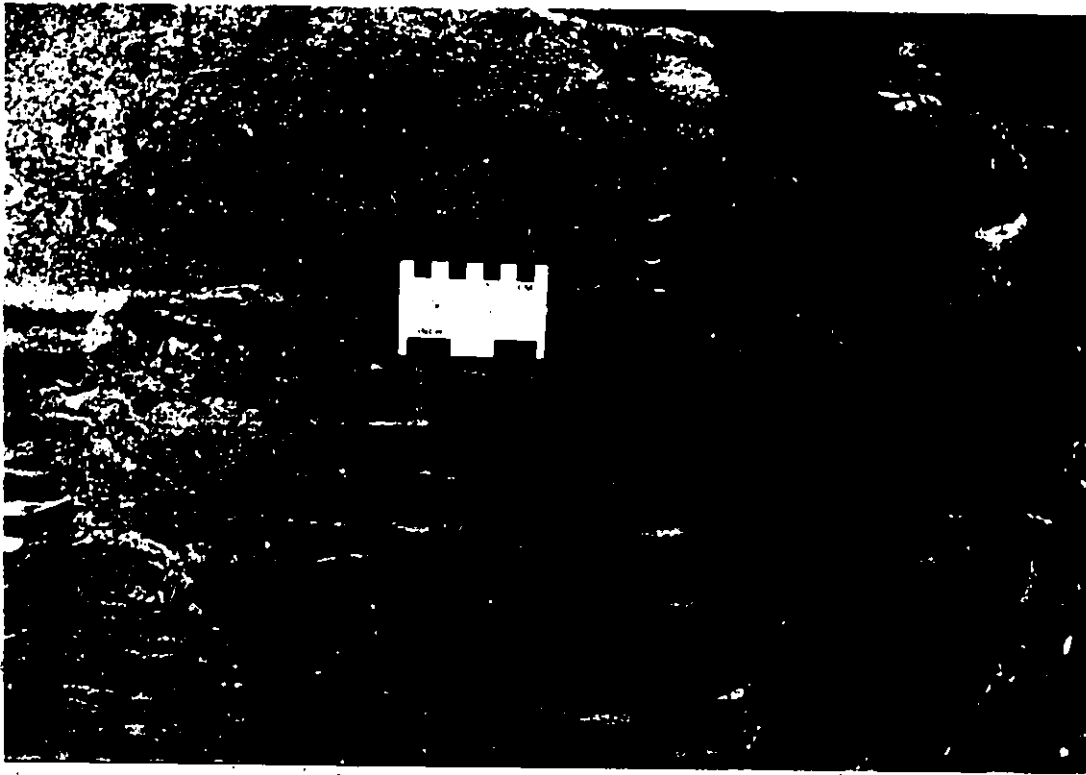


PLATE 2 Laminated to thickly bedded arenites, pebbly greywackes and mudstones of the Belmont Formation exposed on the eastern shore of Manchioneal Bay.

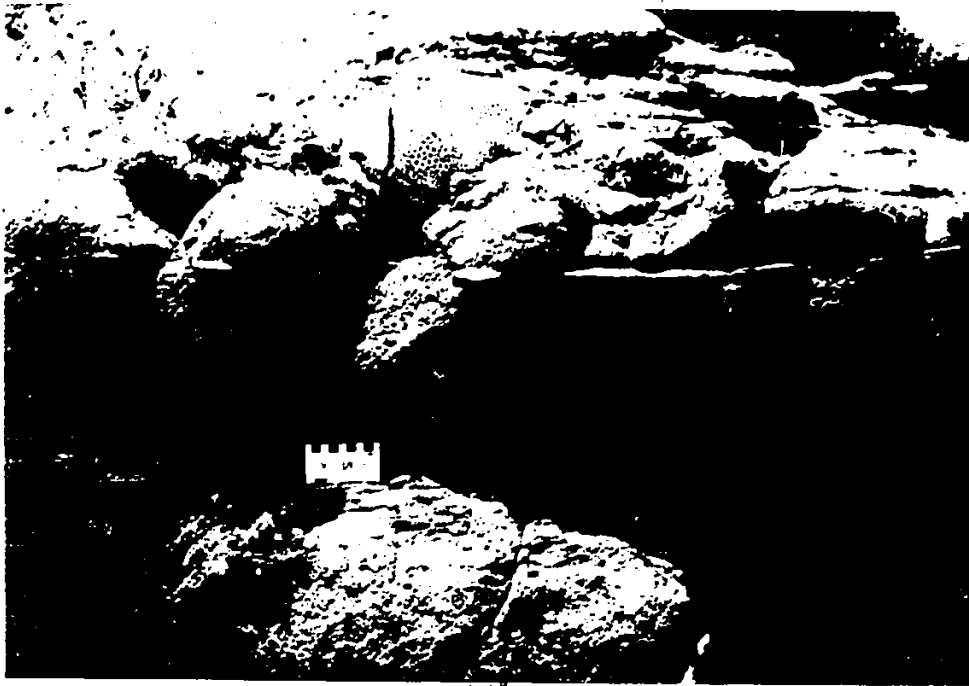


PLATE 3 Clastic marine sedimentary beds of the Belmont Formation (note a large coral fragment included in the sediments).

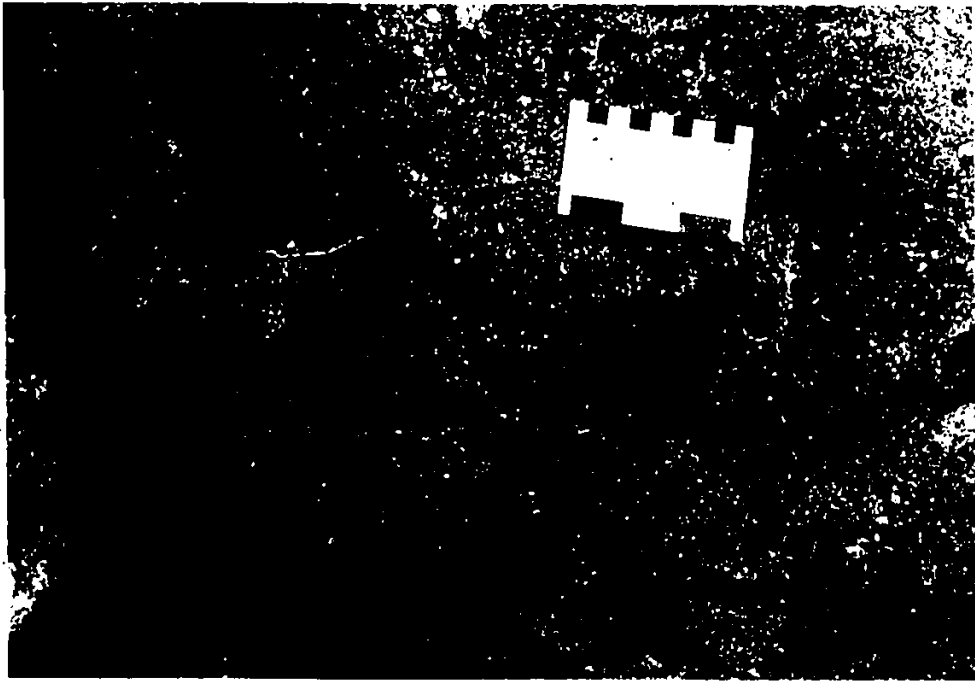


PLATE 4 An APA lapilli-tuff, showing accretionary lapills
(exposed along the shore north of Hillsborough)

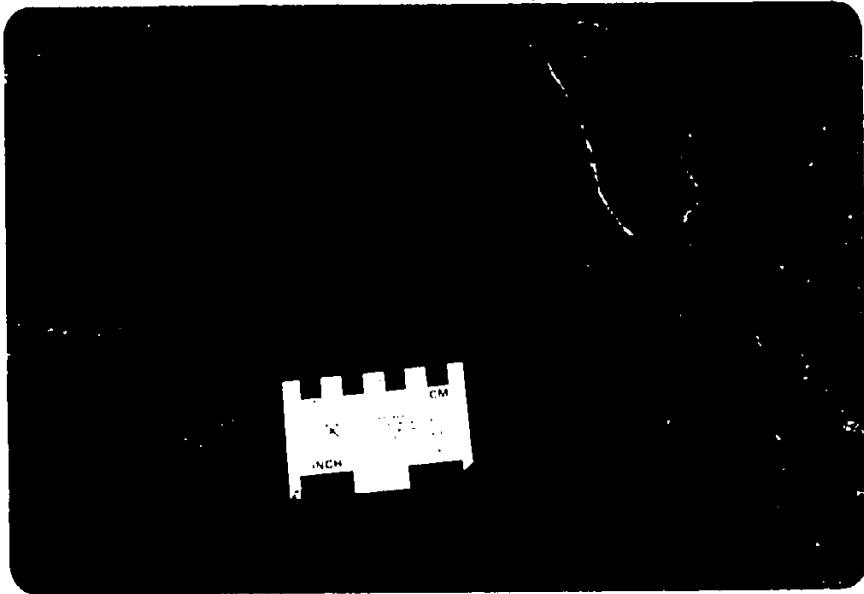


PLATE 5 Bedded APA air-fall tuffs and lapilli-tuffs
(exposed along the shore north of Hillsborough)



PLATE 6 An APA cold avalanche deposit showing subangular and monolithic andesitic clasts set in a finer rudaceous matrix of similar material (exposed along the shore north of Hillsborough)

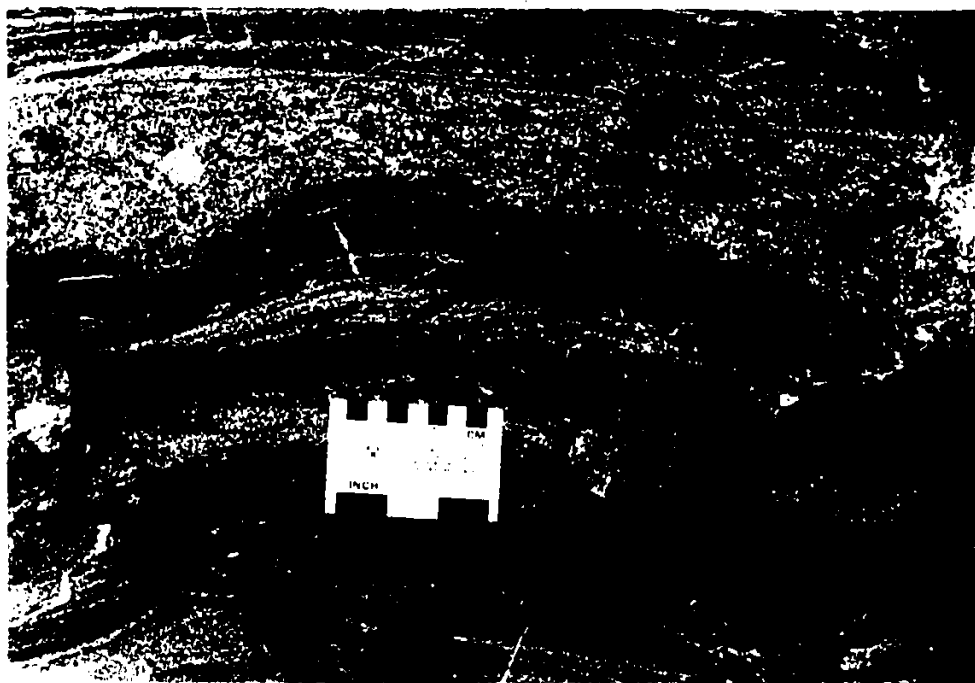


PLATE 7 Laminated, cross-laminated to thinly bedded
APA epiclastic volcaniclastic material
exposed along the southern shore of Tyrrel Bay.



PLATE 8 Fragmented APA epiclastic volcaniclastic beds
exposed along the southern shore of Tyrrel Bay.

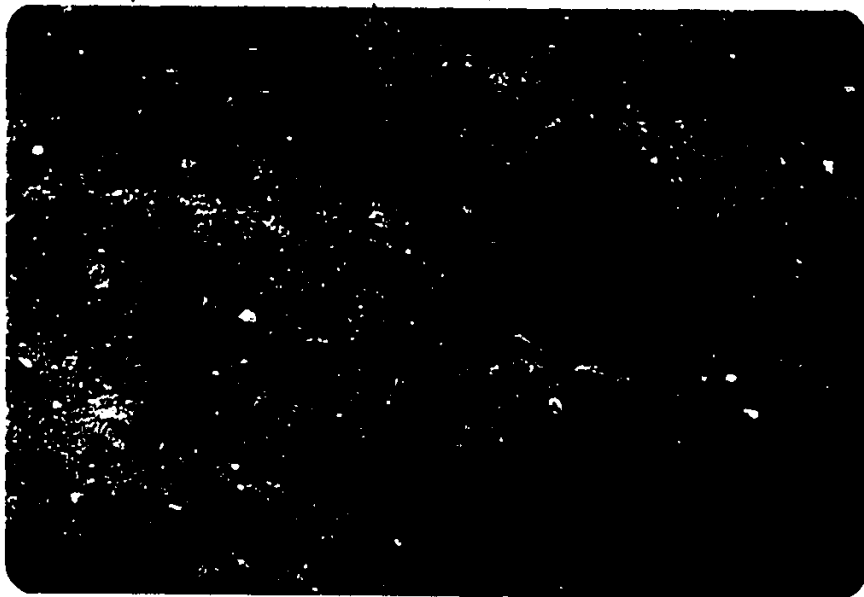


PLATE 9 Poorly sorted APA epiclastic mudflow deposit
exposed along the shoreline north of Hillsborough



PLATE 10 Sub-horizontally bedded CMB volcaniclastic unit (center) exposed along the northern shoreline of Limekiln Bay.



PLATE 11 Sub-horizontally bedded CMB crystal tuffs which include larger blocks of CMB lava (exposed along the northern shoreline of Limekiln Bay)



PLATE 12. Graded beds of CMB crystal-tuffs with clinoproxene and plagioclase crystals (plus CMB lava fragments) set in a muddy green matrix (exposed along the shore at Point Cistern).



PLATE 13 CPA volcanic plug exposed at Belmont (180 m in height)

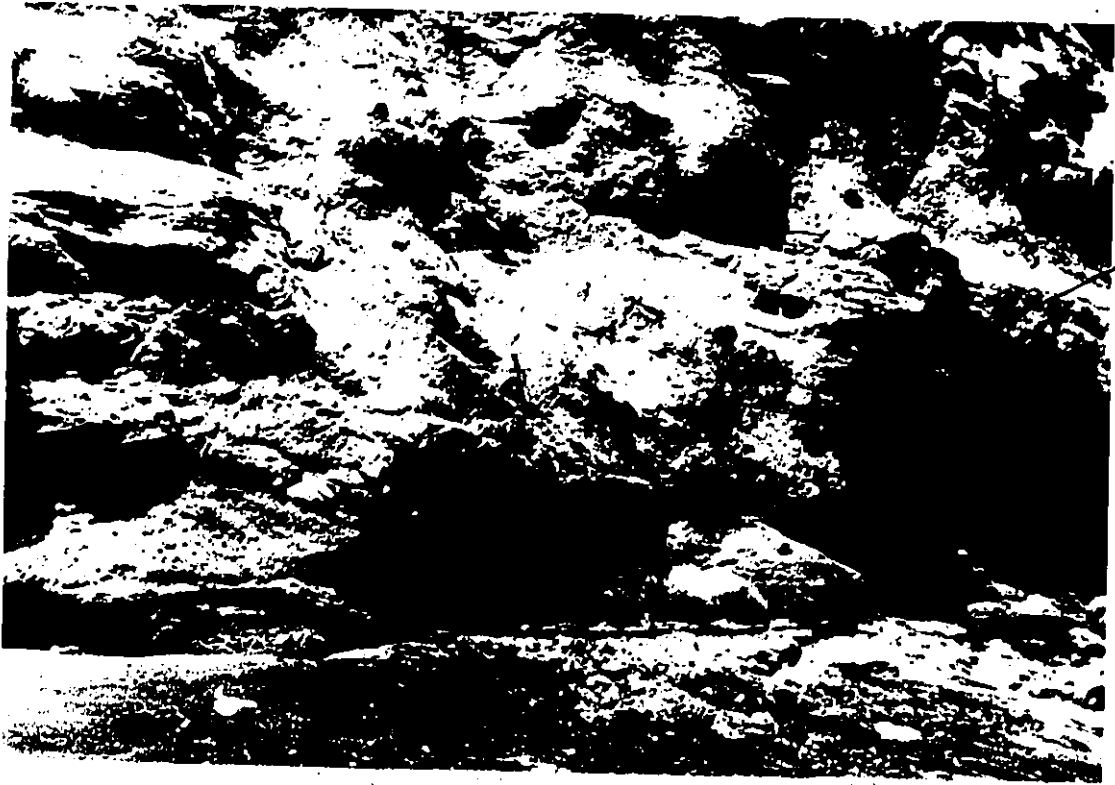


PLATE 14 AMA epiclastic mudflow overlying Belmont beds
on the eastern shore of Manchioneal Bay.



PLATE 15 Brecciated AMA tuffs exposed on the shoreline
at Point Cisterri.

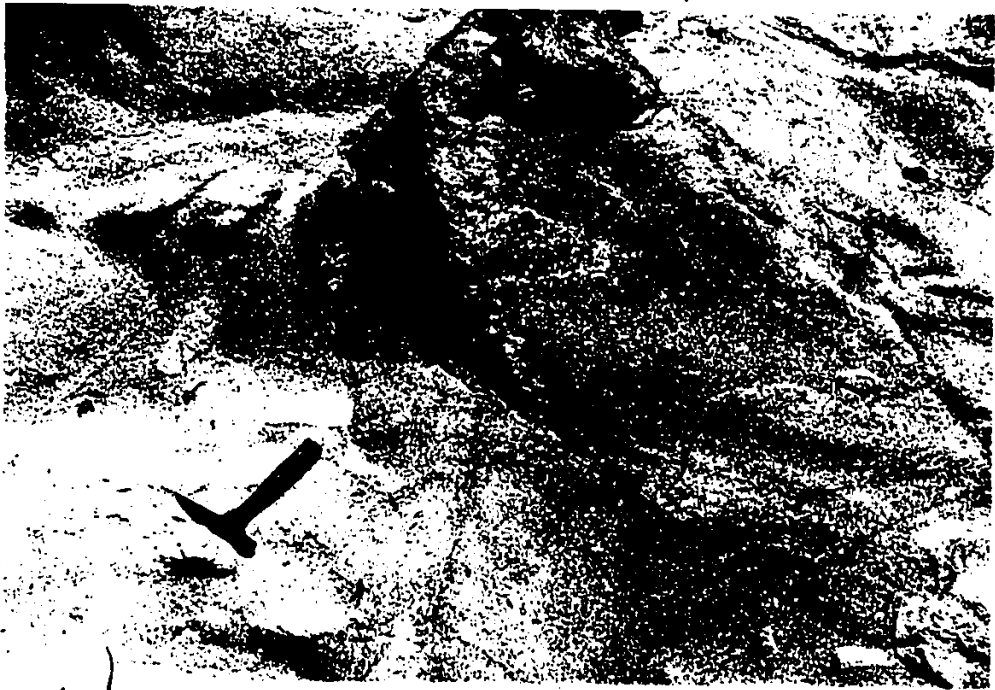


PLATE 18 A mafic plutonic block incorporated in an andesite dyke exposed on the shoreline north of Hillsborough.



PLATE 17 Nipper posing on the beach at Hillsborough Bay (Jack Adam Island in the background).



PLATE 18 Wilcox posing in front of a CMB epiclastic mudflow deposit on the shoreline at Point Cistern.

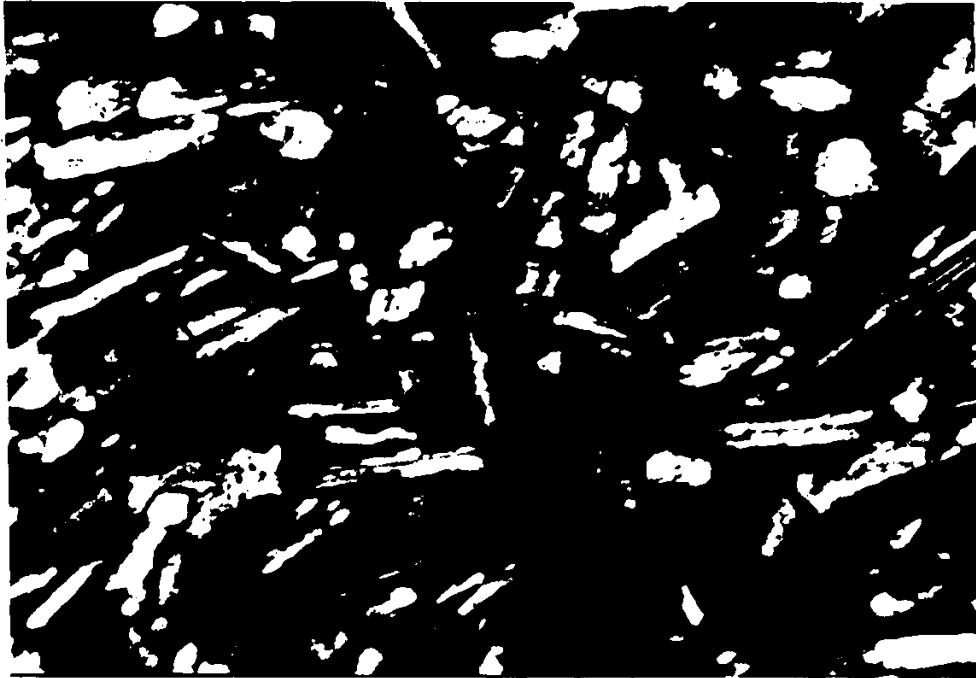


PLATE 10 OBE lava (X15,000) under cross polars showing groundmass plagioclase, clinopyroxene and magnetite, which display an intergranular texture.



PLATE 20 CFA lava (X2,400) under cross polars showing zoned clinopyroxene phenocrysts.



PLATE 21 APA lava (X2,400) under cross polars showing a plagioclase phenocryst with both internal melt channel corrosion and oscillatory zoning (also note the amphibole phenocryst showing marginal alteration to opaque minerals).



PLATE 22 CMB lava (X30,000) under plane polarized light showing groundmass phlogopite adjacent to a clinopyroxene phenocryst.



PLATE 23 CMB lava (X30,000) under plane polarized light showing dendritic-quench overgrowths on intratelluric magnetite crystals (also note alteration of the olivine phenocryst along internal fractures to a green micaceous mineral).

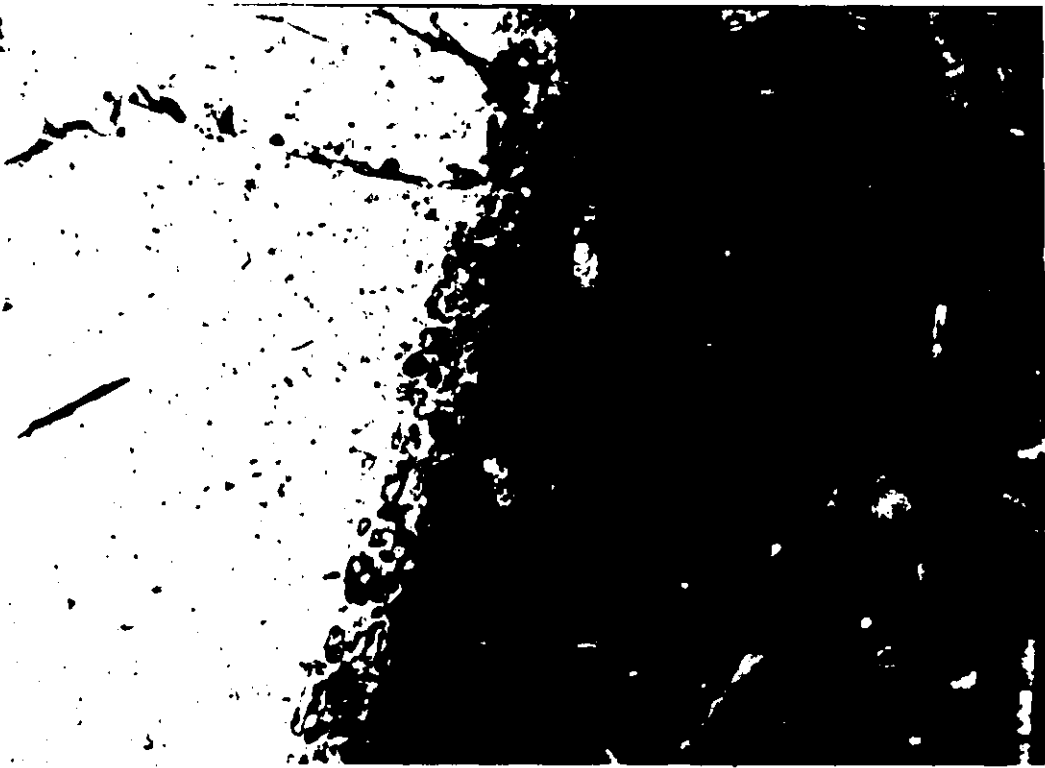


PLATE 24 CMB lava (X30,000) under cross polars showing a fritted marginal overgrowth on a clinopyroxene phenocryst.



PLATE 25 CMB lava (X2,400) under cross polars showing a clinopyroxene phenocryst (center) which envelopes a subhedral olivine phenocryst.



PLATE 26 CMB lava (X2,400) under cross polars showing a clinopyroxene phenocryst which envelopes an euhedral plagioclase phenocryst.

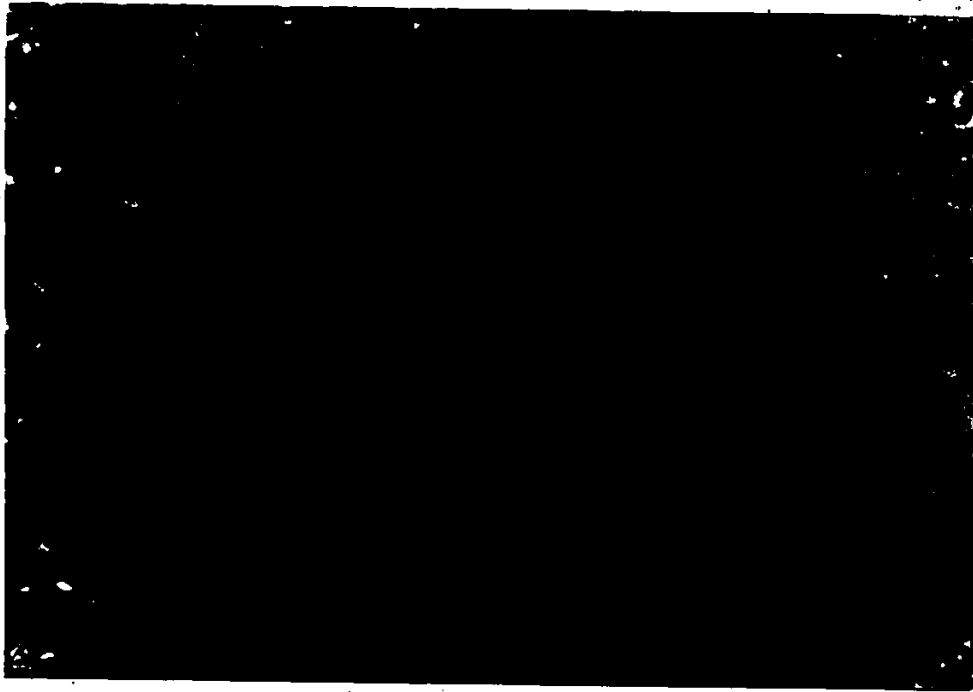


PLATE 27 OMB lava (X37,800) under plane polarized light showing euhedral picotites within an olivine phenocryst.

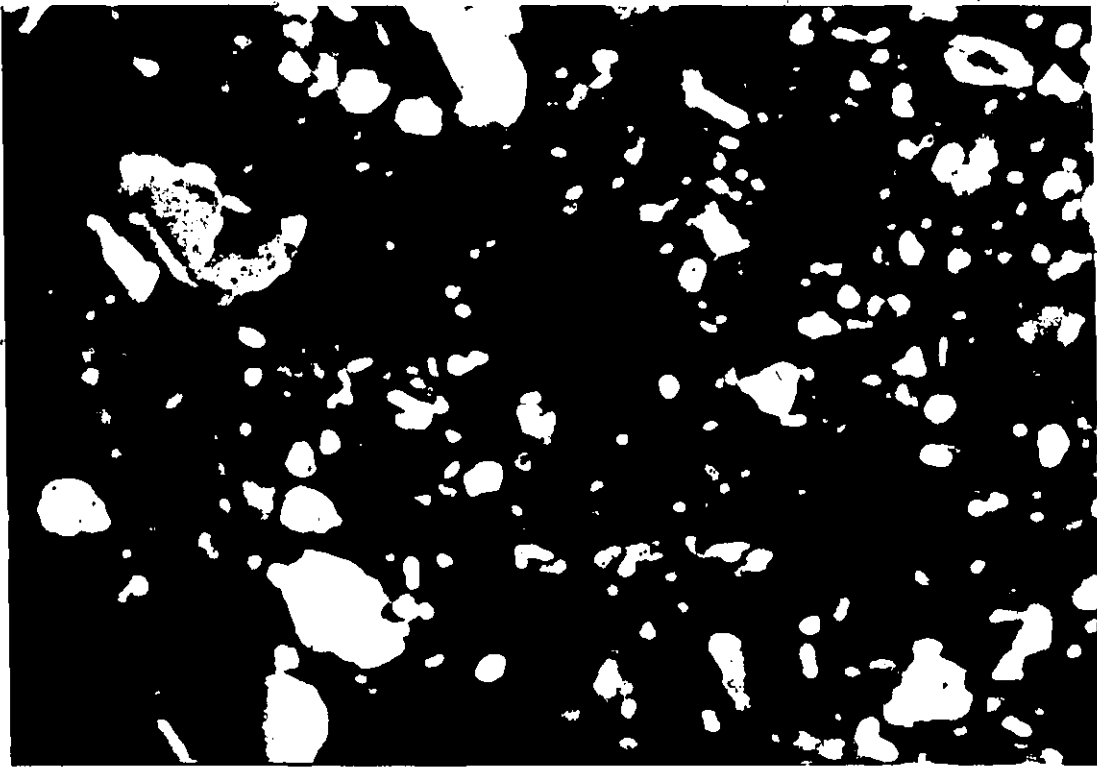


PLATE 28 OMB lava (X2,400) under cross polars showing a clinopyroxene phenocryst (center) with internal melt channel corrosion.

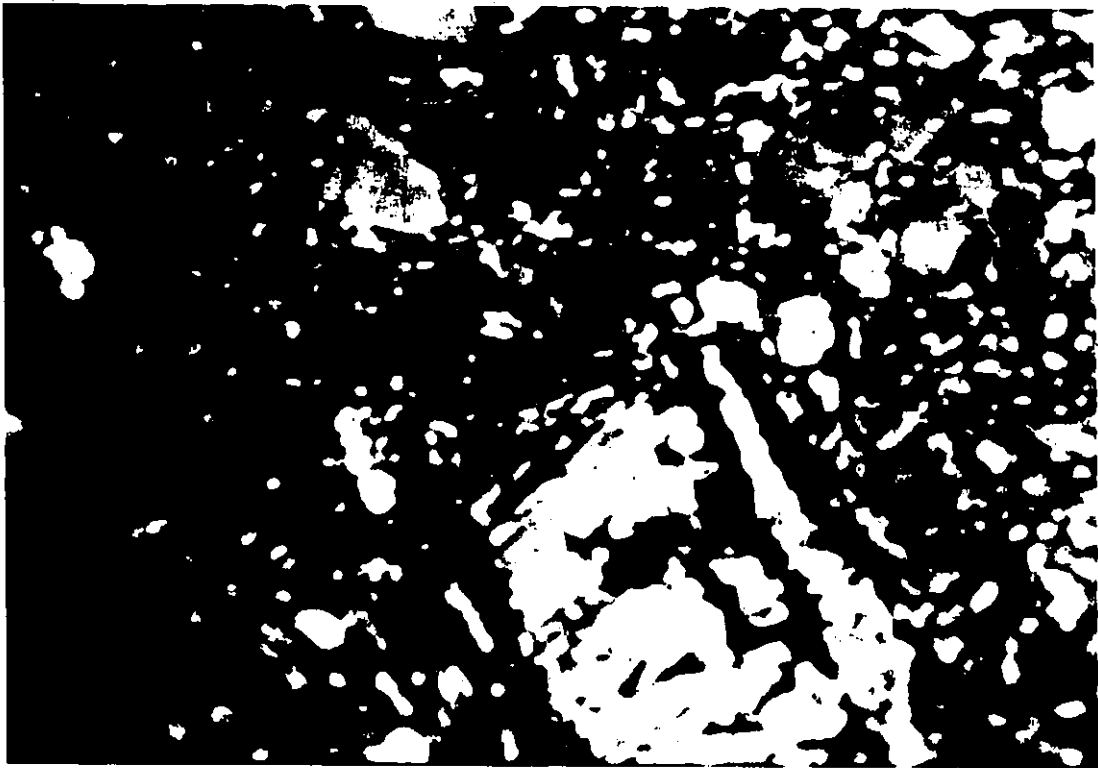


PLATE 29 OMB lava (X2,400) under cross polars showing
an altered plagioclase megacryst.

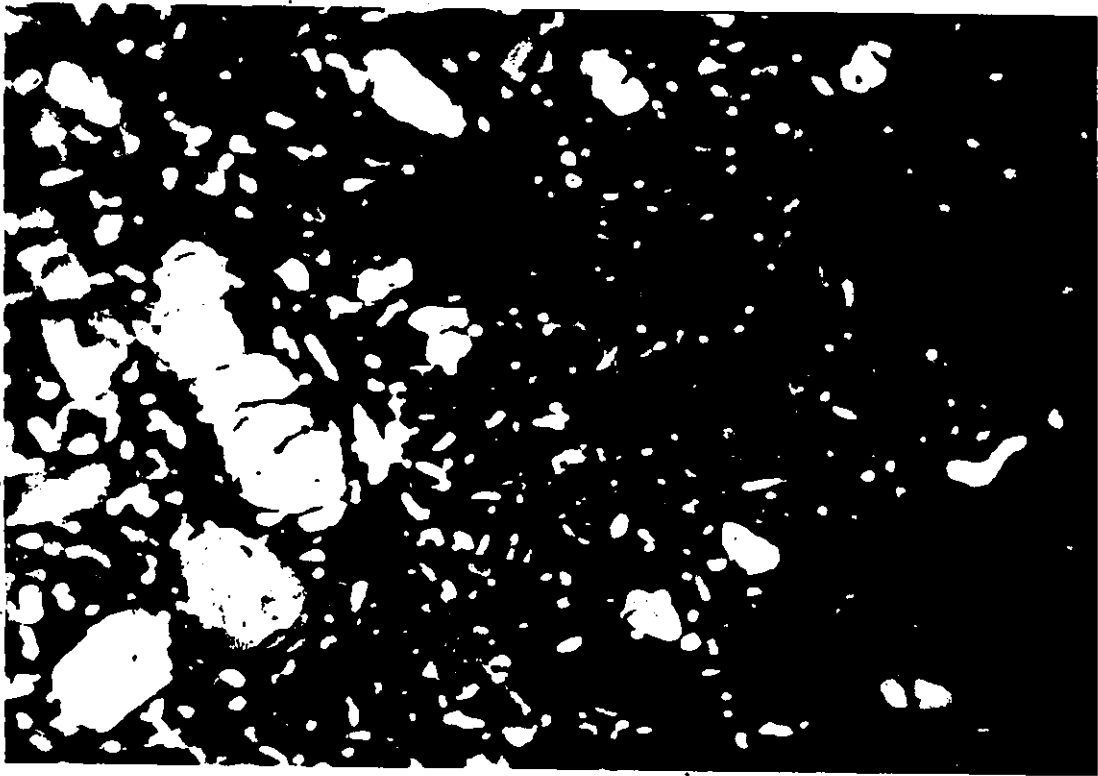


PLATE 39 OMB lava (X2,400) under cross polars showing olivine phenocrysts set in a fine grained groundmass.

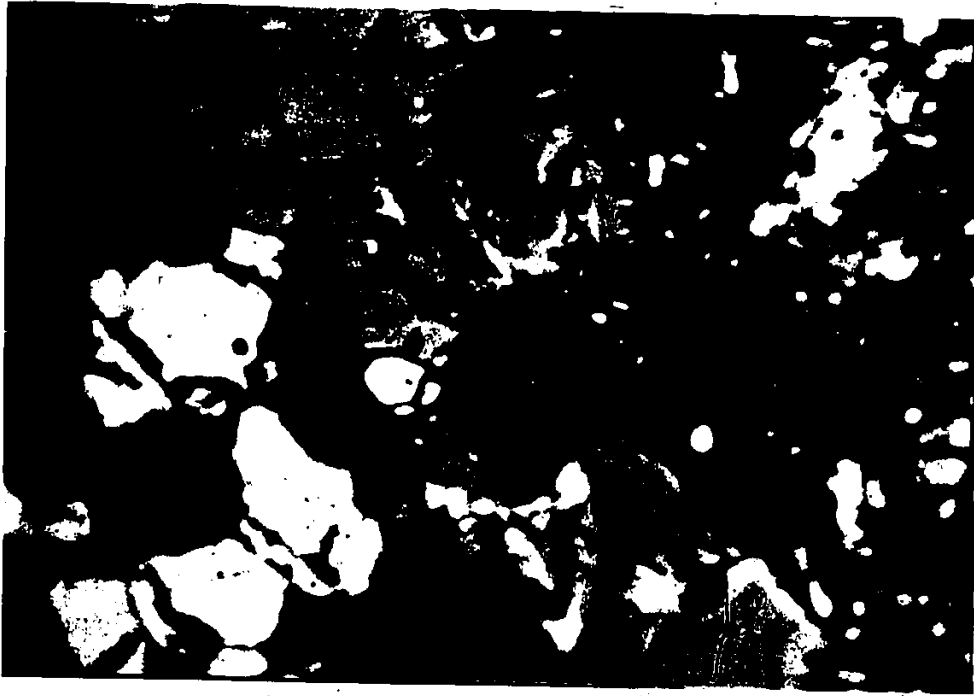


PLATE 31 OMB lava (X2,400) under cross polars showing
a fine grained dunite, cognate xenolith.



PLATE 32 CPA lava (X2,400) under cross polars showing a plagioclase phenocryst with extensive internal melt-channel corrosion.



PLATE 33 AMA lava (X2,400) under cross polars showing an anhedral clinopyroxene which is mantled by an amphibole (note the marginal alteration to opaques on the amphibole).

REFERENCES

- Anderson, A.T., and Gottfried, D., 1971. Contrasting behavior of P, Ti, and Nb in a differentiated high-alumina olivine tholeiite and a calcalkaline andesitic suite. *Geol. Soc. Am. Bull.*, Vol. 82, pp. 1929-1942.
- Arculus, R.J., 1976. Geology and geochemistry of the alkali basalt - andesite association of Grenada, Lesser Antilles island arc. *Geol. Soc. Am. Bull.*, Vol. 87, pp. 612-624.
- Bowen, C.O., 1972. Puerto Rico trench negative anomaly belt. *Geol. Soc. Am. Mem.*, Vol. 132, pp. 339-350.
- Briden, J.C., Rex, D.C., Faller, A.M., Tomblin, J.F., 1978. K-Ar geochronology and palaeomagnetism of volcanic rocks in the Lesser Antilles island arc. *Roy. Soc. Lon. Phil. Trans., Series A, Math. Phys. Sci.*, Vol. 291, pp. 485-528.
- Brown, G.M., Holland, J.G., Sigurdsson, H., Tomblin, J.F., and Arculus, R.J., 1977. Geochemistry of the Lesser Antilles volcanic island arc. *Geochim. Cosmochim. Acta*, Vol. 41, pp. 785-368.
- Burnham, C.W., 1979. Magmas and hydrothermal fluids. In: Barnes H.L., (ed.) *Geochemistry of hydrothermal ore deposits*, 2nd edn., Wiley-Interscience, New York, pp. 71-137.
- Chase, C.G., 1978. Plate kinematics: the Americas, East Africa, and the rest of the world. *Earth Planet. Sci. Lett.*, Vol. 37, pp. 355-368.
- Chase, R.L., and Bunce, E.T., 1969. Underthrusting of the eastern margin of the Antilles by the floor of the western North Atlantic Ocean, and the origin of the Barbados Ridge. *J. Geophys. Res.*, Vol. 74, pp. 1413-1420.
- Cox, K.G., Bell, J.D., and Pankhurst, R.J., 1979. The interpretation of igneous rocks. George Allen and Unwin.
- Dacsh, E.J., 1969. Strontium isotopes in weathering profiles, deep-sea sediments, and sedimentary rocks. *Geochim. Cosmochim. Acta*, Vol. 33, pp. 1521-1552.
- Dale, I.M., and Henderson, P., 1972. The partition of transition elements in phenocryst-bearing basalts and their implication about melt structure. *I. G. C.*, Sec. 10, pp. 105-111.
- Donnelly, T.W., Rogers, J.J.W., Pushkar, P., Armstrong, R.L., 1971. Chemical evolution of igneous rocks of the eastern West Indies: An investigation of thorium, uranium and potassium distributions, and lead and strontium isotopic ratios. *Geol. Soc. Am. Mem.*, Vol. 130, pp. 131-224.

- 2
- Eggler, D.H., and Burnham, C.W., 1973. Crystallization and fractionation trends in the system andesite-H₂O-CO₂-O₂ at pressures to 10 kb. *Geol. Soc. Am. Bull.*, Vol. 84, pp. 2517-2532.
- Fox, P.J., and Heezen, B.C., 1975. Geology of the Caribbean crust in the ocean basins and margins. (eds.) Mairn, A.E.M., and Stehli, F.G., Vol. 3, Chap. 10, Plenum, New York.
- Gast, P.W., 1968. Trace element fractionations and origin of tholeiitic and alkaline magma types. *Geochim. Cosmochim. Acta*, Vol. 32, pp. 1057-1086.
- Gill, J.B., 1981. Orogenic andesites and plate tectonics. Springer-Verlag, Berlin-Heidelberg-New York, Vol. 16.
- Grabert, H., 1971. Die prae-Andine drainage des Amazonasstromsystems. *Geol. Palaeontol.*, No. 20-21, pp. 51-60.
- Green, T.H., Green, D.H., and Ringwood, A.E., 1967. The origin of high-alumina basalts and their relationships to quartz tholeiites and alkali basalts. *Earth Planet. Sci. Lett.*, Vol. 2, pp. 41-52.
- Hanson, G.N., 1978. The application of trace elements to the petrogenesis of igneous rocks of granitic composition. *Earth Planet. Sci. Lett.*, Vol. 38, pp. 26-43.
- Hawkesworth, C.J., O'Nions, R.K., and Arculus, R.J., 1979. Nd and Sr isotope geochemistry of island arc volcanics, Grenada, Lesser Antilles. *Earth Planet. Sci. Lett.*, Vol. 45, pp. 237-248.
- Hawkins, J.W., Natland, J.H., 1975. Nephelinites and basanites of the Samoan linear volcanic chains: their possible tectonic significance. *Earth Planet. Sci. Lett.*, Vol. 24, pp. 427-439.
- Hedge, C.E., and Lewis, J.F., 1971. Isotopic composition of strontium in three basalt-andesite centers along the Lesser Antilles arc. *Contrib. Mineral. Petrol.*, Vol. 32, pp. 39-47.
- Irvine, T.N., and Barager, W.R.A., 1971. A guide to the chemical classification of the common volcanic rocks. *Can. J. Earth Sci.*, Vol. 8, pp. 523-548.
- IUGS Subcommittee, 1973. Plutonic rocks - classification and nomenclature. *Geotimes*, Vol. 18, No. 10, pp. 26-30.
- Jackson, T.A., 1970. Geology and petrology of the volcanic rocks of Carriacou, Grenadines, West Indies, Unpub. M. Sc. thesis, U.W.I.
- Jackson, T.A., 1980. The composition and differentiation of the volcanic rocks of Carriacou, Grenadines, West Indies. *Bull. Volcanol.*, Vol. 43-2.
- Jezeq, P., Hutchinson, C.S., 1978. Banda arc of Eastern Indonesia: petrology and geochemistry of the volcanic rocks. *Bull. Volcanol.*, Vol. 41, pp. 586-608.

- Johnson, R.W., 1976. Late Cenozoic volcanism and plate tectonics at the southern margin of the Bismark Sea, Papua, New Guinea. In: Johnson, R.W. (ed.), *Volcanism of Australia*. Elsevier, Amsterdam, pp. 101-116.
- Keary, P., 1974. Gravity and seismic reflection investigation into the crustal structure of the Aves Ridge, Eastern Caribbean. *Geophys. J. Res. Abstr. Soc.*, Vol. 38, pp. 435-448.
- Leake, B.E., 1978. Nomenclature of amphiboles. *Mineral. Mag.*, Vol. 42, pp. 533-563.
- MacDonald, G.A., 1968. Composition and origin of Hawaiian lavas. *Geol. Soc. Amer. Mem.*, Vol. 116, pp. 477-522.
- Margaritz, M., Whiteford, D.J., James, D.E., 1978. Oxygen isotope and the origin of high - $^{87}\text{Sr}/^{86}\text{Sr}$ andesites. *Earth Planet. Sci. Lett.*, Vol. 40, pp. 220-260.
- Martin-Kaye, P.H.A., 1958. Geology of Carriacou. *Bull. Am. Paleon.*, Vol. 38, No. 175, pp. 395-497.
- Martin-Kaye, P.H.A., 1969. A summary of the Lesser Antilles. *Overseas Geol. Min. Res.*, Vol. 10, pp. 172-206.
- Miyashiro, A., 1974. Volcanic rock series in island arcs and active continental margins. *Am. J. Sci.*, pp. 321-355.
- Nagle, F., Stipp, J.J., and Fisher, D.E., 1976. K-Ar geochronology of the Limestone Caribbeas and Martinique, Lesser Antilles, West Indies. *Earth Planet. Sci. Lett.*, Vol. 29, pp. 401-412.
- O'Nions, R.K., Hamilton, P.J., and Evenson, N.M., 1977. Variations in $^{143}\text{Nd}/^{144}\text{Nd}$ and $^{87}\text{Sr}/^{86}\text{Sr}$ ratios in oceanic basalts. *Earth Planet. Sci. Lett.*, Vol. 34, p. 13.
- O'Nions, R.K., Carter, S.R., Cohen, R.S., Evenson, N.M., and Hamilton, P.J., 1978. Pb, Nd, and Sr isotopes in oceanic ferromanganese deposits and ocean floor basalts. *Nature*, Vol. 273.
- Pearce, J.A., and Cann, J.R., 1973. Tectonic setting of basic volcanic rocks determined using trace element analysis. *Earth Planet. Sci. Lett.*, Vol. 19, pp. 290-300.
- Poldervaart, A., and Hess, H.H., 1951. Pyroxenes in the crystallization of basaltic magma. *J. Geol.*, Vol. 59, pp. 472-489.
- Pushkar, P., 1968. Strontium isotope ratios in volcanic rocks of three island arc areas. *J. Geophys. Res.*, Vol. 73, pp. 2701-2714.
- Pushkar, P., Steuben, A.M., Tomblin, J.F., and Julian, G.M., 1973. Strontium isotopic ratios in volcanic rocks from St. Vincent and St. Lucia, Lesser Antilles. *J. Geophys. Res.*, Vol. 78, pp. 1279-1287.
- Rea, W.J., 1974. The volcanic geology and petrology of

- Montserrat, West Indies. *J. Geol. Soc. Lond.*, Vol. 130, pp. 341-366.
- Rea, W.J., and Baker, P.E., 1980. The geothermal characteristics and conditions of petrogenesis of the volcanic rocks of the northern Lesser Antilles - a review. *Bull. Volcanol.*, Vol. 43-2.
- Robinson, E., and Jung, P., 1972. Stratigraphic and age of marine rocks, Carriacou, West Indies. *Am. Assoc. Petrol. Geol. Bull.*, Vol. 56, No. 1, pp. 114-127.
- Schnetzler, C.C.; and Philpotts, J.A., 1970. Partition coefficients of rare earth elements between igneous matrix material and rock forming mineral phenocrysts -II. *Geochim. Cosmochim. Acta*, Vol. 34, pp. 331-340.
- Shimuzu, N., and Arculus, R.J., 1975. Rare earth element concentrations in a suite of basanitoids and alkali olivine basalts from Grenada, Lesser Antilles. *Contrib. Mineral. Petrol.*, Vol. 50, pp. 231-240.
- Shimizu, N., and Kushiro, I., 1975. The partitioning of rare earth elements between garnet and liquid at high pressures: preliminary experiments. In preparation.
- Sigurdsson, H., Tomblin, J.F., Brown, G.M., Holland, J.G., and Arculus, R.J., 1973. Strongly undersaturated magmas in the Lesser Antilles island arc. *Earth Planet. Sci. Lett.*, Vol. 18, pp. 285-295.
- Smith, A.L., and Roobol, M.J., and Gunn, B.M., 1980. The Lesser Antilles - a discussion of the island arc magnetism. *Bull. Volcanol.*, Vol. 43-2.
- Tomblin, J.F., 1972. Seismicity and plate tectonics of the Eastern Caribbean. *Caribbean Geol. Conf. VI, Isla de Margarita, 1971. Trans: Impreso por Cromotip, Caracas*, pp. 277-282.
- Tomblin, J.F., 1975. The Lesser Antilles and Aves Ridge. In: *The ocean basins and margins*, (ed.) Nairn, A.E.M., and Stehli, F.G., Vol. 3, Chapt. 11, Plenum, New York.
- Tomita, T., 1935. On the chemical compositions of the Cenozoic alkaline suite of the circum-Japan Sea region. *J. Shanghai Sci. Insti., Sect. II, Vol. 1*, pp. 227-306.
- Ujike, O., 1974. Post-eruption oxidation of hornblende phenocryst from Kaitaku, Shodo-shima, Japan. *J. Jpn. Assoc. Mineral. Pet. Econ. Geol.*, Vol. 69, pp. 426-433.
- Van Andel, T.J.H., 1967. The Orinoco delta. *J. Sed. Pet.*, Vol. 37, No. 2, pp. 297-310.
- Wager, L.R., and Mitchell, 1951. The distribution of trace elements during strong fractionation of basic magma - a further study of Skaergaard intrusion, East Greenland. *Geochim. Cosmochim. Acta*, Vol. 1, pp. 129-208.

- Westbrook, G.K., Bott, M.H.P., and Peacock, J.H., 1973. The nature of the Lesser Antilles subduction zone in the region of Barbados. *Nature Phys. Sci.*, Vol. 244, pp. 118-120.
- Whitford, D.J., Jesek, P., 1979. Origin of late-Cenozoic lavas from the Banda arc, Indonesia: trace element and Sr isotope evidence. *Contrib. Mineral. Petrol.*, Vol. 68, pp. 141-150.
- Wyllie, P.J., 1982. Subduction products according to experimental prediction. *Geol. Soc. Am. Bull.*, Vol. 93, pp. 468-476.
- Zielinski, R.A., and Frey, F.A., 1970. Gough Island: evaluation of a fractional crystallization model. *Contrib. Mineral. Petrol.*, Vol. 29, pp. 242-254.
- Zielinski, R.A., 1974. Trace element evaluation of the petrogenesis of a suite of rocks from Reunion Island, Indian Ocean (abstract). *E.O.S.*, Vol. 55, 455 p.

VITA AUCTORIS:

Personal Data:

CALDWELL, Gary Francis

1215 Nottingham Ave., Kingsville, Ontario, N9Y 3K8.

Phone: (519) 733-3548.

Born: January 9, 1958, Windsor, Ontario.

Canadian Citizen.

Single.

Sex: Male.

Education:

1963 - 1967: Attended St. Andrew's School, Windsor, Ont.

1967 - 1972: Graduated from Hugh Beaton School, Windsor, Ont.

1972 - 1977: Graduated from Walkerville C. I., Windsor, Ont.
(5 year Secondary and Honours Diplomas).

1977 - 1981: Graduated from the University of Windsor,
(4 year B.Sc., Honours Geology).

1981 - 1983: Graduated from the University of Windsor,
(2 year M.Sc., Geology).

Employment Experience:

1978 (May - Sept.): Ontario Geological Survey,
77 Grenville Street, Toronto, Ont.

Junior Assistant to Geologist (J. Pirie)
in Redlake, Ont.

1978 - 1979 (Sept. - April): Chrysler's Car Plant,
Windsor, Ont.

Temporary Part Time Worker.

1979 (May - Sept.): Rio Tinto Canadian Exploration Ltd.
85 Richmond St. W., Suite 400, Toronto, Ont.

Junior Assistant to Geologist (D. Clarke)
for gold and base metal exploration around
the area of Kirkland Lake, Ont. (acquired
some experience with carrying out E.M. and
magnetometer surveys).

1980 (May - Sept.): Ontario Geological Survey,
77 Grenville Street, Toronto, Ont.

Senior Assistant to Geologist (N. Trowell):
in Kenora, Ont. Carried out detailed
mapping at a scale of 1:31,680 in the
Gibi Lake area of eastern Lake of the Woods.
Also carried out an undergraduate thesis
on the stratigraphy, petrology and
petrography of the Gibi Lake Metavolcanic
Sequence in the same area.

Our brief account of the geology is
published in Summary of Field Work, 1980
by the Ont. Geological Survey, Miscellaneous
Papers 96, pp. 17 - 20.

1981 (May - Sept.): Shell Canada Resources Ltd.,
400 4th Ave., S.W., Calgary, Alberta,
(Department of Exploration), Southern Foothills
Division, 16th Floor.

Worked under the supervision of Gil Graff as a
summer student geologist. Aided in the partial
mapping and interpretation of the Elk River/Bull
River Area in Southeastern B.C., and performed
field related duties while in Calgary.

1982 (Oct. - April): Chrysler's Car Plant,
Windsor, Ont.

Temporary Part Time Worker.

Awards:

Obtained an undergraduate award certificate by The
Canadian Society of Petroleum Geologists in recognition

of outstanding competence in studies related to Petroleum Geology.

Awarded the privilege of attending the Student Industry Field Trip (1980) which is held and sponsored by The Canadian Society of Petroleum Geologists.

President's Roll of Scholars (University of Windsor), 1978-79 and 1980-81.

Awarded the University of Windsor Postgraduate Scholarship (\$2,500.00) for both the 1981-82 and 1982-83 sessions. (Could not obtain the latter scholarship money while holding the following award):

Awarded the Ontario Graduate Scholarship for 1982-83. (\$1,900.00 per term for three terms).